

SIMULATING COTTONWOOD TREE GROWTH IN FLOOD PLAINS USING THE LIGNUM MODELING METHOD

A Dissertation

presented to

the Faculty of the Graduate School

University of Missouri-Columbia

In Partial Fulfillment

Of the Requirements for the Degree

Doctor of Philosophy

by

MIAOER LU

Dr. David Larsen, Dr. Pekka Nygren, Dissertation Supervisors

AUGUST 2006

The undersigned, appointed by the Dean of the Graduate School, have examined the dissertation entitled.

**SIMULATING COTTONWOOD TREE GROWTH IN
FLOOD PLAINS USING THE LIGNUM MODELING
METHOD**

Presented by Miaoer Lu

A candidate for the degree of Doctor of Philosophy

And hereby certify that in their opinion it is worthy of acceptance.

David Larsen

K. Palaniappan

Stephen G. Pallardy

Milon F. George

Michael Gold

Pekka Nygren

ACKNOWLEDGEMENTS

I want to first thank the University of Missouri Center for Agroforestry and the USDA ARS Dale Bumpers Small Farms Research Center in Booneville, AR for their support for a graduate research assistantship. I also owe a debt of gratitude to my co-advisors (Dr. Pekka Nygren and Dr. David Larsen) who showed me the highlight in forestry science and the ability of scientific thinking in academic research. In the past five years, they have been encouraging, patient, and supportive in my research and course work. They have also been very supportive during my trips out of United States. I also want to thank my other committee members: Dr. Stephen Pallardy, Dr. Milon George, Dr. Kannappan Palaniappan, and Dr. Michael Gold. They have always been generous in providing their help for my research and course works. Dr. Pallardy provided some critical measurement data for my research, and I learned a lot about cottonwood tree growth from him. I also thank Jari Perttunen and Risto Sievänen who helped me in understanding of general LIGNUM modeling structure and programming in new developments of cottonwood simulation.

I would like to thank Dr. Bernard J. Lewis for his generous contribution in editing my dissertation and inexhaustible encouragement. I appreciate the help from Wayne Bishop, Daniel Gibbins, Kenneth Bader, Lauren Murray, Tom Settle, Victor Nieto, and Kristopher Klaus for my field data measurements. I would like to thank Jian Yang and Ian Scott for their help whenever I needed it. Finally, I would like to thank my husband, Zhenqian Lu, and my family in China for their encouragement and support. Their smiles are the sources of my power and motivation in my research.

SIMULATING COTTONWOOD TREE GROWTH IN FLOOD PLAINS USING LIGNUM MODELING METHOD

Miaoer Lu

Under the supervision of Dr. David Larsen and Dr. Pekka Nygren
University of Missouri--Columbia

ABSTRACT

As a flood-tolerant and fast-growing species, cottonwood is a promising species in flood plain and short-rotation forestry. Understanding tree growth will provide critical assistance in flood plain forest management and forest configuration practice. Computer based tree growth simulation models provide a complementary tool for forest managers and scientists to learn the underlying tree growth mechanisms and a tree's response to different growing environments. LIGNUM, a functional-structural tree growth simulation model, was applied to simulation of the cottonwood growth in a flood plain area in central Missouri.

The key characteristics of the LIGNUM model are the linkage between tree spatial structure and physiological function. L-system was adopted in structural derivation of the tree. Physiological processes including photosynthesis and growth allocation were embedded in LIGNUM model. Communication between L-system and LIGNUM model was implemented during model simulation.

Based on the general framework from the previous LIGNUM version, the application of cottonwood growth simulation with LIGNUM modeling method required a

few new developments, including real photon flux data input, a voxel space photon flux interception module, a photosynthesis product module, three nested short time modeling steps, and stand growth simulation. The link to actual weather data enabled better convergence of model results with real world tree growth. The voxel space photon flux interception module replaced tree compartments with regular voxels as the calculation unit, resulting in efficient photon flux interception operation. Three nested short time steps were used according to the growth speed of cottonwood to capture the rapid change in tree structure. The biochemically-derived model on photosynthetic production – Farquhar’s model – was applied to accumulate net leaf CO₂ assimilation all over the tree. The application of LIGNUM in mono-cohort, even-aged, and tightly spaced cottonwood stand is a new extension of the LIGNUM model.

The simulation results reflected well the real cottonwood growth for the first four years. Simulated results respond logically to photon flux input variation. The model is sensitive to several parameters in the photosynthesis module. Further application of LIGNUM model can be used in more complicated forest research.

TABLE OF CONTENTS

| | |
|---|------|
| ACKNOWLEDGEMENTS | ii |
| ABSTRACT | iii |
| LIST OF TABLES | vii |
| LIST OF FIGURES | viii |
| 1. INTRODUCTION | 1 |
| 1.1 Cottonwood and its application in agroforestry and flood plain forests | 1 |
| 1.2 Research problems | 3 |
| 1.3 Tree growth modeling | 5 |
| 1.4 Objectives of this dissertation | 8 |
| 1.4.1 General objectives | 8 |
| 1.4.2 Two specific objectives | 9 |
| 1.5 Outline of dissertation | 10 |
| 2. LITERATURE REVIEW | 12 |
| 2.1 Short-rotation forestry with poplar species | 12 |
| 2.2 Background of tree growth modeling | 14 |
| 2.2.1 Modeling tools | 15 |
| 2.2.2 Modeling hierarchy and application | 16 |
| 2.3 Representative examples of tree growth models | 16 |
| 2.3.1 Empirical models | 17 |
| 2.3.2 Pipe-Model theory | 18 |
| 2.3.3 Process-based models | 19 |
| 2.3.4 Structure-based models | 23 |
| 2.3.5 Functional-structural models | 25 |
| 3. INDIVIDUAL TREE GROWTH MODEL | 39 |
| 3.1 New application of LIGNUM to cottonwood growth | 39 |
| 3.2 Cottonwood modeling with LIGNUM | 40 |
| 3.2.1 General model structure | 41 |
| 3.2.2 Short time step simulation | 49 |
| 3.2.3 Photon flux interception in the tree | 51 |
| 3.2.4 Monte Carlo photon flux interception model | 55 |
| 3.2.4.1 Voxel space | 55 |
| 3.2.4.2 Big leaf | 57 |
| 3.2.4.3 Photon flux interception | 58 |
| 3.2.4.4 Standard diffuse photon flux interception | 64 |
| 3.2.5 Photosynthesis model | 64 |
| 3.2.6 Structure derivation and growth allocation within short time step simulation | 67 |
| 3.2.6.1 Structure derivation | 67 |
| 3.2.6.2 Growth allocation | 71 |
| 3.2.6.3 Root biomass growth | 74 |
| 3.2.7 Communication between L-system and LIGNUM | 75 |
| 3.3 Field data | 76 |

| | | |
|---------|---|-----|
| 3.3.1 | Field site..... | 76 |
| 3.3.2 | Weather data | 78 |
| 3.3.3 | Tree structure | 81 |
| 3.3.3.1 | Branching pattern..... | 81 |
| 3.3.3.2 | Leaf growth..... | 84 |
| 3.4 | Results..... | 85 |
| 3.4.1 | Measured structural patterns of cottonwood..... | 85 |
| 3.4.2 | Model parameterization | 89 |
| 3.4.3 | Model output and validation | 95 |
| 3.4.4 | Running time consumption in Simulation | 105 |
| 3.4.5 | Sensitivity analyses..... | 108 |
| 3.5 | Discussion..... | 113 |
| 3.5.1 | Model evaluation | 113 |
| 3.5.2 | Precision and efficiency of the model..... | 114 |
| 3.5.3 | Model implications | 118 |
| 3.5.4 | Model limitations..... | 120 |
| 3.5.5 | Future research needs..... | 123 |
| 4. | TREE STAND GROWTH MODEL | 124 |
| 4.1 | Forest modeling: Purpose and Foci..... | 124 |
| 4.2 | Simulation of the growth of a cottonwood stand..... | 127 |
| 4.2.1 | General model structure..... | 128 |
| 4.2.2 | Uniformity of tree growth in the stand | 130 |
| 4.2.3 | Voxel model..... | 130 |
| 4.3 | Field data..... | 132 |
| 4.3.1 | The site..... | 132 |
| 4.3.2 | Tree structure | 134 |
| 4.3.3 | Weather data and photosynthetic parameters | 135 |
| 4.4 | Results..... | 135 |
| 4.4.1 | Results from field measurements..... | 136 |
| 4.4.2 | Model parameterization | 145 |
| 4.4.3 | Model output and validation | 145 |
| 4.5 | Discussion..... | 152 |
| 4.5.1 | Stand shading..... | 152 |
| 4.5.2 | Branch azimuth in stand plantation..... | 152 |
| 4.5.3 | Modeling efficiency..... | 153 |
| 4.5.4 | Short-rotation cottonwood stand growth | 154 |
| 4.5.5 | Future research needs..... | 155 |
| 5. | CONCLUSIONS..... | 156 |
| 6. | REFERENCES | 160 |
| 7. | APPENDIX..... | 170 |
| | VITA..... | 174 |

LIST OF TABLES

| | |
|--|-----|
| Table 1. Soil fertility data for open growth plantation. | 78 |
| Table 2. Parameters and constants about structure and physiology. | 91 |
| Table 3. Parameters in cottonwood photosynthesis model with different clones.. | 91 |
| Table 4. Comparison between simulation and field data for cottonwood tree growth in open growth environment. | 100 |
| Table 5. Simulated results of individual tree growth model (4 years) and field observation for 4-year-old tree growth. | 102 |
| Table 6. Sensitivity analysis of parameters for cottonwood growth model..... | 111 |
| Table 7. Sensitivity analysis with variation on parameter combinations. Growth index data – height – is used to test the model sensitivity with parameters. .. | 112 |
| Table 8. Sensitivity test with variation on parameter combinations..... | 112 |
| Table 9. Soil fertility data for 1m ×1m spacing stand growth plantation. | 133 |
| Table 10. Insertion and bending angles of branches for stand and open growth plantation cottonwood trees. | 139 |
| Table 11. Crown height and crown ratio for stand and open-growth plantation cottonwood trees. | 139 |
| Table 12. Frequency of directions for longest branches in cottonwood tree crowns. | 141 |
| Table 13. Modelling parameters in cottonwood stand simulation. | 145 |
| Table 14. Model validation for cottonwood simulation with biomass and height. | 147 |
| Table 15. Height and biomass production for 1×1m spacing cottonwood stand growth. | 150 |

LIST OF FIGURES

| | | |
|-------------------|--|-----|
| Figure 1. | Basic units in LIGNUM modeling..... | 29 |
| Figure 2. | Bud derivation in LIGNUM..... | 29 |
| Figure 3. | General modeling structure for individual tree growth with LIGNUM..... | 43 |
| Figure 4. | Segment and leaf derivation in LIGNUM..... | 45 |
| Figure 5. | Segment and leaf development diagram in individual cottonwood growth. | 46 |
| Figure 6. | Segment split in LIGNUM model..... | 48 |
| Figure 7. | Photon flux overcast distribution in the firmament model..... | 54 |
| Figure 8. | Voxel Space. | 56 |
| Figure 9. | Interception of photon flux in voxel space..... | 60 |
| Figure 10. | Radiation interception in several adjacent voxels..... | 62 |
| Figure 11. | Deviation of bud growth direction in three dimensions..... | 70 |
| Figure 12. | Branch structure measurement..... | 82 |
| Figure 13. | Branch positions in low, medium, and high crown..... | 83 |
| Figure 14. | Azimuth (horizontal bifurcation angle) distribution of branches in cottonwood tree..... | 87 |
| Figure 15. | Inclination (vertical bifurcation angle) distribution of branches in cottonwood tree..... | 87 |
| Figure 16. | Branch growth dynamics..... | 88 |
| Figure 17. | The clonal differences in net CO ₂ assimilation rate among three cottonwood clones. | 92 |
| Figure 18. | Non-linear relationships between net CO ₂ assimilation rate and photosynthetic photon flux density..... | 93 |
| Figure 19. | Light index curve with relative photosynthetic photon flux (PPF)..... | 94 |
| Figure 20. | The visualization of a simulated 4-year-old cottonwood tree..... | 99 |
| Figure 21. | Cottonwoods growing in the study field site in central Missouri. | 100 |
| Figure 22. | Height growth trend of cottonwood simulation and measurement. ... | 101 |
| Figure 23. | Changes in simulated height and leaf area with age in cottonwood simulation..... | 101 |
| Figure 24. | Visualization of results of individual tree growth model for a 10-year-old cottonwood in an open growth environment. | 103 |
| Figure 25. | Visualization of tree growth response with decreasing light level. ... | 104 |
| Figure 26. | The increase of voxel number and tree compartments with age. | 107 |
| Figure 27. | The calculation with pairwise comparison is about the second power of the calculation in voxel model..... | 107 |
| Figure 28. | Tree growth variation with 25% variation in modelling parameters.. | 111 |
| Figure 29. | Increase in voxel space number with age and associated tree growth. | 122 |
| Figure 30. | General modeling structure for cottonwood stand growth simulation.. | 129 |

| | |
|---|-----|
| Figure 31. Voxel space for a simulated cottonwood stand..... | 131 |
| Figure 32. Branch angles distribution for the three clones' cottonwood trees in stand plantation..... | 138 |
| Figure 33. Comparison of the branch insertion angles and bending angles for two plantations and among different cottonwood clones in stand plantation..... | 140 |
| Figure 34. Directional frequencies of the longest branches in cottonwood tree crowns..... | 141 |
| Figure 35. Branch length dynamics for trees growing in stand and open plantations..... | 143 |
| Figure 36. Leaf number dynamics for trees growing in stand plantation and comparison to that of trees in open plantation..... | 144 |
| Figure 37. Visualization of a simulated 4-year-old cottonwood stand growing in a central Missouri environment with 1m×1m spacing..... | 148 |
| Figure 38. Cottonwood stand plantation growth in the field in central Missouri. | 149 |
| Figure 39. Trend in height for measured and simulated cottonwood growth in stand plantation..... | 149 |
| Figure 40. Visualization of 5-year-old tree growth in cottonwood stand..... | 151 |

1. INTRODUCTION

1.1 Cottonwood and its application in agroforestry and flood plain forests

Eastern cottonwood (*Populus deltoides* Bortr. ex Marsh.; hereafter “cottonwood”) is a deciduous poplar species. It is named for the cotton-like fluff in which the seed is enclosed. The botanical name *Populus deltoides* comes from the Greek word *delta*, because its leaves have a heart-like triangular shape.

Eastern cottonwood grows widely in North America and is highly adaptable to different growth environments. The range of this species extends from Quebec in the north to Florida in the south. The north-south distribution extends from latitude 28° N to 46° N. The tolerable ambient temperature can vary from –45 °C to 46 °C (Cooper, 2002). Although eastern cottonwood grows best on moist and fertile soils, it can also survive on deep, infertile sands (Cooper, 2002). Cottonwood is widely distributed along rivers and streams in central Missouri.

As a fast-growing species, cottonwood can grow to more than 30 meters tall with massive trunks more than 1.5 meters in diameter (Cooper, 2002). It can grow to about 10 meters in four years. The biggest cottonwood tree was reported to be 58 meters in height and 180 centimeters in diameter (Putnam *et al.*, 1960). Stand volume for cottonwood can exceed 420 m³ ha⁻¹ of sawed lumber at age 35 (Bull, 1945; Johnson *et al.*, 1976; McKnight, 1950; Williamson, 1913). The wood is light-weight, soft, and relatively weak. Cottonwoods are used as shelterbelts, for firewood, and in intensive

plantations for wood fiber and pulp production. Cottonwood pulp is utilized for book and magazine paper, and food containers. Stem wood contributes the biggest proportion to biomass, and the proportions of total biomass are ranked in the order of stem>branches>leaves (Puri, 1994).

In North America, hybrids between eastern cottonwood and other *Populus* species have been intensively studied for short-rotation forestry (Alig *et al.*, 2000). It has been estimated that short-rotation poplar and cottonwood plantations could supply 40% of the hardwood pulp needs of the U.S. and reduce current pressure for exploitation of natural forests for pulpwood (Alig *et al.*, 2000). There is an increasing interest in poplar wood for use in lumber and oriented strand board, which can be used to make storage products (Pallardy *et al.*, 2003). In India, cottonwood is also common in short rotation forestry (Puri *et al.*, 1994; Singh, 1998; Singh *et al.*, 1997).

Cottonwood is also widely used in agroforestry practices. Introduced cottonwood has become a prime agroforestry species in Northern India, especially in the Indogangetic Plains (Singh, 1998), where it is successfully associated with ginger and turmeric (Jaswal *et al.*, 1993), wheat, rice, pigeon pea and cowpea, as well as with the forages sorghum and berseem (Singh *et al.*, 1997). Silvopastoral practices combining cottonwood with a mixed understory of native grasses and legumes are used for erosion control in New Zealand (Guevara *et al.* 2000). The usage of cottonwood in Northern-American agroforestry practices is also increasing annually.

In projects of University of Missouri Center for Agroforestry (UMCA) flood plain agroforestry, cottonwood is one of the main species studied because of its fast-growth and flood-tolerance properties. A cottonwood clonal trial is being

implemented to identify the potential species and selections in designing agroforestry-related flood plain buffers (Dwyer, 2004). Cottonwood is also the focus of an agroforestry research project on tree/crop interactions. The row orientation effects of a cottonwood stand are being studied for forage production and growth of reed canarygrass on a periodically flooded site (McGraw, 2004). Pallardy (2004) has utilized cottonwood for carbon sequestration and biomass growth study. His study focuses on the physiological and morphological determinants of biomass productivity of poplar clones growing in Missouri River flood plains, leading to the assessment of carbon budgets for cottonwood clonal stands.

1.2 Research problems

Flooding is a serious and frequent problem along the Missouri River and other rivers around the world. Two critical issues are related to flooding. First, what can be done to make good use of the flood plain that is abandoned after flooding? High velocity currents transport sediments into and out of the flooded areas. When the flood recedes, particles are sorted by size with sand first, followed by silt and clay, forming an alluvial deposit or alluvium, which ultimately contributes to the formation of fertile flood plains. It may be feasible to select flood-tolerant crops and/or develop agricultural systems that benefit from these fertile alluvia.

A second issue concerns how to better prevent or at least reduce the damage to flood plains from flooding. Soil erosion is a key problem in flooding. One possible solution can be to bind the soil through the presence of grasses or forests in the flood plain area. Flood plain forests play an especially important role in natural flood control by functioning as natural impoundments and stabilizing the soil against erosion (Klimo,

1998). Flood plain forests also fully benefit from the alluvial deposits that are rich in nutrients. The management of flood plain forests is propitious for flood storage, sediment control, wildlife habitat, timber production, and water quality (Stuart, 1996).

As a flood-tolerant and fast-growing poplar species, cottonwood is a good tree species for flood plain forests. Cottonwood is native to the eastern and Midwest U.S. It grows best on moist, well-drained, fine sandy loams or silt loams. Its wide-spreading root system and rapid growth make it well suited for growth along river banks. The most important feature of cottonwood is its resistance to flood damage. During the 1993 floods in Missouri, mortality of cottonwood was low in areas that were under floodwaters for less than a month, and at least 97% of the large (DBH>20cm) cottonwoods survived even 250 days of flooding (Larsen, 2001, Personal communication). Therefore, cottonwood would seem to be a promising species for flood plain forestry practices, yielding complementary benefits of stabilized soil resources, soil quality improvement, and enhanced sustainability of crop production.

Knowledge of cottonwood growth in flood plains can be helpful in flood plain forest management. A better understanding of the functional-structural adaptations of the plants growing in a flood plain environment is important for the development of sustainable production systems. As a complementary tool for field experiments and measurement, computer-based tree growth simulation models are also used in designing field experiments and deriving conceptive experimental results. The research in this dissertation seeks to better understand and model the growth functioning of cottonwood in a flood plain with the LIGNUM modeling method. The functional-structural modeling approach LIGNUM has been used in the growth simulation of Scots pine (Perttunen *et*

al., 1998), jack pine (Lo *et al.*, 2001) and sugar maple (Perttunen *et al.*, 2001). Thus this adaptation of LIGNUM to cottonwood represents another extension of the LIGNUM model.

The goal of this dissertation was to simulate the growth of cottonwood in a flood plain area under a specific environment and varied stand spacing with the aid of computer technology. The study uses the LIGNUM modeling method to simulate the volume and biomass growth of cottonwood in the flood plain area of central Missouri. LIGNUM is a functional-structural tree growth modeling method initially developed in Finland and designed to simulate tree growth with computer technology. The growth model can be used to produce a quantitative assessment of cottonwood growth in a flood plain area, which in turn may be useful in evaluating the possibility of utilizing cottonwood stands as riparian buffers in flood plains.

1.3 Tree growth modeling

In the study of cottonwood growth, modeling is a conventional tool for examining the growth of cottonwood, understanding underlying biological growth hypotheses, and predicting tree growth. This growth modeling study includes two parts—examining the cottonwood growth data sets and simulating the tree growth.

What is a model?

A model can be used to represent real-world entities and processes either by an abstract or a physical entity (Kimmins, 1987). A good model can provide an accurate representation of certain properties of the entity or process under consideration. Encoded in a computer program, a model may become a valuable tool for understanding the properties and behavior of complex systems. A model can never represent the entire real

world entity with complete accuracy; but it can simulate many functions of interest to researchers. In forestry, models may be used to predict the future condition of a forest in relation to its present state, or the effects of particular treatments on a forest over time (Robinson and Ek, 2000).

Tree growth modeling

A tree growth model is designed to answer questions about how trees grow, how they are affected by environmental factors and management practices, as well as the kinds of products and profit potentials that may be derived from them. Both the structure and physiology of a tree are very complex. However, scientists have uncovered many relationships connecting tree structure and physiological processes with tree growth. Based on these relationships, modeling may be used to simulate tree growth and provide information of interest for scientists. Tree growth simulation models are designed to simulate the change of tree size in terms of volume and structure. Relevant information may include tree biomass, height, yield, canopy form, and other aspects. Such a model can also be used to simulate different plant growth environments in terms of, for example, variation in radiation levels, extent of fertilization or irrigation, etc., to predict and test plant growth patterns.

With the help of fast-calculating computers, tree growth modeling has evolved dramatically in recent years. Tree growth simulation is a powerful research method to construct, render, and study digital trees in their specific environments, while observing and controlling all stages of their development.

Tree growth models have a long history of describing whole-forest dynamics in the form of growth and yield tables (Robinson and Ek, 2000). Overall there are several

types of forest models, including gap models (Friend *et al.*, 1993; Nilson, 1971; Bugmann, 2001; Lindner *et al.*, 1997), growth and yield models (Stage, 1973; Stage *et al.*, 1998; Hamilton, 1991; Mitchell, 1975), and functional-structural models (Perttunen *et al.*, 1996, 1998, 2001; Sievänen *et al.*, 2000).

Functional-Structural Modeling and LIGNUM

Many computer-based tree growth simulation models focus on either physiological processes or crown structure development of a tree. Tree physiological processes take into account tree metabolism, energy flow, and biomass budget. Growth is derived from the carbon balance of physiological processes such as photosynthesis, respiration and resource allocation. Other processes such as nutrient cycling and water supply also affect tree growth. Tree structure involves tree branching patterns and branch development in space. The spatial tree structure determines the photon flux intercepted by the whole tree as well as carbohydrate distribution in growth allocation. Both physiological processes and spatial structure are important in tree growth and its modeling.

A tree growth model which includes both physiological and structural factors is called a *functional-structural tree model* (FSM). An FSM is designed to be capable of effectively integrating physiological processes of tree growth with tree morphology. A functional-structural tree model of particular interest here is the LIGNUM model (Perttunen *et al.*, 1996, 1998, 2001; Sievänen *et al.*, 2000). This specific research study will employ the LIGNUM modeling approach.

To simulate tree growth, the LIGNUM model starts from an initial bud. Bud derivation in the model constructs the spatial tree structure with branches in terms of

azimuth, angle and position. Based on the structural pattern, radiation interception is simulated in a radiation interception submodel, which leads to estimates of physiological processes such as photosynthesis, respiration, and growth allocation. The growth allocation submodel distributes net growth to the whole virtual tree in the form of diameter growth and length elongation, which results in structural development.

1.4 Objectives of this dissertation

The objective of this dissertation is to simulate cottonwood tree growth in a flood plain environment with the LIGNUM modeling method. LIGNUM has been designed to capture the three-dimensional structure of a tree species in simulating its growth and development in different environments. This project intends to examine the growth of the individual cottonwood tree in terms of both structure and physiology, and to simulate the growth of a stand plantation of cottonwood in the Missouri River flood plain area.

1.4.1 General objectives

The growth of the whole tree is determined by the development of and interaction among tree organs, including stem, branches, leaves, and roots. Models can be used to simulate tree growth in response to a variety of genetic and environmental factors. The general objective of this tree growth simulation project is to understand and explain the underlying functioning of cottonwood with respect to volume and biomass growth, to simulate the effects of flooding and weather conditions in central Missouri on cottonwood growth, and to assess the possibility of utilizing the cottonwood plantation in flood plain forestry.

1.4.2 Two specific objectives

Two specific objectives of this dissertation include individual tree growth simulation for cottonwood with the LIGNUM modeling method and the extended application of LIGNUM simulation from the individual tree to the cottonwood stand with variable spacing.

Individual cottonwood tree growth simulation

The first objective is to simulate individual cottonwood tree growth with the LIGNUM model. This model has been used to simulate the growth and yield of eastern cottonwood (*Populus deltoides* Bart. ex. Marsh.) in an open-growth environment. The relationships of different tree components and growth allocation have been described in the model. A parameter system specific to the cottonwood tree growing in central Missouri flood plain environment has been developed for the model. Several new developments in LIGNUM modelling for cottonwood are also incorporated into this model, including the use of real weather data and a biochemically derived photosynthesis model (Le Roux *et al.*, 1999; von Caemmerer and Farquhar, 1981). Different time steps for physiological processes and structure updates (Sievänen *et al.*, 2004), and utilized voxel space for estimating the interception of photon flux (Perttunen *et al.*, 2004) represent additional innovative features of this model.

Cottonwood stand simulation

The second objective of this study is to simulate cottonwood growth in a dense, short-rotation plantation stand. The interactions between adjacent trees and the effects on tree growth are studied. Cottonwood is a shade intolerant tree species (Cooper, 2002). Mutual shading in the stand will dramatically affect tree growth. The stand spacing and

its effects on tree growth and biomass production will also be examined.

Stand simulation can help to verify empirical tree growth research. Enhanced understanding of tree growth mechanisms can also help to improve empirical modeling research. Empirical models are based entirely on statistical assumptions derived from growth measurement data. The research on tree growth mechanisms and processes can provide reasonable biological interpretations for assumptions and parameters in the empirical models. The consistency between empirical modeling and functional-structural tree modeling will clearly lend confidence to modeling research.

1.5 Outline of dissertation

This dissertation describes and explains how the LIGNUM model may be applied to simulate the growth and yield of eastern cottonwood (*Populus deltoides* Bart. ex. Marsh.) in a wide-spaced, open growth plantation, and a dense, tight-spaced plantation. Several new developments in LIGNUM modelling are incorporated herein. The simulation of LIGNUM for a plantation stand is itself a new development in LIGNUM modelling.

The first part of the dissertation introduces this project. It describes the concept of a tree growth model and the purposes of such a model. The model LIGNUM, which is used in this project, is generally introduced. This part also identifies the significance of the LIGNUM method to tree growth modeling.

Part II is a literature review of past and current research on tree growth modeling. It considers some historical background of tree growth modeling as well as the classification of different types of tree growth models. Several well known modeling methods are introduced, and the advantages and disadvantages of these models are

compared.

The third part of the dissertation introduces the individual cottonwood growth model with LIGNUM. It includes sections on data collection and observation, methodology in terms of structural derivation and physiology of growth, new developments in LIGNUM, and results and discussion.

Part IV introduces the stand cottonwood growth model with LIGNUM. It includes sections on data collection and observation, methodology in terms of structural derivation and physiological growth, and results and discussion.

The final chapter of this dissertation makes conclusions on the developments on the individual model and stand model, and considers the significance of this research, as well as its implications for future studies.

2. LITERATURE REVIEW

During the long history of tree growth modeling, many kinds of models focusing on different modeling aspects have been developed. Different models are used for different purposes and have specific functions. Some models utilize statistical, empirical equations. Some are combined with fast calculating computer tools. Some models are designed to simulate individual tree growth, and some predict the output of forest production. Some models focus on a tree's physiological growth processes, while others focus on the structural pattern of the tree crown. Some models are adapted for practical forest management, while others are more likely to yield a research explanation for plant science. In summary, most modeling efforts reflect interests in wood production, environmental considerations, and tree growth understanding and explanation.

This chapter introduces the background in tree growth simulation. A variety of tree growth simulation models have been developed in forestry historically, from conventional empirical field experiments to advanced functional-structural models. After a brief look at short-rotation forestry with poplar species as the context for this research, the chapter describes these kinds of tree growth models and reviews several representative examples. The advantages and disadvantages of several functional-structural models are also compared.

2.1 Short-rotation forestry with poplar species

Poplars have been widely used in forest industries for timber and fiber

production. One of the most desirable aspects of poplar is its rapid growth that allows for a short rotation period. With the increasingly intensive utilization of forest land, the wood products industry is facing more and more economic and environmental pressures. It is imperative to develop sustainable wood production sources. Poplar and its hybrids have displayed the capacity for rapid biomass accretion (Anderson *et al.* 1983; Ranney *et al.* 1987; Ceulemans *et al.*, 1992). They are highly suitable for short-rotation forestry because of their high biomass production rates and rapid juvenile growth (Ceulemans *et al.*, 1992).

Short-rotation forestry "refers specifically to the unique practice of growing trees in evenly spaced rows on cultivated land much like an agricultural crop" (Christopherson *et al.* 1989). The primary goal of short rotation forestry is to "produce an optimum amount of woody biomass over as short period of time as possible, naturally with as low costs as possible" (Short Rotation Forestry Handbook, 1996). Short rotation forestry can produce high wood yield for particular end uses in a short period of time through intensive management (Short Rotation Forestry Handbook, 1996; the Minnesota Hybrid Research Cooperative [MHPRC, 1999]); diversify agriculture and forestry; as well as establish protection against wind and water erosion in a short period, and intercept nutrient runoff near streams, rivers and wetlands (MHPRC, 1999). Short rotation forestry has become more and more popular in countries such as Austria, Canada, Denmark, Italy, the Netherlands, Sweden, United Kingdom, USA, and Brazil (Short Rotation Forestry Handbook, 1996).

According to the Short Rotation Forestry Handbook (1996), poplars were chosen as the lead model genus for short rotation forestry; almost half of the research

effort of the Short Rotation Woody Crops Program has focused on poplar research. Foci of research in short rotation forestry include determining disease and insect risks, accurate costs, accurate productivity estimates, and other special challenges such as plantlet multiplication and weed control. Given its properties of quick growth and wood production, Eastern Cottonwood (*Populus deltoides*) is one of the best species for short rotation forestry.

2.2 Background of tree growth modeling

Tree growth involves the elongation of tree height, thickness of stem diameter, and extension of branches and leaves. Trees absorb solar energy mainly through leaf photosynthesis. The net CO₂ assimilation after subtracting respiration is transformed into biomass and contributes to tree growth throughout the tree, including its stem, leaves, and roots. Tree growth is closely related to tree physiology and tree architecture.

The purpose of tree growth modeling in forest research and management is to explain tree growth mechanisms, predict future tree growth, and answer questions regarding the effects of certain treatments on a forest over time.

There is a long history for forest models since forests have been managed (Robinson and Ek, 2000). Early models of whole-forest dynamics were mostly based on expert knowledge or historical statistics with an assumption of stable tree growth environments (Botkin, 1993). These empirical forest growth models had been used for more than a century in the forms of growth and yield tables (Robinson and Ek, 2000). Models that focus on the behavior of individual trees have continued to evolve steadily since the 1960s combining more additional modeling elements in biological theories and

environmental factors (Vanclay, 1995).

2.2.1 Modeling tools

With the development of tree growth modeling, more and more methods have been adopted in efforts to improve model efficiency and simplification. Most of these methods can be categorized into two groups.

Statistical equations

The early modeling methods were comprised mostly of sets of statistical equations. One popular example is the growth and yield table that simulates whole-forest production. A yield table is expressed in terms of total standing volume. It is a type of growth table which lists expected productivity or volumetric yield for a given age, site quality, forest density, and forest management regime. The statistical model is derived from sample data of tree measurements and is applied to a broader area with the same forest type and environment to predict forest yield.

Computer modeling

With the development of tree growth research, forest scientists discovered more and more rules about the internal physiological processes and morphological structure of trees. This knowledge has been applied within complex tree growth modeling procedures and used for further tree growth study. The implementation of complex models requires fast and precise calculations. Computer programming techniques and software are continuously being refined in the area of tree growth modeling.

2.2.2 Modeling hierarchy and application

According to Munro (1974) and Shifley (1990), models for forest ecosystems can be categorized into one of three types. The first type is the *whole stand model*, which focuses on and produces aggregate stand-level statistics. Whole stand models usually have some components that simulate forest dynamics in terms of growth and mortality. The second type is the *size-class model*, which treats trees similar in size or some other features as a group. Trees of the same species and size in diameter and height are placed in one group. The third type is the *individual-tree model*, which considers each tree as a unique entity. The individual tree model is used to simulate the relationships between organs in the tree, from roots to leaves. The above hierarchy results in a variety of methods for forest modeling.

The application of different models also varies. Some growth models, such as empirical equation models, are utilized as tools to provide information for forest management in forest industries. The empirical model derived from a set of sample data is assumed to be applicable to an entire area. However, it cannot be applied in other areas with different environments. Other growth models, such as the organ-based individual tree model, aim at producing basic explanations at the level of forestry science. Such modeling research is intended to improve our understanding of the processes and factors affecting forest and tree growth at a certain hierarchical level.

2.3 Representative examples of tree growth models

The most basic tree growth model utilized in forestry is the empirical model, which makes use of field data to create statistical descriptions and equations for tree

growth. Process-based models, which take into account the physiological processes of the tree, are more elaborate forest growth models. There are different kinds of such models depending on particular research questions and practical interests. The pipe model theory is a special tree physiological process theory that describes the relationship between tree sapwood and leaf foliage, as well as the diameter distribution and carbon allocation throughout the tree. Repeated iterations of tree branching lead to another type of tree model -- the morphological model. These models aim at a detailed description of the plant's structure and its development in space.

Different types of models provide different kinds of information and have advantages for different kinds of prediction problems. The selection of a model depends on the modeling purpose and the information needed. Each model has essential features and limitations. In order to overcome the latter, some modelers began to create hybrids of process-based and morphological models, creating what are called functional-structural models. Other hybrids are designed to combine features of the traditional empirical model and the physiological process model.

2.3.1 Empirical models

Empirical models, the first type of forest growth model developed, predict tree growth as a function of time and space (Robinson and Ek, 2000). Conventional empirical models are comprised of mathematical equations based on statistical assumptions. Time is an explanatory variable in a growth curve; it can be used to obtain the value of the variable under consideration (e.g., height) at the specific time by referring directly to the function (Robinson and Ek, 2000). Some measure of spacing is usually used to assess

competitive interactions among objects (Martin and Ek, 1984), either directly, as a collection of tree distances, or indirectly, e.g., as a local basal area. These models are statistical descriptions based on curve-fitting approaches (Botkin *et al.*, 1972). Empirical growth and yield models are usually developed from large amounts of field data to meet the needs of managers. They are best applied in practical forest management situations to predict or evaluate forest production in terms of basal area and wood volume.

A representative example of an empirical model is the Richards equation:

$y = a(1 - e^{-bt})^c$ (Richards, 1959; Pienaar and Turnbull, 1973; Robinson and Ek, 2000; Zeide, 2004). This equation can use a single variable (t) such as tree age to describe the development of a particular tree dimension y , such as tree diameter or height. This description does not consider any other factors related to growth and is highly artificial. However, this simple equation is straightforward and easy to apply in practice. Empirical growth models are usually effective in short-term applications in which no major change in environmental factors or management practices occur.

2.3.2 Pipe-Model theory

Shinozaki *et al.* (1964) developed the pipe-model theory by envisioning a tree as a bundle of unit pipes, each of which supplies a particular amount of leaf area with water. These authors found a direct correlation between the total cross-sectional area at any horizontal level and the leaf mass above that level. The amount of leaves existing above a certain horizontal level in a plant community is always proportional to the sum of the cross-sectional areas of the stems and branches at that level. The more leaves they support, the thicker the branch diameters.

As a result of the "Pipe Model Theory", the analysis of branching structure has shifted away from structural allometry (scaled physical measurements) toward vascular allometry (physiological measurements) (Aratsu, 1998).

2.3.3 Process-based models

Process-based models attempt to simulate tree or forest growth in terms of the underlying physiological processes that determine growth and the way a forest stand is affected by the physicochemical environment. A process-based model is a model of a system and its behavior at a given level of complexity, based on submodels of the constituent processes that together determine the behavior and responses of the system (Landsberg, 1986, 2003).

Process-based tree growth models are designed to track the particular processes that drive tree growth (Robinson and Ek, 2000). The growth of a tree is determined by the allocation of carbon, which is controlled by physiological processes such as photosynthesis, respiration, and the transport of carbohydrates. The excess of photosynthate after maintenance and growth-related respiration is stored in the plant body and can be transformed into energy for growth. Shading by neighboring trees reduces radiation interception and photosynthesis, which leads to the focal tree's self-pruning.

Process-based models have the potential to be far more flexible than models constructed directly from empirical relationships and can be used in a heuristic sense to evaluate the consequences of change and the likely effects of stimuli (Landsberg and Gower, 1997; Landsberg *et al.*, 2001). Contemporary process-based models can provide good estimates of growth and biomass productivity at various scales. Combined with

conventional models, they can provide information of the type required by managers and planners.

A number of process-based models have been developed to simulate tree growth based on physiological processes. These models can be classified into several categories. A stand growth model such as that developed by Mäkelä and Hari (1986) is based on individual tree growth; TREGRO (Weinstein and Yanai, 1994) is an individual tree growth model; BIOMASS (McMurtrie and Landsberg, 1992; Sampson and Allen, 1999) and 3-PG (Landsberg and Waring, 1997; Landsberg *et al.*, 2001) are stand-level models; and FOREST-BGC (Running and Gower, 1991; Running and Coughlan, 1988) is a regional forest ecosystem model.

Mäkelä and Hari's model

Early in 1986, Mäkelä and Hari described a stand growth model in which biomass production was determined by physiological processes. The stand model was based on individual tree growth. The individual tree model described the annual photosynthetic production and its allocation to different growth compartments. It used shaded photosynthetic radiation ratio rather than defining a competition index for photosynthetic production. The tree geometry was used in allocating growth. Canopy closure was represented in terms of maximum needle biomass. For all these phenomena, biological assumptions were applied to explain the physiological processes involved in tree growth.

FOREST-BGC

FOREST-BGC (Running and Coughlan, 1988; Running and Gower, 1991;

Hunt *et al.*, 1991) is an ecosystem process model that is designed to calculate the carbon, water and nitrogen cycles within a forest ecosystem. The ecosystem processes involved in FOREST-BGC include canopy interception and evaporation, transpiration, photosynthesis, growth and maintenance respiration (Running and Coughlan, 1988), carbon allocation above and below-ground, litterfall, decomposition and nitrogen mineralization (Running and Gower, 1991).

Leaf area index (LAI) is considered to be a critical variable in the model for calculating a variety of interrelated ecosystem processes. FOREST-BGC includes daily and yearly components. The daily component calculates the photosynthesis and maintenance respiration each day on the basis of incoming short-wave radiation, air temperature, dew point, and precipitation. The daily information including photosynthesis, evapotranspiration, and respiration is summed annually. The annual sum of photosynthesis and respiration serves as input to the yearly component of the model, which is concerned with tree respiration and growth allocation. Annual tree growth results are allocated to leaves, stem, and roots.

This model was used in 1984 to simulate the annual hydrologic balance and net primary production of a hypothetical forest stand in seven contrasting environments across North American (Running and Coughlan, 1988). A further development of FOREST-BGC focused on leaf/root/stem carbon allocation with stand water and nitrogen limitations (Running and Gower, 1991).

The FOREST-BGC simulation model has been tested with field measurements from the Oregon Transect Ecological Research project (OTTER). High correlations between predicted and measured data were found for aboveground NPP, stem biomass,

and average leaf nitrogen concentration (Running, 1994).

3-PG model

The Physiological Principles in Predicting Growth (3-PG) model (Landsberg and Waring, 1997; Landsberg *et al.*, 2001) is a combination of a process-based model and some empirical relationships from experiments and measurements, thereby enhancing the potential value of model results in practical forest management applications.

The model calculates total carbon fixed from utilized photosynthetically active radiation, obtained by correcting the photosynthetically active radiation absorbed by the forest canopy for the effects of soil drought, atmospheric vapour pressure deficits, and stand age. Gross primary production (P_G) is calculated as a linear function of photosynthetically active radiation (PAR) and canopy quantum efficiency. The latter is a conversion factor affected by atmospheric humidity, air temperature, water balance, and nutrition. In 3-PG model, the ratio of net primary production (P_N) to gross primary production (P_G) is relatively constant for trees (Landsberg and Waring, 1997). There is also a simple relationship that can be used to estimate the amount of carbon allocated below ground. The tree growth patterns and carbon allocation to foliage and stems are all determined by a procedure based on allometric ratios. Effects of nutrients, including that of soil fertility level on below-ground allocation, have also been incorporated in the model (Landsberg and Waring, 1997).

Korzukhin *et al.* (1996) concluded that process-based models are more likely to meet the information challenges presented by ecosystem management because they offer significant advantages over empirical models for increasing our understanding of and

ability to predict forest behavior. However, process-based models remain closely connected with empirical models. On the one hand, process-based models are based on measurable field data. Modeling hypotheses are derived from observation data. Such hypotheses are similar to the statistical assumptions in empirical models. In addition, some empirical models are derived from purely biological principles. Each parameter in such models has a process-based interpretation (Thornley, 1976; Thornley and Johnson, 1990). Mäkelä and Hari (1986) recognized the need to develop process-based growth and yield models simultaneously with more traditional statistical ones.

2.3.4 Structure-based models

In contrast to process-based models, morphological or structure-based models focus on the spatial architecture and branching pattern of a tree. Although the shape of a tree can be affected by environmental conditions, the canopy architecture is genetically determined. The genotype of a tree species determines characteristics of its branching pattern, including branching angle, branching arrangement, segment length, and the relative growth rate of terminal and lateral branches. Branch architecture in effect reflects an iterative pattern whereby branch structure is preserved among scales – *i.e.* similar structure is displayed in different branch orders. All of the known vascular plants can be classified into less than 30 architectural patterns according to simple morphological characteristics (Hallé *et al.*, 1978; Jaeger and De Reffye, 1992).

Morphological models focus primarily on representing spatial plant architecture and branching patterns (Prusinkiewicz and Hanan, 1989; Prusinkiewicz, 2001; Godin, 2000). They usually start from an algorithmic structural model and end with graphic

results. These models are used to describe tree structure via the application of morphological rules. Morphological models are in essence a formal way to represent three-dimensional branching structures of trees. Hallé *et al.* (1978) identified the basic concepts of architectural analysis to be the architectural model and reiteration. Honda (1971) demonstrated that complex crown shapes may be obtained using a limited number of geometric parameters and that plant architecture is very sensitive to changes in these parameters. Based on the regular branching patterns, many structural tree models adopt existing algorithms such as the Lindenmayer system (*L-system*) (Lindenmayer, 1976; Prusinkiewicz and Hanan, 1989), fractals (Oppenheimer, 1986; Hearn and Baker, 1994), specific branching processes (Kawaguchi, 1982; Aono and Kunii, 1984), or other mathematical models (Fisher, 1992; Jaeger *et al.*, 1992).

The Lindenmayer system (*L-system*) is the most widely used method for simulating plant architecture. The L-system was developed by Aristid Lindenmayer (1968, 1971) and was initially intended to describe the development of multicellular organisms. The L-system is a string-rewriting system. It contains sets of rules and symbols that simulate growth processes. It works well for growth that involves repetition of an identical simple process, such as branching.

Research on L-systems has focused on the question of what phenomena can be described with formal languages. The theory, tools, and applications that utilize an L-system framework for modelling plants and their environment have been developed by Prusinkiewicz (Prusinkiewicz and Hanan, 1989, 1992), Kurth (1994) and others (Hanan, 1988). Prusinkiewicz has developed an L-system-based modeling software package *L-studio/cpfg*, which utilizes Windows software for creating simulation models and

performing virtual experiments using L-systems. After defining the initial status of a tree, a set of derivation rules are used to develop the tree growth process from one status to another. The virtual tree is constructed through an iterated derivation process.

2.3.5 Functional-structural models

Among plant growth models, which range from simple to extremely complicated, physiological processes and structural morphology are two critical properties that must be accommodated. Both process-based models (PBMs) and morphological modeling approaches have advantages and limitations. The PBMs do not have reference to the three-dimensional crown structure, which can affect radiation interception and growth allocation. Morphological models, on the other hand, are limited in their capacity for describing tree functions. These two basic approaches are, however, to a certain degree complementary and can be combined into a better modeling approach by reducing the limitations of each. Such combined models make up what is called *functional-structural tree modelling* (FSM) [Sievänen *et al.*, 2000]. The functional-structural tree models bridge the gap between PBMs and tree architecture models by depicting an accurate 3-D perspective of plants as an aid to analyzing plant behavior.

“Computational plant models or ‘virtual plants’ are increasingly seen as useful tools for comprehending complex relationships between gene function, plant physiology, plant development, and the resulting plant form” (Prusinkiewicz, 2004). The 3-D computer tree growth model is a digitized simulation system that can be constructed without restrictions as to season or weather conditions. Such a model can also be

duplicated, parameter-modified, and mechanism-improved for analysis relatively more easily than is the case with field experiments. Computer modeling allows to scientists to make virtual recreations of trees and their growth processes.

Most computer models represent a plant as a collection of elementary units such as bud, leaf, internode, branching point, and stem segment (Perttunen *et al.*, 1996; Rauscher *et al.*, 1990; Godin *et al.*, 1999). Such models are designed to integrate the activities of elementary units as they contribute to the functioning of the whole plant. Both morphological structure and physiological processes can be included in the same model. Computer models also have the obvious advantages of enhanced computational speed, the ability to employ a wide range of mathematical techniques, and potential utility in developing programming tools.

LIGNUM

LIGNUM (Perttunen *et al.*, 1996, 1998, 2001; Sievänen *et al.*, 2000) is a tree model developed by researchers at the Finnish Forest Research Institute, the University of Helsinki and the Helsinki University of Technology. LIGNUM is designed to capture the three-dimensional structure of a tree species and at the same time to model its growth and development. The model combines both process-based and morphological modeling approaches for tree growth simulation.

LIGNUM was first parameterized for young Scots pine growing in southern Finland (Perttunen *et al.*, 1996, 1998). The underlying modeling hypothesis is that general tree growth concepts, including the pipe model theory, architectural growth rules, physiological processes, and carbon allocation mechanisms, are applicable to all tree species (Perttunen *et al.*, 2001). Lo *et al.* (2001) developed the LIGNUM application for

jack pine simulation. LIGNUM has also been applied to broad-leaved tree species, including sugar maple (Perttunen *et al.*, 2001). This study defined the basic model structure for broad-leaved trees and provided strong evidence that the structural description used in LIGNUM is general enough to be applied to broad-leaved species. The cottonwood simulation in this study represents the adaptation of the LIGNUM model to another deciduous tree species.

The key to integrating morphological and process-based models is to consider the tree in terms of suitable units and use them to model both metabolism and spatial structure (Perttunen *et al.*, 1996). The LIGNUM model treats a tree as a collection of a large number of simple units that correspond to organs in a real tree (Perttunen *et al.*, 1998). Sievänen *et al.* (2000) called these structural modules *idealized elementary units* (IEU) and noted that they are a common feature of functional-structural models. Four structural modules similar to real world counterparts are used to represent the above-ground part of a tree: *tree segment*, *bud*, *axis* and *branching point* (Figure 1). These may also be referred to as tree compartments.

The *tree segment* and *bud* (Perttunen *et al.*, 1996, 1998, 2001) are basic units in both the tree and the model. The unit *bud* is an embryonic shoot, the growing point of the tree from which new shoots, leaves and flowers may develop. The *tree segment* is the section between two branching points to which the leaves (for broad-leaved trees) are attached. A *leaf* consists of a petiole connecting to a tree segment and bearing a leaf blade. All metabolic functions are modeled at the segment or bud level (Perttunen *et al.*, 2001). The *axis* and *branching point* are aggregate units each consisting of a number of sub-units. A branching point occurs where one or more tree segments joint together.

There is no actual organ in the real tree corresponding to a branching point; it is used to simplify the growth modeling process in connecting tree segments to one another. An axis is a sequence of tree segments and branching points terminating in a bud. A tree is the special axis that includes all compartments of the tree.

These units within the model tree are organized into a list structure. This in turn facilitates computer programming for simulating tree growth by operating the list collection (Perttunen *et al.*, 2001). The root system in LIGNUM is modeled with only one parameter denoting its mass (Perttunen *et al.*, 2001).

These units or compartments represent both physiological and structural attributes of the above-ground part of a tree. Based on these compartmental units, the model describes the three dimensional structure of the tree crown and determines the growth allocation in terms of the metabolism taking place in these units. The physiological processes can also be explicitly related to the tree structures in which they are taking place.

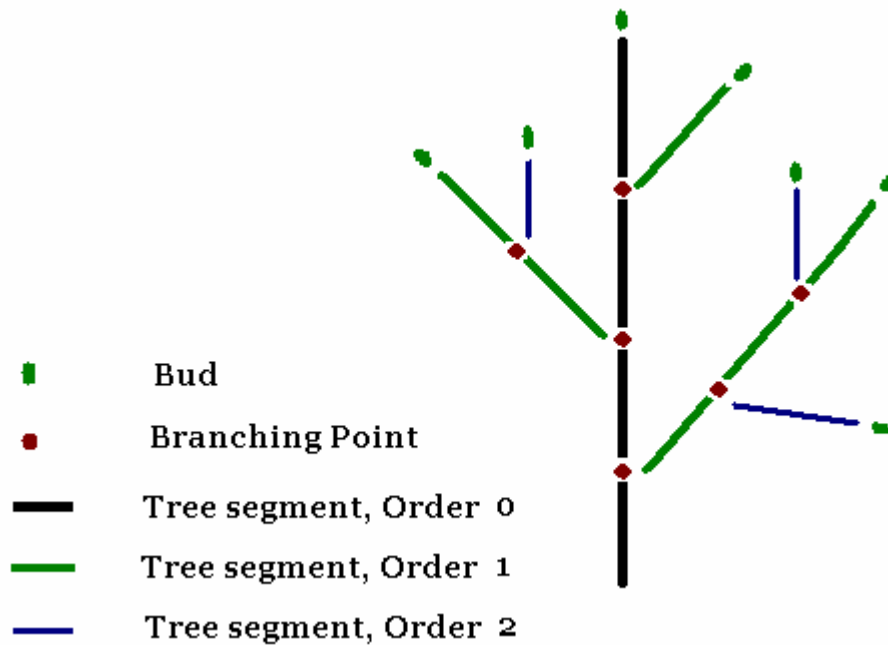


Figure 1. Basic units in LIGNUM modeling: An axis is a sequence of tree segments and branching points, terminating with a bud. A branching point may include one or more axes.



Figure 2. Bud derivation in LIGNUM. In the first derivation, the bud develops into a segment, a young lateral leaf emanating from the branching point, and a tip bud. The new tip bud develops into a segment, a young lateral leaf, and a tip bud in the second step. The first young lateral leaf develops into a mature leaf.

The L-system is applied to develop tree branching structure with these idealized elementary units. The bud is the most active unit in LIGNUM modeling. It determines the tree's structural development and branching pattern (Figure 2).

The growth of the four tree compartments is based on several rules in the model. The development of a new tree compartment begins with a bud, which emerges from a branching point. The rule sequence for tree development may be described as:

$$\begin{array}{l} B \longrightarrow TS [BP] B \\ BP \longrightarrow B \end{array}$$

where B is a *bud*, BP denotes a *branching point*, and TS is a *tree segment*. The list -- TS[BP]B -- derived from B is called an *axis* and denoted as A. The square bracket means a new sub-axis begins at the left bracket and ends with the right bracket. These two rules establish that a bud will develop into an *axis* containing a *tree segment*, a *branching point*, and an ending *bud*. The branching point itself contains a new *bud*.

Based on the above derivation rules, the development of a bud after two derivations may be expressed as (Figure 2):

$$\begin{array}{c} B \\ TS [BP] B \\ TS [B] B \\ TS [TS [BP] B] TS [BP] B \end{array}$$

A pair of square brackets contains a sub-order axis. The sequence of tree compartments is grouped into lists as axes. Every list is an axis consisting of tree segments, branching points and buds. LIGNUM uses a two-way list (*or* double-link list) as the list structure (Perttunen *et al.*, 1996). Every tree compartment in the list is connected to both the preceding and following element. There is a first element and a last element. The

two-way list enables the model to implement all operations efficiently.

Based on this structural derivation, the LIGNUM model calculates the shading relationships between tree compartments within the 3D structure and computes the annual interception of solar irradiance by each compartment. Intercepted irradiance is used in estimating leaf photosynthesis, and net primary production (NPP) is obtained by deducting the respiration losses in each tree compartment from the whole tree photosynthesis. Carbon allocation within the tree is estimated following the pipe model principles (Shinozaki *et al.*, 1964), i.e., according to the relationships between the growth of foliage and water-conducting and supporting organs -- branches and stem -- needed to support it. Tree structure is updated according to the carbon allocation.

The LIGNUM model simulates tree growth and development with an annual time step using the four modular units. The available photosynthetic products drive the annual growth of the tree after accounting for respiration losses. The tree structure affects radiation interception and the photosynthetic rate. The allocation of photosynthates is controlled by physiological processes, according to the pipe model theory (Shinozaki *et al.*, 1964a, 1964b; Perttunen *et al.*, 1996) and the branching rules.

The model is programmed using the C++ language. It has a tree compartment template which serves as a basis for development of a class representing each structural component: *TreeSegment* class, *Bud* class, *BranchingPoint* class, *Axis* class and *Tree* class. The program treats the tree as a collection of lists that constitute these classes. The tree as a whole is an aggregate list consisting of all other lists and tree compartments. Based on these lists, the program simulates physiological processes with recursion. LIGNUM uses functions to simulate the tree's physiological processes and every

function is applied to each idealized elementary unit by means of four algorithms that traverse the tree compartment lists.

ECOPHYS

ECOPHYS (Rauscher *et al.*, 1990; Host *et al.*, 1990) is a functional-structural model for poplar. It simulates the whole-tree growth of young *Populus* trees by integrating physiological processes and morphological structure of tree canopies.

The purposes of the ECOPHYS model include the study the physiological factors that influence the growth of *Populus*, evaluation of clones for intensive culture practice, simulating the growth of poplars under different growth environments with varied irradiance or temperature, testing basic concepts of plant physiology, improving the predictive understanding of tree growth, and providing a framework for integrating observations into ecophysiological theory (Rauscher *et al.*, 1990; Host *et al.*, 1990).

The model incorporates the processes of photosynthesis, respiration, photosynthate (PSYN) distribution, and growth allocation (Rauscher *et al.*, 1990). The basic operational unit in ECOPHYS is an individual leaf in the tree; the leaf is the major receptor of environmental variables and the regulator of plant response to these variables (Dickson *et al.*, 1991).

The input variables for the ECOPHYS model include nutrients, solar radiation, precipitation, and soil water data. There are sub-models for photosynthetic production, nutrient transport, soil water movement and uptake, respiration, and leaf shading (Wu, 1999).

There are four primary modules in ECOPHYS that govern poplar growth

simulation (Rauscher *et al.*, 1990). These include the radiation interception submodel, the photosynthetic production submodel, the photosynthate allocation submodel (growth allocation), and the dry matter production and dimensional growth submodel. Several supporting modules are also used to modify physiological, environmental, and simulation parameters.

For the radiation interception submodel, the quantities of direct and diffuse solar radiation received by a leaf are calculated based on solar altitude and azimuth and the leaf shading patterns. The latter are determined geometrically by projecting each leaf in a three-dimensional coordinate system and determining the area of each leaf that is shaded by other leaves.

Whole-tree photosynthetic production is the principal driving variable for growth. It is a function of irradiance, temperature, leaf area, and parameters of the photosynthesis/radiation response model (Rauscher *et al.*, 1990). It is calculated in the photosynthetic production submodel by a leaf-specific photosynthesis function based on leaf radiation interception.

In the third module, photosynthates (PSYN) are accumulated and diminished by the leaf maintenance respiration. The remaining PSYN is allocated throughout the tree based on experimentally derived transport coefficients. The photosynthate transport coefficients used by ECOPHYS were determined by ^{14}C tracer studies in controlled environments and also in the field (Dickson, 1986; Isebrands and Nelson, 1983; Larson, 1977). Photosynthates may be transported upward to other leaves or up stem internodes, or downward to lower stems, the original hardwood cutting before planting, and the roots. Newly-emerged leaves retain all of their photosynthates, while expanding leaves

transport most of their photosynthates upward to stem internodes. Mature leaves transport most of their photosynthates downward to stem internodes, hardwood cutting, and roots. Transported photosynthates are ultimately used for maintenance and growth respiration, and converted to structural biomass.

The last submodel is dry mass production and dimensional growth. This is used to convert net CO₂ assimilation to overall biomass increase of the tree. The increased biomass is then converted into volume increment in line with the wood density of cottonwood.

AMAP

The plant modeling program AMAP (Reffye *et al.*, 1995; Reffye *et al.*, 1997; Godin *et al.*, 1999) has been developed in the International Center of Agronomic Research for Development (CIRAD), France. The program begins with analysis of plant architecture and adds physiological concepts into a dynamic tree simulation process. In order to construct plant architecture and study tree growth, a software package was developed to record the detailed tree structure data and to reconstruct a 3D virtual plant.

The software package *AMAPmod* is utilized in plant architecture analysis (Godin *et al.*, 1997) to support plant modeling. *AMAPmod* provides users with a methodology and corresponding set of tools to measure plants, create databases, and analyze information extracted from these databases (Godin *et al.*, 1999). Two components included in *AMAPmod* are structural database and a query-language (AML) (Godin *et al.*, 1997).

AMAPmod adopts a multiscale tree graph (MTG) to construct the topology of tree architecture at different scales, from tree scale, axis scale, growth unit scale, to internode scale (Godin *et al.*, 1997; Godin and Caraglio, 1998). The multiscale nature of MTG results from the decomposition of the plant into larger or smaller components. MTGs are suitable for representing plant topology with respect to scale and time. At a given scale, topology expresses succession and branching relationships between plant components with a directed graph, which includes vertices and edges. Vertices represent botanical entities and edges correspond to physical connections among these entities (Godin *et al.*, 1997). The *AMAPmod* package also combines “the multiscale tree graph (MTG) approach and 3D digitizing to allow for explicit identification of the relationships between multiscale topology and geometry” (Godin *et al.*, 1999).

Based on three-dimensional architectural plant models, a numeric radiation model is applied to describe the radiation budgets of individual plant parts and entire plants within each virtual scenario (Mialet-Serra *et al.*, 2001). Other physiological processes, such as water cycle, are also embedded in the architectural plant model (Reffye *et al.*, 1997). The plant is depicted as a serial connection of vegetative organs, which conduct water from roots to leaves. The growth cycle of the plant includes three steps: production of new growth units by the buds; transport of water in the hydraulic structure; and production and allocation of photosynthates within the plant (Reffye *et al.*, 1997).

MAESTRO

MAESTRO (Wang and Jarvis, 1990a; Wang *et al.*, 1995) is an array model that is used to predict the spatial distribution of radiation, photosynthesis, and transpiration for

individual tree crowns in a stand and for the whole stand. Hourly average solar azimuth and zenith angles, latitude and longitude are used to calculate radiation interception. Tree crown structure is defined in terms of spatial distribution, inclination and orientation of all tree compartments and their geometric properties. The tree compartments include leaves, twigs, branches, and trunk. The simulation models use four structural properties: crown shape, total leaf area and spatial distribution of leaves within the tree crown, and the leaf inclination angle distribution (Wang and Jarvis, 1990b). Using the simulated radiation environment, MAESTRO calculates the photosynthesis, transpiration, and evaporation of intercepted water within the crown of a single target tree. The model is especially suited to pure, wide-spaced stands. Results are of interest to plant physiologists, micrometeorologists and forest managers.

Advantages and disadvantages of current FSMs

As functional-structural models, ECOPHYS, AMAP, and LIGNUM have many properties in common. All of these models incorporate structural dynamics and physiological processes related to tree growth. They use leaf photosynthates to drive tree growth and assess the impacts of environmental stresses on growth. They produce an interactive graphical display of the tree so that the user can view the tree growth and examine the tree simulation. Each model also addresses model validation questions by comparing predicted data to field measurements.

The three modeling approaches also exhibit a number of differences. In ECOPHYS leaves are the primary modeling unit, with each individual leaf of the tree included in the model. The model accumulates the photosynthetic production from every individual leaf and uses the PSYN as the currency of tree growth. Based on the processes

of photosynthesis, respiration, and photosynthate distribution and growth, the PSYN accumulated by leaves is consumed or allocated among all tree components. The simulation of PSYN for all individual leaves is a large and time consuming task. Because of this, the ECOPHYS model is only used for juvenile poplar under near-optimal conditions (Rauscher *et al.*, 1990). In addition, the model does not describe root growth.

The AMAP model primarily uses *AMAPmod* database to describe tree architecture. Although more and more physiological processes are added into the model, the primary focus still remains on tree structure. Some other limitations of AMAP modeling include the large amount of field work needed to understand and measure the architectural development of more complex species. Moreover, the model requires a large amount of computer time (Reffye *et al.*, 1997).

While the ECOPHYS model is a growth model applied to juvenile poplar clones, the LIGNUM model is intended to be a general model. LIGNUM simulates tree growth through four idealized elementary units. These modular units describe structural features of the tree crown and key physiological processes. With these units, the total photosynthetic production of all leaves is simulated with a one-year time step. LIGNUM uses the pipe model theory (Perttunen *et al.*, 1996) to determine the growth allocation in each tree component based on these units. The usage of modular units in tree growth simulation increases the modeling flexibility and dramatically reduces the modeling calculation requirements. Moreover, the LIGNUM model can also be used for simulating the growth of root systems.

In summary, these three models use different theories for tree growth and have different modeling emphases. ECOPHYS focuses on physiological processes and AMAP

primarily on tree architecture. The LIGNUM model attempts to combine physiological process with tree architecture.

The advantages of the LIGNUM model for tree growth simulation are:

1) The combination of a process-based model with a tree architecture model can remove or at least reduce the limitations of both modeling approaches.

2) LIGNUM uses simple tree units to simulate the actual tree organs in a natural way, including 3D architecture and interactions. It is an extension of existing methods of modeling plant growth and development and is expected to have applications to plant modeling in the future.

3) The elementary units simplify computation, thereby avoiding the large computing requirements that have accompanied other approaches.

4) The rule-based modeling method makes full use of existing tree growth theories.

5) The model has the flexibility for producing concise or detailed descriptions of a tree if necessary.

6) LIGNUM represents an approach developed to be a general modeling tool. It can be adapted to several tree species.

3. INDIVIDUAL TREE GROWTH MODEL

As an individual tree growth simulation model, LIGNUM is designed to simulate the growth relationships between organs within a tree, from the uppermost leaves to the lower root system. The model has been developed primarily to enhance understanding of mechanisms underlying tree growth and a tree's response to different growing environments. It is used to explore the relationship of physiological processes within the tree to the tree crown structure, and overall growth. Cottonwood growth simulation is one of new applications of the LIGNUM model.

3.1 New application of LIGNUM to cottonwood growth

LIGNUM is a ruled-based, individual tree growth model. A desirable feature of a ruled-based model is its modular structure, which is conducive to generality and can be easily redefined for parameters and model equations. The simulation of cottonwood represents an application of broadleaf species simulation with LIGNUM in a central Missouri environment. In this study, the general framework of the LIGNUM model is adapted to the simulation of cottonwood. There are basically two major adaptations taking place in the cottonwood simulation – module improvements and parameters adaptation.

Changes in parameters intend to better reflect the specific growth habits of this species. Three major parameter sets changed in the model include tree structural parameters, growth allocation parameters, and photosynthetic parameters. Tree crown structure is a factor affecting the interception of solar radiation. Photosynthetic

parameters are used to affect photosynthetic production. Growth allocation parameters determine the structural output of simulation. Changes in these parameters will affect total photosynthetic production and biomass accumulation correspondingly. Because of variation in this species' genotype and phenotype, adaptation of LIGNUM to cottonwood growth simulation requires that several innovations be incorporated in the LIGNUM methodology. Module improvements in cottonwood simulation include real photon flux data input, the shorter modeling time step, the submodel for solar energy interception, the photosynthesis submodel, and respiration and growth allocation rules.

The application of the LIGNUM model in simulating the growth and yield of eastern cottonwood (*Populus deltoides* Bart. ex. Marsh.) in a wide-spaced agroforestry plantation system and a dense short-rotation plantation represent further extensions of LIGNUM development.

3.2 Cottonwood modeling with LIGNUM

The simulation of cottonwood tree growth is expressed in the form of structure derivation and biomass allocation. The tree growth process consists of two components – the L-system and LIGNUM system. L-system is a set of rewritable rules that are used to construct and derive tree structure. Structure derivation constructs the structural frame of the tree, including branching pattern, number of segments, and leaf distribution. The LIGNUM system allocates the tree's net growth to each part of the tree. A given segment is thickened in diameter and elongated in length as a result of biomass allocation. The size of individual leaves increases with time.

3.2.1 General model structure

Tree growth

Tree growth is the result of carbon allocation in each part of the tree. The dimensions of tree growth include the extension of tree height, the expansion of stem diameter, the development of roots, and the increase of total tree volume and biomass.

Biomass increment of cottonwood is determined as the difference between the net carbon assimilation by leaves and tree respiration in the stem and branches:

$$G(\text{growth}) = P(\text{photosynthesis}) - M(\text{respiration}) \quad (\text{E } 1)$$

Carbon is used as the currency of energy flow in the program. Photon flux interception in each part of the tree is calculated with self-shading among tree compartments. The adopted photosynthesis submodel in LIGNUM calculates the net CO₂ assimilation, which is the total leaf photosynthesis minus leaf respiration. Net CO₂ assimilation is summed from all leaves in the entire tree. The accumulated net carbon assimilation after subtracting the total maintenance respiration of woody part is the carbon available for tree growth. The net carbon is then allocated to tree parts all over the tree in the form of segment elongation and stem diameter increase. Growth respiration that is assumed to be proportional to biomass production is subtracted to calculate net increase in tree size. Tree growth leads to a change in tree structure, which in turn affects radiation interception in next growth cycle.

Modeling structure diagrams

The *modeling time step* is the time period for an individual cycle of the process being modeled. Although an annual time step is a ubiquitous selection to match with the

natural tree growth cycle, cottonwood growth simulation uses a shorter time step to simulate the interception of photon flux and tree growth more precisely. The cottonwood simulation applies three nested time steps in tree growth simulation: an annual time step, a structural time step, and a physiological time step.

The annual time step matches the natural annual cycle of tree growth. The median structural time step is used to capture the structural developments in cottonwood growth. In the flow of the entire model, canopy structure is updated from time to time so that its changing effects on photosynthetic photon flux density, photosynthetic production and tree growth may be captured. The physiological time step is even shorter than the structural time step and is explained in detail in section 3.2.2.

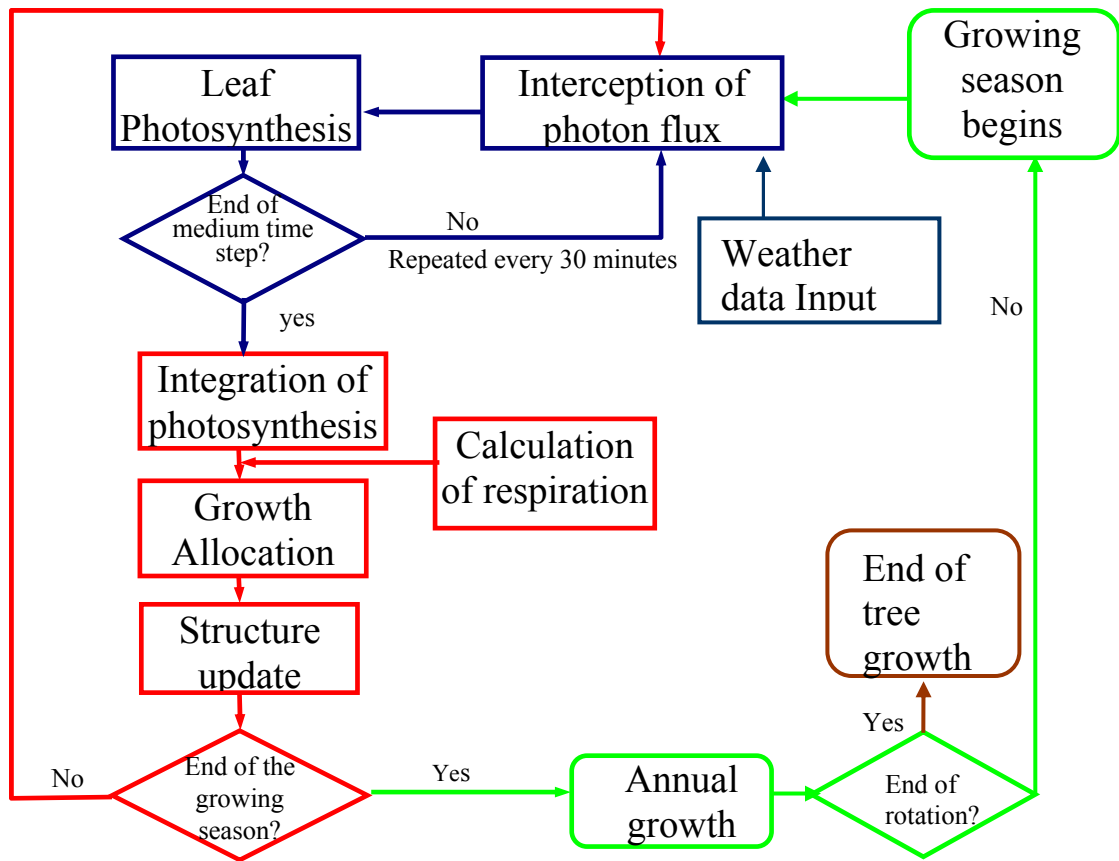


Figure 3. General modeling structure for individual tree growth with LIGNUM. The inner loop is the photosynthesis cycle repeated every 30 minutes. The intermediate loop is the structure update cycle with a longer interval, called structural update time step or medium time step. The outermost loop is the growing season cycle.

Figure 3 shows the three nested loops in the modeling procedure. The green cycle is the annual growing season time step, and the red cycle is structural time step for structure update. The blue cycle represents the physiological time step for interception of photon flux and photosynthesis

The inner physiological loop collects the intercepted photon flux and photosynthesis every 30 minutes and sums up total photosynthesis for use in subsequent structure updates. The middle structural loop integrates the net CO₂ assimilation from the inner loop to obtain the net growth of biomass after subtracting for respiration. The net growth of biomass is allocated into each part of the tree and updates the tree structure. The structure update is implemented several times each year rather than annually. The outer loop encompasses all these procedures within the annual growth cycle.

In the short time step simulation, annual tree growth and structure updates are accomplished several times in one growing season. The growth of cottonwood begins from each active bud. Each bud could develop into a new branch, which would include several segments and branching points. Each branching point carries one lateral bud, which creates a leaf and may lead to further branch development. New leaves emerge from branch tips one by one with their supporting segments. Older leaves grow in size in the process of maturation. Naturally, the derivation of segments and leaf development are part of a continuous process resulting in tree growth. However, the simulation model artificially separates this continuous process into several phases.

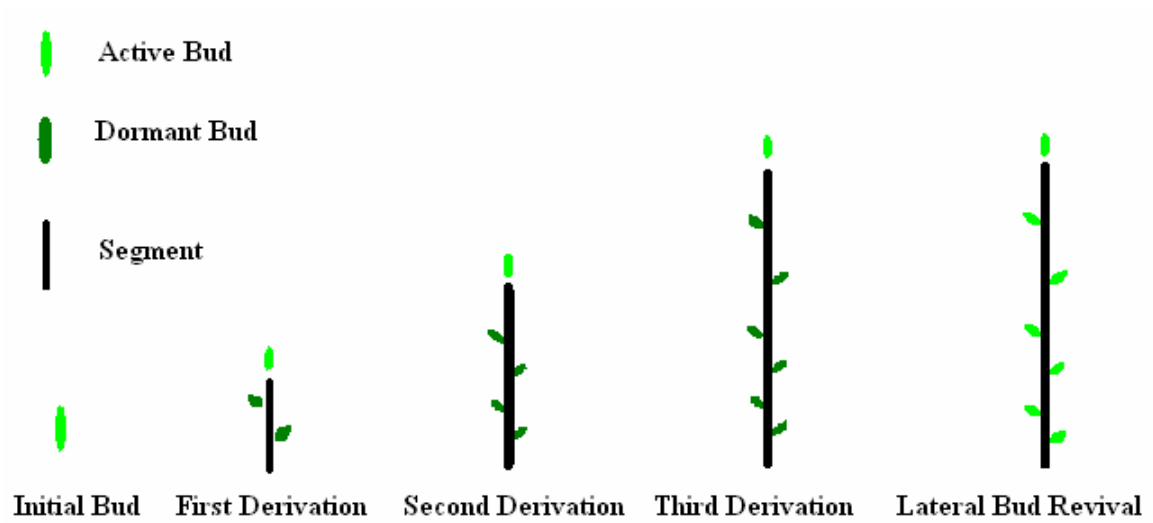


Figure 4. Segment and leaf derivation in LIGNUM. The continuous process of branch derivation is arbitrarily separated into four steps. All lateral buds are set as dormant until the beginning of the next growing season.

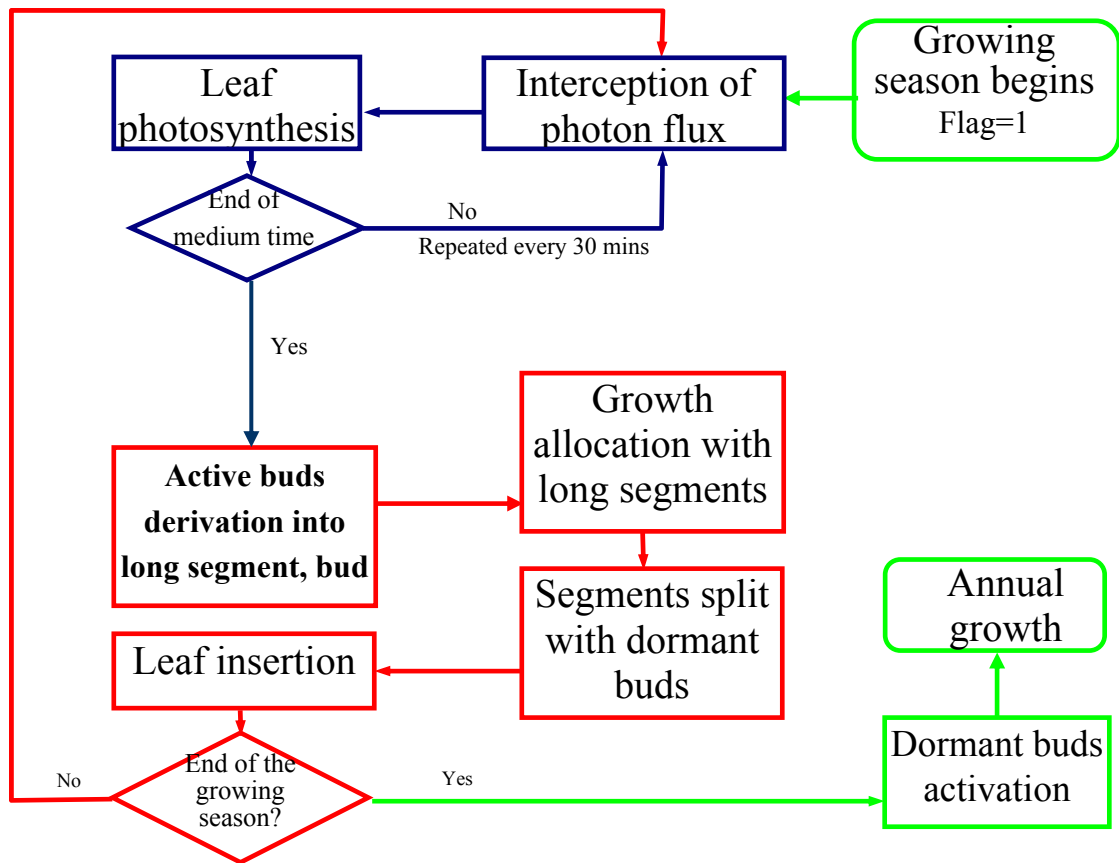


Figure 5. Segment and leaf development diagram in individual cottonwood growth. Branch derivation includes an expansion step and a split step. Lateral buds from segment split are dormant and would be reactivated at the beginning of next growing season.

During a single growing season, only the top bud of each branch is set as active and serves as the basis for deriving a new segment in the next step. All other lateral buds are set as dormant with respect to bud derivation. These dormant buds do not become active until the beginning of next growing season (Figure 4; Figure 5). All buds, both active and dormant, create new leaves each time buds are created. These leaves play an important role in photon flux interception and photosynthesis for the tree. All leaves are shed at the end of the growing season.

During tree growth, two steps are used in structure derivation in both LIGNUM system and L-system. The first step is “expand”, in which active buds expand into new segments and new buds. Although each bud may generate several segments and buds in each structural derivation, there is only one long segment and one top bud derived in the first L-system derivation. This long segment is used in growth allocation for both length elongation and diameter thickness. The second step is “split”, in which the long segment is divided into several short segments and new lateral buds according to the branching pattern of the particular species being modeled (Figure 6). The resultant length elongation and diameter thickness of the long segment depend upon the available net CO₂ assimilation. The number of new segments in “split” is determined by the branch length elongation. This process is repeated in the next time step at the tip of the branch. All leaves have the potential to develop a new branch in next growing season.

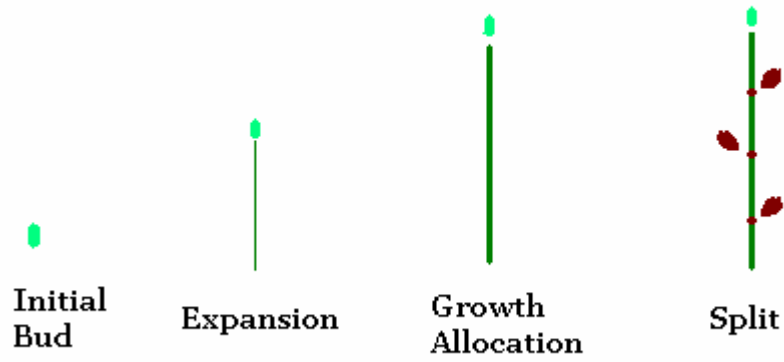


Figure 6. Segment split in LIGNUM model. In structural derivation , a long segment and a new bud are developed from an active bud. This long segment is used in growth allocation in terms of length elongation and diameter increment. The long segment is split into several short segments and new lateral buds.

Both “expand” and “split” are included in the structure derivation via L-system. Growth calculation and allocation are modeled within the LIGNUM system. Thus there must be frequent communication between LIGNUM and L-system as key drivers of the overall modeling process. Further details on the communication between LIGNUM and L-system are discussed in section 3.2.7.

3.2.2 Short time step simulation

The modeling time step is the time period of the particular process cycle that is being modeled. Cottonwood is a fast-growing species, and the annual time step may ignore some growth details and structural changes within the growth cycle. Thus, a shorter time step for modeling structural development was employed in this study for simulating cottonwood. Instead of accumulating the total net CO₂ assimilation and making an annual growth allocation, modeling processes, such as simulate interception of photon flux, growth allocation, and structure update, are implemented several times a year. This model calculates and allocates net primary production (NPP) into tree compartments and updates tree structure in a cycle of weeks rather than yearly. There are three different length time steps nested in the cottonwood growth simulation model.

The annual time step mimics the natural annual cycle of tree growth. The tree intercepts photon flux with segments and leaves in tree crown. The photons absorbed in the leaves are converted into energy in the photosynthesis submodel. Net carbon assimilation after respiration is then allocated to each part of the tree. The tree structure is updated with tree growth and all leaves are shed in the winter.

In the overall model configuration, the canopy structure is updated periodically

so that it may affect photon flux density within the tree crown structure, as well as photosynthetic production and tree growth. Tree structure is updated several times during a single growing season. The structural time step is a fraction of the annual cycle. The length of this time step is selected so that canopy expansion during the time period is detectable in modeling structural update. These more frequent structural updates can capture the important structural changes. At the same time, the structural time step is long enough to simplify the model calculations.

The physiological time step is even shorter than the structural time step. Physiological processes, including interception of photon flux and leaf photosynthesis, are affected not only by tree structure but also by the radiation environment. When real weather data is utilized in cottonwood simulation, photon flux interception and leaf photosynthesis are calculated in the model every 30 minutes under the variable photosynthetic photon flux density affected by solar position and cloudiness. The interception of photon flux is calculated applying a voxel space model. Photosynthesis and respiration are calculated in terms of intercepted photon flux and biomass, respectively. Real-time calculation of photon flux interception and photosynthesis enable simulation results to reflect the real growth. The length of physiological time step is selected so that there will be a photosynthetically important change in unshaded photon flux density. The net CO₂ assimilation is accumulated and allocated into tree growth and structure update in the structural update step.

The determination of time steps for physiological processes (a fraction of a day) and structural update (a fraction of the growing season) consider both computational efficiency and accuracy in addition to biological criteria.

3.2.3 Photon flux interception in the tree

In this cottonwood simulation study, real weather data were used as the input for the model. The weather data include photon flux density and air temperature (T_a) recorded every ten minutes according to real solar time (RST) at the field site of the two model systems simulated (New Franklin, Missouri, USA 39°1' N, 92°46' W, 197m altitude). The measured photosynthetic photon flux densities were divided into diffuse (Q_d) and direct (Q_b) components using the relationship between measured and potential global radiation (Nygren *et al.*, 1996; Weiss and Norman, 1985). The direct component is the photon flux from sun that passes directly through the atmosphere without any scattering. Solar position defines the direction of the direct photon flux. The diffuse component is the photon flux scattered in the atmosphere due to contact with aerosols such as dust and water vapor. An object on the ground receives diffuse flux from all directions of the visible hemisphere, but the relative importance of different sky regions depends on local and temporal atmospheric conditions. Both direct and diffuse photon fluxes were used to model photosynthesis in the LIGNUM cottonwood simulation.

In order to simulate tree growth in response to photon flux, the distribution of photon flux in the whole sky is set in LIGNUM by means of the Firmament submodel (Perttunen *et al.*, 1996; 1998; 2001). Photosynthetic photon flux density is divided into several sectors according to a standard overcast distribution (Ross, 1981) [Figure 7]. The Firmament submodel deals with direct and diffuse fluxes separately.

With the standard overcast distribution (Figure 7), the upper hemisphere is divided into several sectors in both horizontal and vertical directions. These sectors are

divided so as to have as equal solid angle as possible. Both the number of inclinations and the number of azimuth can be set in the model. Let N_i denote the number of divisions in vertical inclination and N_a the number of divisions in horizontal azimuth. The number of the azimuth (N_a) defined in the model is the mean number of sectors contained within the inclination zones. There is a zenith sector at the top of the hemisphere with its direction pointing directly upward. The total number of sectors in the hemisphere is equal to $(N_i \times N_a + 1)$. The total area of the upper hemisphere is 2π ; thus the area of the zenith sector is equal to $2\pi / (N_i \times N_a + 1)$. The width of the inclination zone is equal to $(\pi/2 - \text{angle of zenith segment}) / N_i$. The width of sectors in the same azimuth is the same, and there are different numbers of sectors at each inclination level. Figure 7 presents a sketch of sector positions in the standard overcast distribution.

The diffuse flux in each sector from the sky is distributed according to the zonal brightness of the standard overcast (Ross, 1981):

$$d_{(inc)} = \frac{(6/7) (1 + 2 \sin(inc))}{2\pi} \quad (E 2)$$

where inc is the elevation of the sector positioned in the sky hemisphere, and $d(inc)$ is the fraction of diffuse flux from sector inc out of the total diffuse flux received by the sphere. According to the equation, the brightness for each sector is determined exclusively by the sector inclination. The amount of solar photon flux received by each sector increases with the increase of its altitude position. The equation of $d_{(inc)}$ is scaled so that the flux on the horizontal plane is equal to 1:

$$\int_0^{\pi/2} 2\pi \cdot \cos(x) \times d(x) \sin(x) dx = 1 \quad (E 3)$$

where $2\pi \cos(x)$ is the area of the horizontal plane surface of the unit sphere, and $d(x) \sin(x)$

is the photon flux density on horizontal plane surface. When diffuse photon flux is set with Q_d in the Firmament submodel, the diffuse brightness for each sector is $Q_d \times d_{(inc)}$ according to the sector position.

Each sector has a specific direction. Both direct and diffuse components reach the growing tree through these sectors. Diffuse flux occurs in every sector, and the direct flux penetrates from one sector in the directional pathway of the flux. The photon flux available for photosynthesis at a particular point is the sum of the photons intercepted through all these sectors.

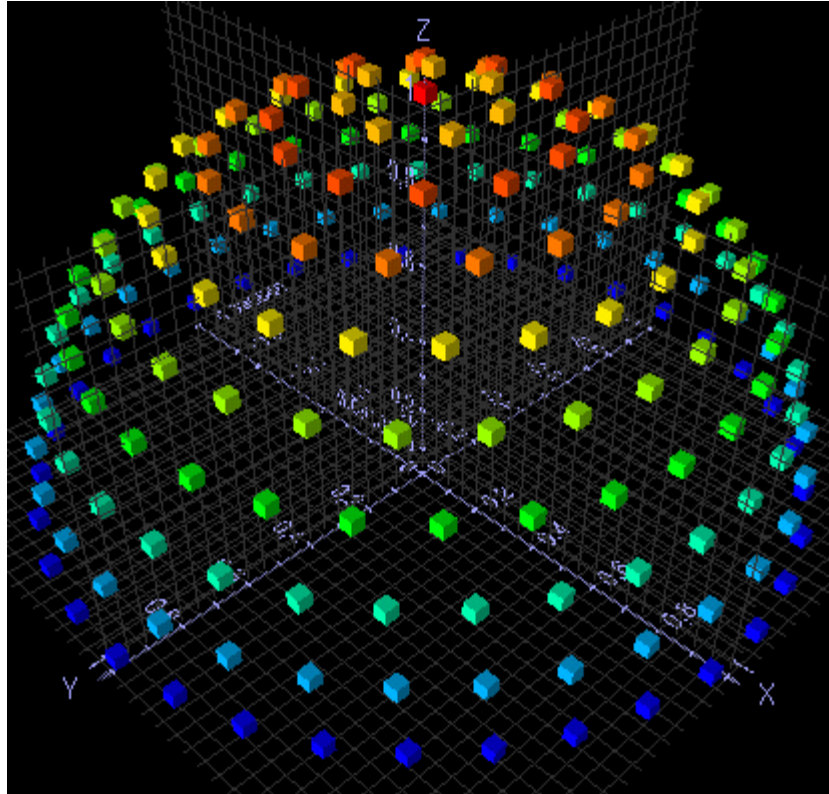


Figure 7. Photon flux overcast distribution in the firmament model. The upper hemisphere is divided into several sectors in both horizontal and vertical directions. These sectors are divided so as to have an equal solid angle. The photon flux received by each sector increases with the increase of sector's latitude in the sphere. The color in the figure denotes the different amount of incoming photon flux densities of each sector. The red sector in the zenith position receives the greatest amount of photon flux. (Figure courtesy of Jari Perttunen)

3.2.4 Monte Carlo photon flux interception model

Not all photons are available for photosynthesis. Only the photon flux intercepted by the tree compartments is converted into energy for tree growth. Interception of direct photon flux (Q_b) and diffuse photon flux (Q_d) is determined by incident photon flux, mutual shading of leaves and the optical properties of leaves. In earlier versions of LIGNUM, radiation transmission in a tree segment was calculated according to Oker-Blom and Smolander (1988), and mutual shading between all segments was estimated using analytical geometry (Perttunen *et al.* 1998; 2001). The voxel space model was subsequently introduced into LIGNUM to reduce the heavy computational load associated with the radiation interception model. Instead of calculating the mutual shading of each leaf in the tree canopy, the voxel space model utilizes voxel boxes as the calculation unit, which simplifies calculations substantially.

3.2.4.1 Voxel space

Voxel space is the space in which the tree grows. The 3D tree growing space is divided into small imaginary cubic boxes called voxels. Just as a pixel is the basic pictorial planar element in a two-dimensional vision, a voxel is the basic volumetric element in a three-dimensional vision. In an individual tree simulation, the size of voxel space may be extended to accommodate the growing tree. The number of voxels increases with tree growth, which can save calculation redundancy in juvenile tree simulations. Interception of photon flux is calculated based on these voxels. The 3D tree structure generated by LIGNUM defines the position of each leaf within the voxel space. Every tree component occupies one or more voxels (Figure 8).

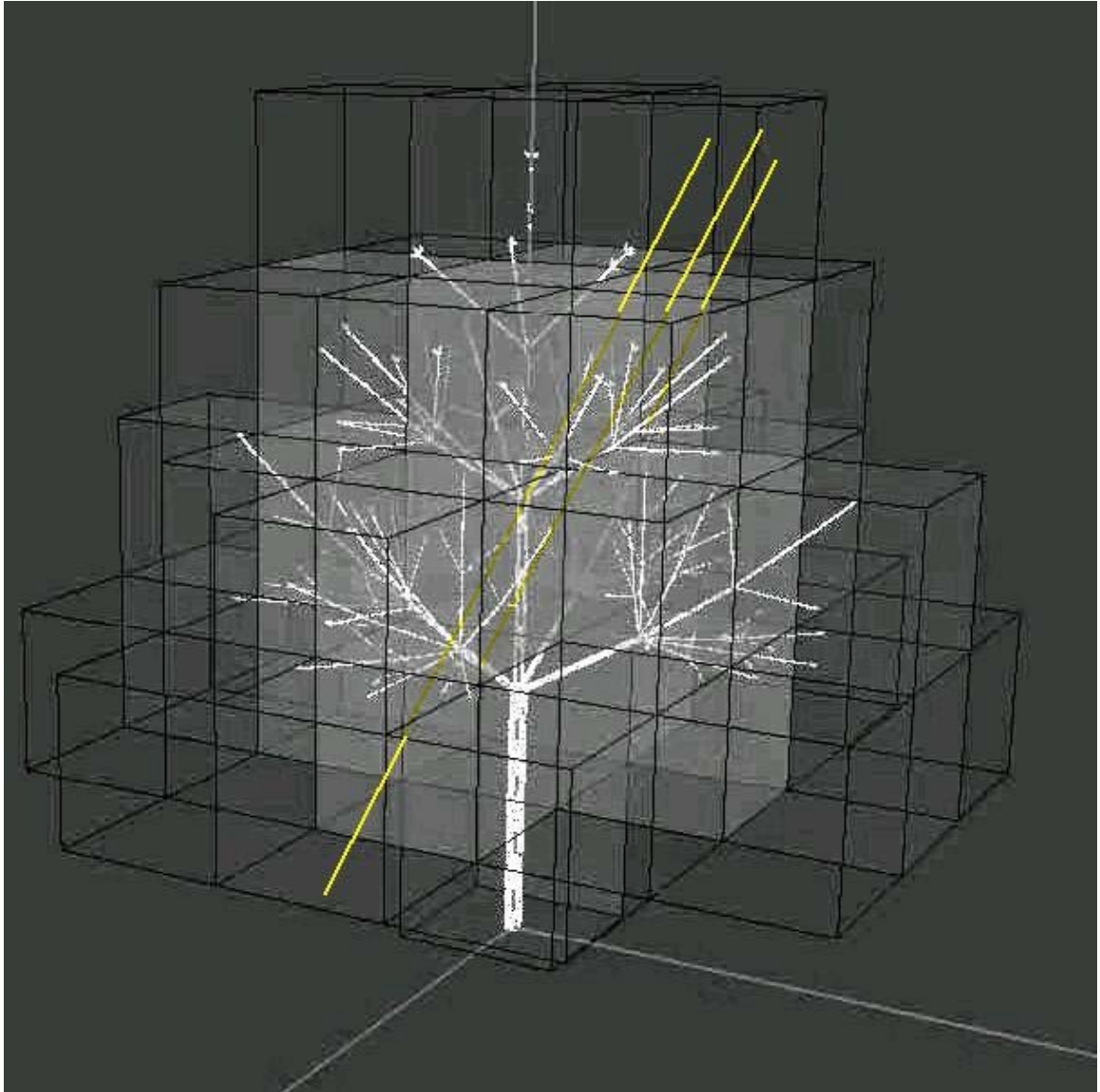


Figure 8. Voxel Space. The voxel space divides the growing space of the tree into cubic voxels. Tree compartments including leaves and segments are added into each voxel. The more tree compartments a voxel contains, the greater the possibility that voxel will intercept the photon flux. (Figure courtesy of Mika Lehtonen)

The voxel acts as the unit for calculating photon flux interception. All leaves and segments in one voxel are added up as the content of that voxel. The greater the biomass content is in a given voxel, the greater the likelihood of that voxel intercepting incoming photon flux. A beam might be intercepted by one of the voxels in its pathway or go completely through the tree growing space. The size of a voxel is similar to the size of a pixel in 2-dimensional representation. The bigger the voxel, the less accurate the resolution of voxel space becomes. The size of a voxel is selected according to the size of the growing tree in order to simplify the calculation of photon flux interception while assuring that the modeling result accurately reflect reality.

Given a standard overcast sky, the voxel space receives diffuse flux from each sector in the sky in a specific direction. The direct flux, Q_b , is emitted from the apparent direction of the sun. Intercepted Q_b and Q_d in each voxel are combined to yield the total incoming photon flux for the leaves in that voxel.

3.2.4.2 Big leaf

There may be one or more leaves and/or tree segments in a given voxel. Each leaf possesses a different leaf area and leaf angle. For each leaf, there is an angle between the leaf's normal direction and the incoming photon flux. Let α denote the angle between the normal direction of a leaf and the direction of incoming flux. The interception of photon flux by the leaf is the result of incoming flux multiplied by $\cos(\alpha)$. In order to simplify the photon flux interception cosine correction in the cottonwood growth simulation, one big leaf is generated to represent all leaves in a given voxel. The normal of the big leaf (that is, the direction perpendicular to the plane of the leaf blade) thus

determines the general direction of exposure for all leaf components in the voxel. The big leaf normal is calculated as the leaf-area-weighted sum of all individual leaf normals in the voxel.

$$N = \sum (N_i \times LA_i) \quad (\text{E } 4)$$

where N is the general big leaf normal; LA_i is the leaf area of a specific leaf, and N_i is the normal of the specific leaf. The leaf area of the big leaf is in essence the total area of the leaves in the box. The big leaf and its normal are used to calculate photon flux interception for each specific flux direction. If α is the angle between the normal of big leaf and the incoming photon flux direction, then the photon flux received by the big leaf is calculated as the product of the original flux density multiplied by $\cos(\alpha)$.

3.2.4.3 Photon flux interception

Two voxel space models are available: the green voxel space model and the Monte-Carlo voxel space model (LIGNUM). The green voxel model sets an attenuation value for each voxel as a function of the amount of tree compartments inside the voxel. The radiation beam is attenuated when it goes through the voxel. All the voxels in the beam pathway may absorb some radiation according to their position in the path and the amount of the tree compartment they occupy. The green voxel model is deterministic in nature. Given the specific tree structure and photon flux environment, photon flux absorbed by each voxel is determined.

On the other hand, the Monte-Carlo voxel space model is stochastic in nature. It is used in the cottonwood simulation to calculate the mutual shading among voxels in the path of radiation beams. The interception of photon flux is affected by whether the

flux passed through other voxels before reaching the focal voxel. In effect, the voxels in front of the focal voxel in the photon flux path are shading voxels.

3.2.4.3.1 General rules for photon flux interception

Voxel space and big leaf in the voxel are used to calculate the amount of photon flux possibly intercepted by each voxel. In this study, the calculation of the intercepted total photon flux, Q_i , proceeded according to the following steps:

1) Mutual shading is based on the relative geometric position of tree segments. For each voxel, a path was traced towards each sky sector and a list of voxels on that path was generated. Each path was used to calculate a fraction of the diffuse photon flux (Q_d) from each sky region. Solar position determines the direction of direct photon flux (Q_b). The path corresponding to the direct photon flux direction is used to calculate the direct photon flux interception.

2) Along each path, Q_b or directional Q_d flux components might undergo one of two transformations: (a) they may be intercepted by shading voxels, which are those before the focal voxel in the list; or (b) they may reach the focal voxel.

3) A “big leaf” is used to describe optical properties of leaves (Monteith, 1965; Ross, 1981). The normal of the “big leaf” is the leaf-area-weighted sum of all individual leaf normals in a voxel box. Bigger leaves influence the big leaf normal more than do smaller ones.

4) In this study, a “Monte Carlo voxel” approach was employed for determining whether or not a voxel intercepted the photon flux. In so doing, the projected big leaf and voxel surface areas perpendicular to flux direction from each sky region n -- $A_l(n)$ and $A_v(n)$, respectively -- are calculated (Figure 9). The probability (p) of the directional flux interception within the voxel is the ratio $A_l(n)/A_v(n)$. The Bernoulli process is used to determine whether or not a flux is intercepted by the voxel i with the probability of p_i .

$$Bernoulli(p_i) = \begin{cases} 1 & \dots \text{probability } p_i \\ 0 & \dots \text{probability } 1 - p_i \end{cases}$$

The $Bernoulli(p_i)$ function has result either 1 or 0. A result of 1 for the Bernoulli process means that the photon flux is intercepted by the voxel.

5) The absorbed photon flux is thus a fraction of the incoming photon flux. Leaf optical properties will determine the flux ratio of interception, transmission and reflection. When exposed to photon flux, a single layer of leaves is considered to absorb 80% of the incoming photosynthetic photon flux, with 10% being transmitted through the leaf, which may be intercepted and absorbed by the another layer of leaves. Reflection and scattering of the photosynthetic photon flux in the canopy were not considered in

current model version. In the case of non-interception, the whole flux passes through the voxel. When there is more than one layer of leaves in the voxel, 90% of the photosynthetic photon flux is considered to be intercepted by the voxel biomass.

6) The total photon flux intercepted by a focal voxel is calculated as the sum of all fluxes — direct and diffuse -- from each sector. The intercepted photon flux is shared equally by all leaves in the voxel.

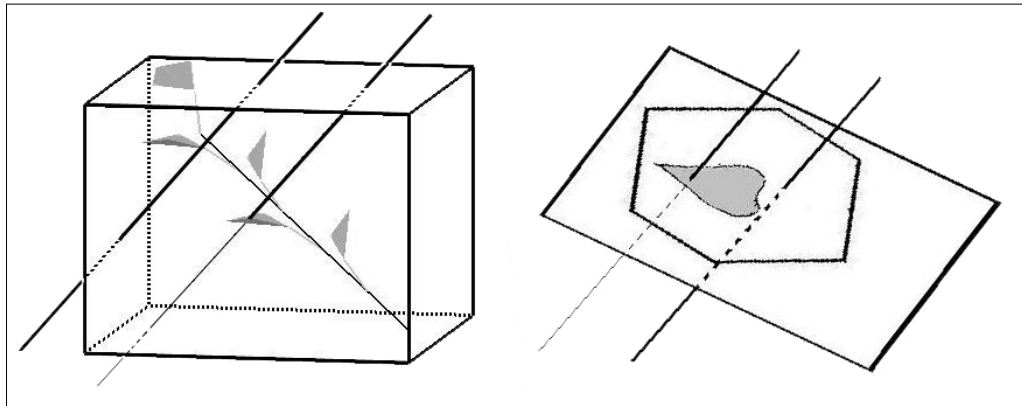


Figure 9. Interception of photon flux in voxel space. Left: A general voxel with a tree segment and leaves. A photon flux entering the voxel from a sky region may pass through the voxel (thick line) or be intercepted by tree compartments (thick line turning thin). Right: Projection of the voxel (polygon) and big leaf area (shaded area in polygon) to the plane perpendicular to the photon flux from the sky region.

3.2.4.3.2 *Photon flux interception in shading voxels*

If a voxel is a shading voxel in the pathway of the flux, four scenarios are possible (Figure 10):

- a), the photon flux may penetrate all the shading voxels and reach the focal voxel;
- b), the photon flux may be transmitted through the foliage of one shading voxel, which has one layer of leaves;
- c), the photon flux may be absorbed by the foliage of one shading voxel, which has more than one layer of leaves;
- d), the photon flux may be transmitted through the foliage of one shading voxel and be intercepted by another shading voxel.

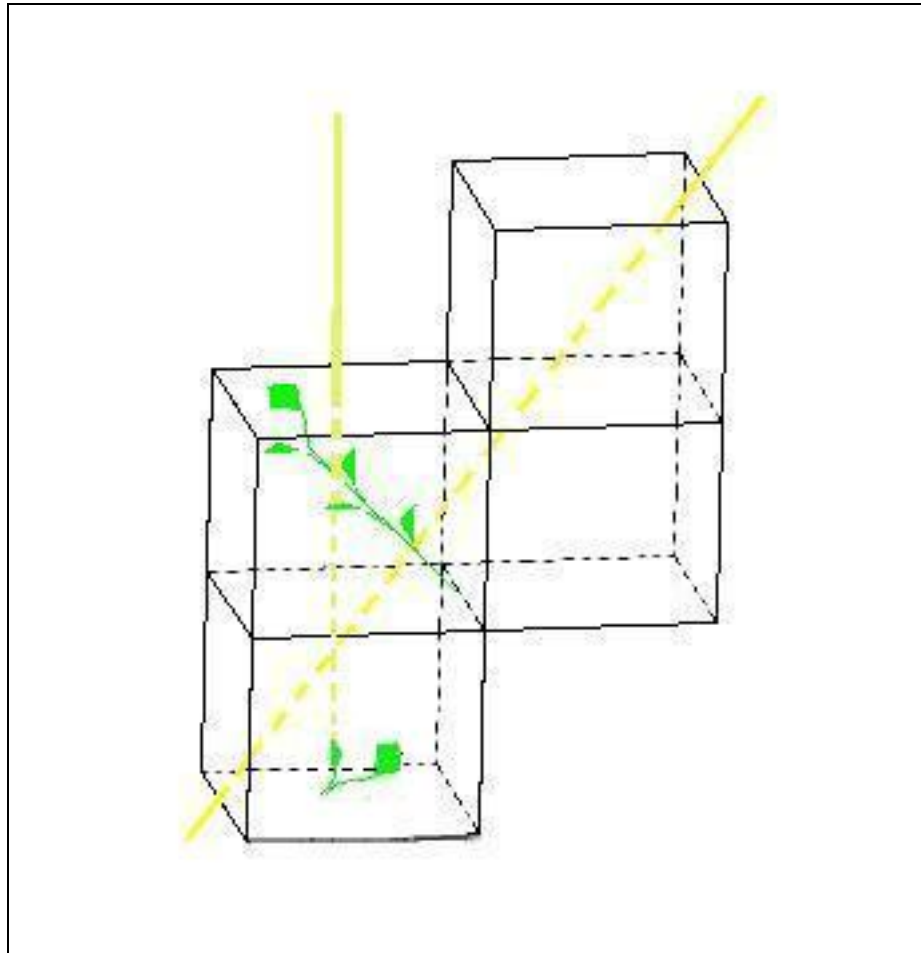


Figure 10. Radiation interception in several adjacent voxels. There are four scenarios for an incoming photon flux: a) the photon flux may penetrate to the focal voxel without contact with foliage in shading voxels; b) the photon flux may be transmitted through the foliage of one shading voxel, which has one layer of leaves; c) the photon flux may be absorbed by the foliage of one shading voxel, which has more than one layer of leaves; d) the photon flux may be transmitted through the foliage of one shading voxel and be intercepted by another shading voxel.

3.2.4.3.3 Photon flux interception by focal voxel

In the cottonwood growth model, if the photon flux is transmitted through the foliage of more than two layers of leaves in the beam path -- either in a single voxel or in two voxels -- before the flux reaches the focal voxel, then the focal voxel is in essence completely shaded and will not receive photons from this beam. If a photon flux penetrates without interference through all the previous voxels and reaches the focal voxel, the latter will receive the full amount of photons in the beam. Thus, in the case of a flux reaching a given focal voxel, the flux might have never been intercepted by shading voxels in its path, or it may have been intercepted by one layer of leaves in a preceding voxel, with only the transmitted radiation reaching the focal voxel. In these two cases, the focal voxel would receive 100% and 10% of the original incoming photon flux, respectively. As noted earlier, in the first case, 80% of these photon fluxes will be absorbed by the foliage in the focal voxel if there is only one layer of leaves in that voxel; or 90% will be absorbed if there is more than one layer of leaves in it. In the second case, 90% of received photon flux will be absorbed by the focal voxel.

Either direct beam or diffuse flux may reach a focal voxel. The total photon flux intercepted by one voxel is the sum of the diffuse photon flux intercepted by that voxel from all directions and the direct photon flux; and this sum is shared by all leaves in the voxel.

The self-shading of leaves in the focal voxel is also considered in the cottonwood voxel space model. When the leaf area index in the voxel is greater than 1, there are several layers of leaves in the voxel and these leaves in effect shade one another. Since all leaves are considered as having the same priority, these leaves have to share the

incoming photon flux equally. When the tree crown leaf area index (LAI) is bigger than 1, the incoming photon flux density for the leaves in one voxel equals the incoming photon flux for the voxel divided by the LAI.

3.2.4.4 Standard diffuse photon flux interception

The photon flux interception was affected by tree structure. Each photosynthesis process with 30-minute interval is implemented based on current tree structure. However, tree structure update didn't keep the same pace as photosynthesis. Within the structural update time step, the tree structure remained unchanged. Because tree structure keeps the same during structural time step cycle, each voxel gets similar fraction of diffuse photon flux. In order to simplify the photon flux interception calculation, the standard diffuse photon flux interception was applied. Within the tree structure update cycle, diffuse photon flux interception by each voxel was only calculated in the first photosynthetic process with new structure to create a standard distribution of intercepted diffuse photon flux. The standard distribution described the amount of intercepted diffuse photon flux in each voxel as a fraction of total input diffuse photon flux. For the rest of the photosynthetic processes in the same structural time step, these fractions were used to calculate the diffuse photon flux interceptions in each voxel with new diffuse photon flux input value until next structure update.

3.2.5 Photosynthesis model

In previous versions of the LIGNUM model, it was assumed that the relationship between the solar radiation and the photosynthetic production by the leaves was linear or almost so. In this cottonwood simulation, leaf photosynthesis (P) is

modelled as a function of intercepted total photon flux (Q_i) and temperature (T_a) according to Farquhar's approach (Le Roux *et al.*, 1999; von Caemmerer and Farquhar, 1981). The photosynthetic production calculated from Farquhar's approach is the net CO₂ assimilation of leaves after subtracting leaf respiration. The total net CO₂ assimilation of all leaves is used for the respiration of other compartments of the tree and tree growth.

The net CO₂ assimilation rate, A_l ($\mu\text{mol m}^{-2}\text{s}^{-1}$) (von Caemmerer and Farquhar, 1981) is calculated as:

$$A_l = (1 - \Gamma^* / C) V_c - R_d, \quad (\text{E } 5)$$

where A_l is the net CO₂ uptake rate per unit leaf area ($\mu\text{mol m}^{-2} \text{s}^{-1}$); R_d is daytime respiration rate of leaves ($\mu\text{mol m}^{-2} \text{s}^{-1}$), i.e. respiration related to metabolic processes other than photorespiration; Γ^*/C is the ratio of the rates of photorespiration and carboxylation; C is the intercellular CO₂ concentration in a leaf ($\mu\text{mol mol}^{-1}$), corrected for solubility relative to 25°C; V_c is the carboxylation rate ($\mu\text{mol m}^{-2} \text{s}^{-1}$); Γ^* is the CO₂ compensation point of photosynthesis in the absence of daytime respiration ($\mu\text{mol mol}^{-1}$).

The equation for Γ^* is:

$$\Gamma^* = \frac{0.5V_{O_{\max}}K_cO_i}{V_{c_{\max}}K_o}, \quad (\text{E } 6)$$

where $V_{c_{\max}}$ is the maximum ribulose biphosphate (RuP₂) saturated rate of carboxylation ($\mu\text{mol m}^{-2} \text{s}^{-1}$); $V_{O_{\max}}$ is the maximum RuP₂ saturated rate of oxygenation ($\mu\text{mol m}^{-2} \text{s}^{-1}$). O_i is the intercellular concentration of O₂ in the leaf, corrected for solubility relative to 25°C (mmol mol^{-1}). K_c is the Michaelis constant for CO₂ (mmol mol^{-1}), and K_o was the Michaelis constant for O₂ (mmol mol^{-1}). The relationship between $V_{O_{\max}}$ and $V_{c_{\max}}$ is estimated (Long 1991):

$$V_{o \max} = 0.21 \times V_{c \max} . \quad (\text{E } 7)$$

Farquhar *et al.* (1980) predicted an abrupt change in the dependence of photosynthetic rate on intercellular pressure of CO₂ as the limitation on photosynthesis changed from RuP₂(ribulose biphosphate)-saturated carboxylation rate to RuP₂ regeneration rate. The RuP₂ saturated rate of carboxylation (μmol m⁻² s⁻¹) is:

$$W_c = \frac{C \cdot V_{c \max}}{C + K_c (1 + O \cdot K_o)} . \quad (\text{E } 8)$$

The RuP₂ limited rate of carboxylation (μmol m⁻² s⁻¹) is:

$$W_j = \frac{J}{4.5 + 10.5 \cdot \Gamma_* / C} , \quad (\text{E } 9)$$

where J is the potential rate of electron transport (μmol m⁻² s⁻¹), which depends on absorbed photon flux (Q ; μmol m⁻² s⁻¹).

$$J = \frac{J_{\max} \cdot Q}{Q + 2.1 \cdot J_{\max}} , \quad (\text{E } 10)$$

where J_{\max} is the light-saturated potential rate of electron transport (μmol m⁻² s⁻¹). Thus, carboxylation rate V_c in eq. (E 5) was:

$$V_c = \min\{W_c, W_j\} . \quad (\text{E } 11)$$

In this study, the temperature dependence of O and C is modelled according to Long (1991). Most constants used in the photosynthesis model were also obtained from Long (1991) [see table 2 in 3.4.1]. Farquhar's model provides the instantaneous photosynthetic rate per unit leaf area per unit time.

Leaf respiration rate is subtracted from photosynthetic rate to yield net C uptake. The leaf respiration rate is adjusted by temperature (T_a) with a temperature

coefficient.

$$R_d' = R_d \times Q_{10}^{(T'-T)/10} \quad (\text{E } 12)$$

where R_d is the respiration rate at temperature T ; R_d' is the respiration rate at temperature T' ; Q_{10} is the temperature coefficient ($Q_{10}=2$ as default). Q_{10} defined the change of respiration rate with temperature increasing by 10°C . In this project, R_d is the measured data from experiment with temperature 25° , and R_d' is the adjusted value according to temperature variation. Net C uptake is integrated over the leaf area of the whole tree; at night time, net C uptake is negative because of foliage respiration; net primary production (NPP) is estimated as the difference between foliar net C uptake and respiration by the woody parts of the tree.

3.2.6 Structure derivation and growth allocation within short time step simulation

3.2.6.1 Structure derivation

The tree growth simulation begins with a very simple tree structure of a single stem segment and attached buds, including an apical bud and a lateral bud. The bud is the key element in structure derivation. In each growing season, buds develop into segments, branching points, and new buds, which in the model are represented as a list of tree compartments. There are three major steps in structure derivation with L-system rules: derivation, split, and bending.

1. Derivation

When a bud is active, it will expand into a long segment attached with a new

apical bud and a new lateral bud at the end of the segment. Both the segment and the apical bud will have the same orientation as the original bud. The lateral bud will vary from the original direction. The direction of the lateral bud is determined by two angles: *Roll* and *pitch* (Figure 11). Pitch angle is the angle at which the lateral bud deviates from the original direction. It can also be called the insertion angle of the lateral bud. If the pitch value is 0, the direction of lateral bud would be the same as the original direction. If the pitch value is 90, the two buds would be perpendicular to each other. Thus the pitch angle is the angle at which the sub-branch deviates from that of the mother branch. *Roll* is the angle of the lateral bud changing direction in azimuth. There are 360 potential directions from north to west, and back to north. Roll angle is the angle from direct north in a clockwise direction. The angle between the directions of the lateral bud and the apical bud ultimately becomes the branching angle between the sub-branch and mother branch after both buds develop. The joint point of these two buds is the branching point.

2. Split

In actual cottonwood growth, several segments usually develop from one bud, with each attached a lateral bud. In the L-systems of the LIGNUM model, only one branch segment develops from a single bud at first (Figure 6). The branch is elongated and thickened during growth allocation, and thereafter is split. The split function involves splitting the entire segment into several segments and accompanying lateral buds. The number of segments is determined by the length of the initial segment. The direction of each lateral bud at the end of a segment deviates from the original direction according to the derivation process described above.

3. Bending

Because of the eutropic growth of the tree, the tree branch does not continue to grow in the exact direction of the initial branching insertion angle. Most branches, especially the lower branches, tend to bend upward in order to grow toward the sunlight. The structure derivation with L-systems also considers branch bending. The entire derived segment may not necessarily follow the original direction dictated by the old bud, but rather tend to alter that direction to favor upward growth. This branch bending happens gradually, and stops before the segment grows straight upwards.

H: Roll axis
L: Pitch axis
U: Turn axis
Segment grows along H
direction

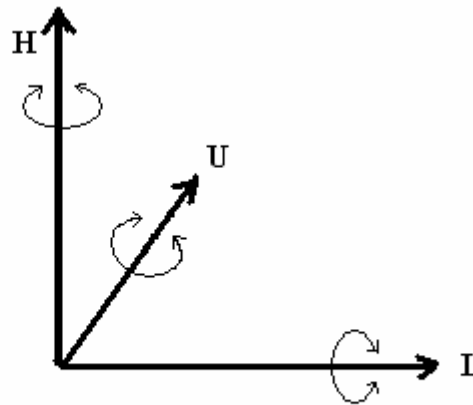


Figure 11. Deviation of bud growth direction in three dimensions. Apical bud and its segment grow along direction H. The rotation along the L axis controls inclination of lateral bud derivation (insertion angle); the rotation along the H axis controls lateral bud deviation in azimuth (azimuth angle).

3.2.6.2 Growth allocation

In the cottonwood simulation model, tree growth reflects the allocation of net primary production, N_p , or the difference between the net C assimilation by the foliage of a tree, A_t , and the maintenance and growth respiration of other tree compartments. This is depicted by:

$$N_p = A_t - \sum R_{mi} - k \times (A_t - \sum R_{mi}) \quad (\text{E } 13)$$

where R_{mi} is the maintenance respiration of the i^{th} compartment of the tree. R_{mi} is proportional to the existing biomass in each compartment, and k is the proportion of growth respiration (R_{gi}) out of the C available for growth. The factor k is assumed to be equal to all tree compartments and R_{gi} is, consequently, proportional to production of new woody biomass:

$$\sum R_{gi} \propto N_p . \quad (\text{E } 14)$$

The growth respiration of foliage is embedded in Farquhar's photosynthesis model (E5). The same function was used for leaf night respiration rate as for daytime respiration (E12). Whole-tree net C assimilation A_t is calculated by integrating net C assimilation by individual leaves, A_l , over the whole canopy during calculation period. Growth occurs only when the net C assimilation by foliage exceeds the maintenance respiration demand by tree organs including leaves, sapwood, and roots. The net primary production is allocated via the following equation:

$$N_p = iW_n(\lambda) + iW_o(\lambda) + iW_r(\lambda) \quad (\text{E } 15)$$

where iW_n (kg) is the new tree segments and buds, iW_o (kg) is the woody biomass growth

in thickness of existing tree segments, iW_r (kg) is the new root growth, and λ is a non-unit factor that is used to adjust the tree growth. The total demand for photosynthetic production caused by a new tree segment at the time of its emergence is not known, so the balance of this function must be solved iteratively. The new growth of the tree including segment, buds, and root is defined as a function of the parameter -- λ . The final new tree growth is obtained by tuning up the λ value so as to maintain the balance of equation (E15).

Vigor index

For above-ground structural development and the growth allocation, one of factors is the vigor index (VI) of each segment (Nikinmaa *et al.* 2003). Vigor index is the amount of growth located on each segment. The more the vigor index value, the more growth will be allocated on the segment.

Vigor index of each sub-segment was determined by product value of the mother branch's vigor index and the vigor index ratio of the sub-segment. To calculate vigor index, the woody axes from the base of the tree to the tip of the shoot are tracked in LIGNUM. Vigor index ratio related to the relative diameter of the axis among axes from the same branch point. At each branch point, the diameters of the dividing axes are compared to calculate the vigor index ratio of each axis. Value 1 is assigned to the axis with the greatest diameter at a branching point. A value reflecting the ratio between the cross-sectional areas of the axis of interest and the thickest axis at the branching point is assigned to each thinner axis. The vigor index of each axis is the product of each vigor index ratio and their mother branch's vigor index. The axis of interest retains this value until the next branch point, where the calculation is repeated. This procedure is continued

until the shoot at the tip of the axis is reached. If the VI value of the axis below the branching point is denoted by v_{i-1} , the equation for the VI value at the subsequent branching point i ($i = 1, \dots, n$) is:

$$v_{i(j)} = \left(\frac{d_j}{d_m} \right)^2 v_{i-1} \quad (\text{E } 16)$$

where d_j is the diameter of axis j and d_m is the largest diameter of the axes at the branching point ($d_m = \max(d_j | j = 1, \dots, n)$, where $1, \dots, n$ denote the axes at the branching point).

If $r_{i(j)}$ denotes the vigor index ratio between the cross-sectional areas of the axis of interest and the thickest axis at the branch point, then:

$$r_{i(j)} = \left(\frac{d_j}{d_m} \right)^2, r_{i(j)} \leq 1. \quad (\text{E } 17)$$

where i is the index of axis below branch point, j is the index for one of the axis above branch point. Given the above, the value of VI for a shoot is:

$$VI = \prod_0^n r_i, \quad (\text{E } 18)$$

where VI is the value of the vigor index for the shoot of interest, $i=0$ is the basal section of stem before the first branch point and n is the shoot of interest ($r_0 = v_0 = 1$).

The thicker branch after one branching point keeps the same VI as that of the branch before the branching point. Usually the main stem retains the largest VI value 1. For other branches, the VI value decreases with increasing branching order.

Radiation environment factor

Another factor influencing tree structure growth and biomass allocation is the

radiation environment. A tree compartment that absorbs more radiation grows faster than one that is more shaded by other compartments. The radiation index acts as a factor in segment elongation along with vigor index. The radiation index ranges from 0 to 1 following the photosynthesis product curve as a function of absorbed photon flux (Figure 17; Figure 18). When the tree segment grows under full sun, the radiation index is set to 1. When tree segments grow under a photon flux density below the light compensation point of photosynthetic rate (Figure 18), the radiation index is set to 0. For all other segments growing in intermediate radiation environments, a radiation index from 0 to 1 is assigned according to the radiation index curve function, which is consistent with the photosynthetic curve function (Figure 18).

The effects of vigor index and radiation factor were multiplicatively applied to segments' growth in tree growth allocation.

3.2.6.3 Root biomass growth

In contrast to the detailed structural description for the shoot, the root growth in LIGNUM model includes only biomass. Root biomass growth applies the relationship among root mass, shoot mass, and foliage mass growth. A portion of root mass is assumed to die annually (Perttunen *et al.*, 1996).

Root respiration

It is assumed that there is no heartwood in the roots. Root maintenance respiration is proportional to the total root biomass. Root growth respiration is proportional to the amount of root growth.

Root growth

According to the pipe model theory, the transportation system in a tree involves the interconnected network of roots, stem vessels, and leaves. The root growth corresponds to the growth of foliage and woody shoot. The relationship among root mass, shoot mass, and foliage mass growth was used to assess root growth in the LIGNUM model. The root growth is proportional to the new foliage mass growth with a constant ratio through the whole tree growth span.

Root senescence

In root biomass simulation in the current version of the LIGNUM model, the coarse and fine roots are not distinguished. The total root masses including both coarse and fine roots are considered to have equal root senescence rates. Thus each year a constant fraction of total root mass will turn over.

3.2.7 Communication between L-system and LIGNUM

The LIGNUM model utilizes the L-system method to construct and derive tree structure. Based on this derived tree structure, LIGNUM allocates tree biomass growth to segment length, segment diameter, foliage, and root growth. In each structural time step, L-system and LIGNUM communicate back and forth to implement tree structure derivation and growth allocation.

From an initial active bud, L-system produces an L-string as a depiction of tree structure, which is converted into a virtual tree in the LIGNUM system. The L-string provides the virtual tree with its structural pattern, which includes branch azimuth, inclination, and position among others. Interception of photon flux takes place in LIGNUM system through the tree's structural pattern, which results in physiological

processes such as photosynthesis, respiration, and growth allocation. The allocation of growth leads to structural extension in length and diameter. Structure is also affected by the tree's self-pruning with self shading of tree crown. Finally, after tree physiological processes and growth allocation have been accounted for, the virtual tree in the LIGNUM system is translated back into L-string as the axiom of the next L-string structure derivation.

The above communication between LIGNUM system and L-system occurs iteratively for each structural update cycle in simulation.

3.3 Field data

Based on above modeling description, corresponding field data were collected as modeling parameter and input data. Field data used in model included photon flux environment data, tree structure data, and photosynthetic parameters. The measured field data including height and biomass were also used to validate the model.

3.3.1 Field site

Model parameterization and validation were based on data measured in an eastern cottonwood plantation. The plantation was established on the Missouri River flood plain at the University of Missouri's Horticulture and Agroforestry Research Center (HARC) at New Franklin, MO, USA (92°46' W; 39°01' N; 197m altitude). The field floods occasionally in spring and early summer. The soil was fertile, moderately well-drained and permeable (Pallardy *et al.*, 2003). The soil fertility data is show in Table 1. The cation exchange capacity (CEC) in the soil is quite consistently distributed with soil depth. The CEC slightly decreases from surface to 40cm depth and increases from

40cm to 80cm depth with maximum value 28.9 ($\text{cmol } 100\text{g}^{-1}$) and minimum value 16.4 ($\text{cmol } 100\text{g}^{-1}$). The calcium content shares the same pattern as CEC in soil depth distribution with maximum value 18.2 ($\text{cmol } 100\text{g}^{-1}$) and minimum value 9.6 ($\text{cmol } 100\text{g}^{-1}$). The soil surface with 10 cm depth contains abundant nutrition including N (0.286%), K (0.7 $\text{cmol } 100\text{g}^{-1}$), and P (73.4 ppm). The soil nutrition, especially N content, decreases dramatically with increasing soil depth until about one fifth of the maximum values at the depth of 60cm.

Table 1. Soil fertility data for open growth plantation.

| Depth (cm) | Total C (%) | Total N (%) | Bray P (ppm) | CEC(cmol 100g-1) | Ca(cmol 100g-1) | Mg(cmol 100g-1) | K(cmol 100g-1) |
|-------------------|--------------------|--------------------|---------------------|-------------------------|------------------------|------------------------|-----------------------|
| 0 - 10 | 2.5 | 0.286 | 73.4 | 28.9 | 18.2 | 4.1 | 0.7 |
| 10 - 20 | 1.3 | 0.148 | 35.2 | 23 | 15.3 | 3.4 | 0.4 |
| 20 - 30 | 0.8 | 0.099 | 31.8 | 17.3 | 12.1 | 2.7 | 0.3 |
| 30 - 40 | 0.8 | 0.079 | 23.2 | 16.4 | 10.6 | 2.4 | 0.2 |
| 40 - 50 | | | | | | | |
| 50 - 60 | 0.6 | 0.066 | 18.0 | 17.7 | 9.6 | 2.7 | 0.2 |
| 60 - 70 | | | | | | | |
| 70 - 80 | 0.5 | 0.055 | 78.0 | 26.8 | 14.6 | 5.7 | 0.4 |

Parameterization data were measured in an alley cropping experiment (hereafter “open plantation”). The cottonwood plantation was planted with 6 × 18 m spacing in April 2001 in association with white clover (*Trifolium repens* L.). The cottonwood clone was a selected Midwestern industry clone. No within-row canopy closure had occurred before the measurements in summer 2002 and 2003. Thus, the alley cropping was considered to be an open-growth plantation.

Additional parameterization data were also obtained from a cottonwood stand plantation that was established adjacent to the alley cropping plant. This plantation was established using 20-cm long cuttings in May 1999. The stand was planted with 1×1 meter spacing. The growth of the stand served as a reference for the validation of simulation results and modeling predictions.

3.3.2 Weather data

Data collection

Weather data were collected using an automated weather station (Campbell Scientific, Logan, UT, USA). The weather station recorded global radiation, photosynthetic photon flux density, net radiation, wind speed, soil temperature, air

temperature, air humidity, and rainfall. Li-Cor LI-190SB Quantum sensor (Li-Cor, Inc., Lincoln, NE, USA) was used for measuring photon flux density, Kipp & Zonen CM6B pyrometer with heating/ventilation unit (Kipp & Zonen BV, Delft, The Netherlands) was used for global radiation, and HMP45C-L integrated temperature/relative humidity probe (Vaisala Ltd, Helsinki, Finland) for air temperature. Photosynthetic photon flux density and temperature were used in the current model, and global radiation was applied for estimating direct and diffuse components of incident photon flux density. Other weather data were not used in this study. The photosynthetic photon flux density (Q) is the density of solar photon flux (400nm to 700nm waveband when measured as radiation) that is absorbed by plant chlorophyll and used as energy for photosynthesis. All radiation data were cosine corrected. Data were measured every 10 seconds and the average values were recorded at 10-minute intervals by a CR23X data logger (Campbell Scientific).

Data processing

The date for weather data was recorded as Julian dates. The logger time was converted from central time to real solar time (RST) for ease of calculations.

The LIGNUM model uses direct and diffuse photon flux in the firmament model. The measured value of Q is the sum of direct and diffuse components. In this project, the ratio (Φ_b) of the direct component of photon flux to the measured total photosynthetic photon flux density value was estimated (Nygren *et al.*, 1996; Weiss and Norman, 1985):

$$\Phi_b = \frac{r_b(PAR)}{r_g(PAR)} \left[1 - \left(\frac{0.9 - r_{obs}/r_g(SWR)}{0.7} \right)^{2/3} \right] \quad (E 19)$$

where $r_b(PAR)$ and $r_g(PAR)$ are potential direct and global radiation of photosynthetically active wavebands; r_{obs} is measured global short-wave radiation, and $r_g(SWR)$ is potential global short-wave radiation. The potential direct and global photosynthetically active radiations were calculated (Nygren *et al.*, 1996; Weiss and Norman, 1985):

$$r_b = r_0 \left(\bar{d}/d \right)^2 \sin \phi \tau^{(p_a p_0^{-1} \sin^{-1} \phi)} \quad (E 20)$$

$$r_g = 0.5 r_0 \left(\bar{d}/d \right)^2 \sin \phi \left[1 + \tau^{(p_a p_0^{-1} \sin^{-1} \phi)} \right] \quad (E 21)$$

where r_0 is the average value of the solar constant; \bar{d} is the yearly average of the distance between the Earth and the Sun; d is the actual distance between the Earth and the Sun calculated according to McCullough and Porter (1971); ϕ is the solar elevation angle relative to the horizon; τ is atmospheric transmittance; p_a is atmospheric pressure at the study site; and p_0 is the atmospheric pressure at sea level; $r_g(SWR)$ is calculated with equation (E21) using $r_0 = 1380 \text{ Wm}^{-2}$ (Ross, 1981); r_b is calculated using $r_0 = 600 \text{ Wm}^{-2}$ (Weiss and Norman, 1985).

The ratio Φ_b is called the direct fraction of photosynthetic photon flux density. The relationships between Q and its direct and diffuse components, Q_b and Q_d , respectively, were given by the equations:

$$Q = Q_d + Q_b, \quad (E 22)$$

$$Q_b = \Phi_b \times Q, \quad (E 23)$$

$$Q_d = (1 - \Phi_b) Q. \quad (E 24)$$

The direction of Q_b is computed as a function of latitude, Julian day, and RST (Gates, 1980; Ross, 1981).

The equation for Φ_b reveals that the ratio of the measured global short-wave radiation (r_{obs}) to the potential global short-wave radiation ($r_g(\text{SWR})$) should not exceed 0.9 (Weiss and Norman, 1985). In data processing, the $r_{obs}/r_g(\text{SWR})$ ratio was set at 0.9 if calculation yielded a result greater than 0.9.

3.3.3 Tree structure

Structural data collection involved detailed tree structure measurement, tracking of leaf area development, and woody biomass measurement. Tree structure measurement includes branch diameter, length of internode segment, and branch angles.

3.3.3.1 Branching pattern

Two- and three-year-old trees were sampled in the open growth plantation to obtain the branch structural pattern. Three trees with large, average, and small diameter at breast height (DBH) were selected for measurement. Measurement of tree structure included branch base diameter, branch bifurcation angle, internode segment diameter, and segment length. The data were organized by branching order. The lowest order was the tree stem, which was set as order 0. The main branches or those attached directly to the stem were assigned to order 1 and the order number increased with increasing branch bifurcation (Figure 1). The tree heights were also obtained for trees from two- to five-years old in open growth plantation for the purpose of model validation.

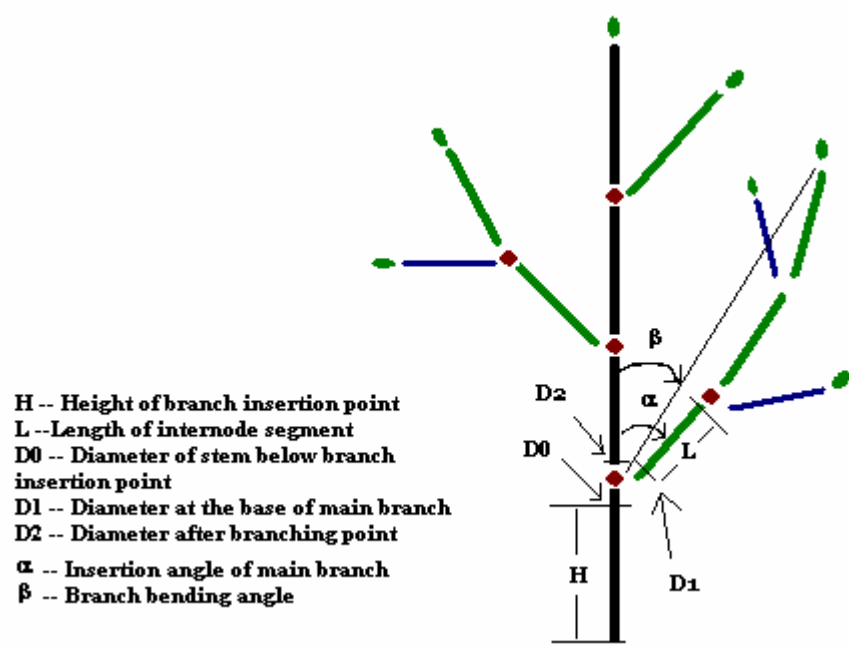


Figure 12. Branch structure measurement including branch height, diameter bifurcation, branch angles both in azimuth and inclination, and branch bending

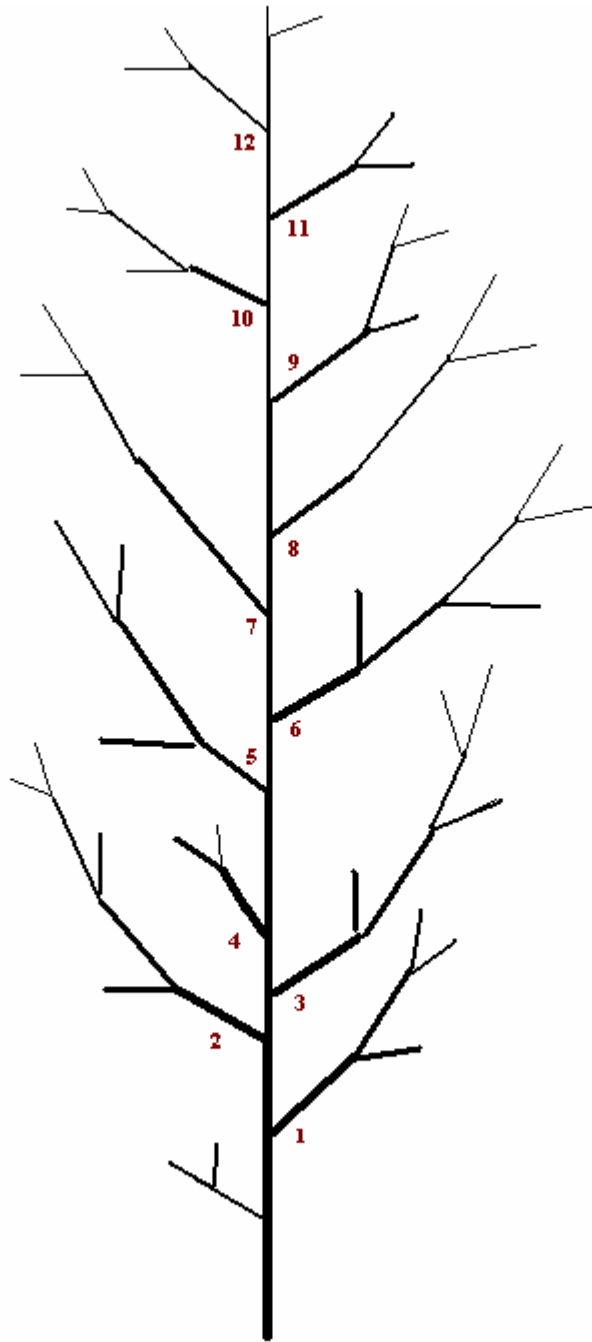


Figure 13. Branch positions in low, medium, and high crown. Branches 1, 2, 3, and 4 are low positional branches; branches 5, 6, 7, and 8 are medium positional branches; branches 9, 10, 11, and 12 are high positional branches;

Each main branch was recorded in terms of height of branch insertion point, internode segment length, diameter of main branch, diameter of stem below main branch, insertion angle of the main branch, and the angle of branch bending (Figure 12). Similar structural measurements were implemented for twelve selected main branches. The twelve main branches were selected from the stem from each tree: four from a lower position, four from a middle position, and four from an upper position. The lower position is at the bottom of the main tree crown, the upper position at the top of the tree crown, and the middle position intermediate to lower and upper positions (Figure 13). The structural measurement in each main branch includes branch basal diameter (D1 in Figure 12), diameters in each bifurcation point (d1, d2, d3 in Figure 12), length of internode segment, and bifurcation angle of sub-branches. The structural bifurcation is tracked in each selected main branch until the last order of the branch.

3.3.3.2 Leaf growth

In the spring, new leaves emerge in succession. New leaves were selected to follow up leaf emergence and expansion dynamics. The leaves were selected from trees in a stand plantation with 1m by 1m spacing so that leaves from both sunny and shaded positions can be collected for comparison study. There are three cottonwood clones in the stand. For each clone, fifteen leaves were selected from sunny positions and the other fifteen from shaded positions. The fifteen leaves from the same clone may come from five trees, three leaves each. Selected leaves were measured for length and width every other day. At the end of the leaf tracking, leaf areas of the selected matured leaves were measured by scanning. Via regression analysis, a linear relationship was obtained

between leaf area and the product of leaf length and width. The leaf area growth was applied in the LIGNUM model in simulating the interception of photon flux and photosynthesis.

3.4 Results

The objective of cottonwood modelling with the LIGNUM modelling method is to simulate tree growth under a specific growth environment based on tree growth knowledge and to verify hypotheses relative to plant science. The results in this subchapter include the measured structural patterns and photosynthetic parameters from laboratory experiments, simulated results based on these structural patterns and parameters, and modelling evaluation. The model evaluation is implemented through model verification, sensitivity analysis of parameters, and model prediction.

3.4.1 Measured structural patterns of cottonwood

Branch angles

Branch angle includes branch azimuth (Figure 14) and branch inclination (Figure 15). Branch azimuth is the horizontal bifurcation angle between the sub-branch and the mother branch. Branch inclination is the vertical bifurcation angle between the sub-branch and the mother branch, which include insertion angle and bending angle. The branch angles affect branch development and partly determine structural pattern of the tree crown. The strengths of azimuth frequency in Figure 14 are not significantly different in each direction. The azimuth measurement data are considered to be randomly distributed. The radar chart in Figure 15 reveals that branch insertion angles range mostly

from 30° to 70° with an average value of 44° and a standard deviation of 14°. The above features of branch angles provided the branch derivation pattern for the cottonwood growth simulation with LIGNUM.

Branch growth dynamic

Branch growth dynamic includes branch elongation in length and leaf emergence and maturation for new branches. New branches exhibited active growth from April to September, with final elongation length averaging about 0.7m (Figure 16b). New leaves emerged along with branch length elongation. The average leaf numbers increased from April and reached a maximum number of *ca.* 35 before leaf fall began in August (Figure 16a). Some branches had as many as 60 leaves.

Leaf growth dynamics

The time interval between emergences of two concatenated leaves was about 1 to 2 days. It took about 10 days from emergence to full leaf maturity. The leaf mass may be expressed in terms of leaf area and specific leaf area factor. The specific leaf area factor varied during the growing season. For this study the measured value for specific leaf area in matured leaves in the cottonwood tree was 15 m² kg⁻¹.

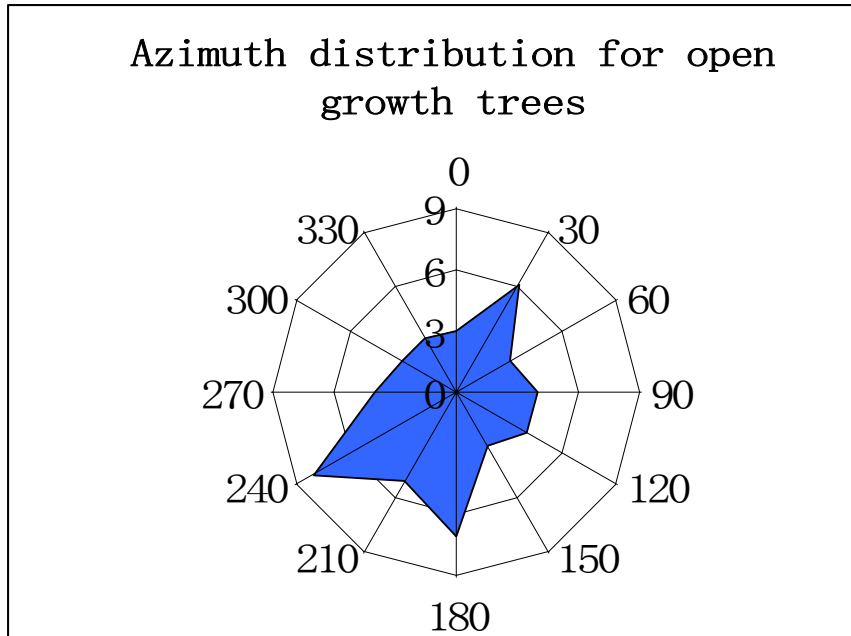


Figure 14. Azimuth (horizontal bifurcation angle) distribution of branches in cottonwood tree. The blue area is the frequency of branch azimuths. The strength in each direction is the frequency of branch azimuths.

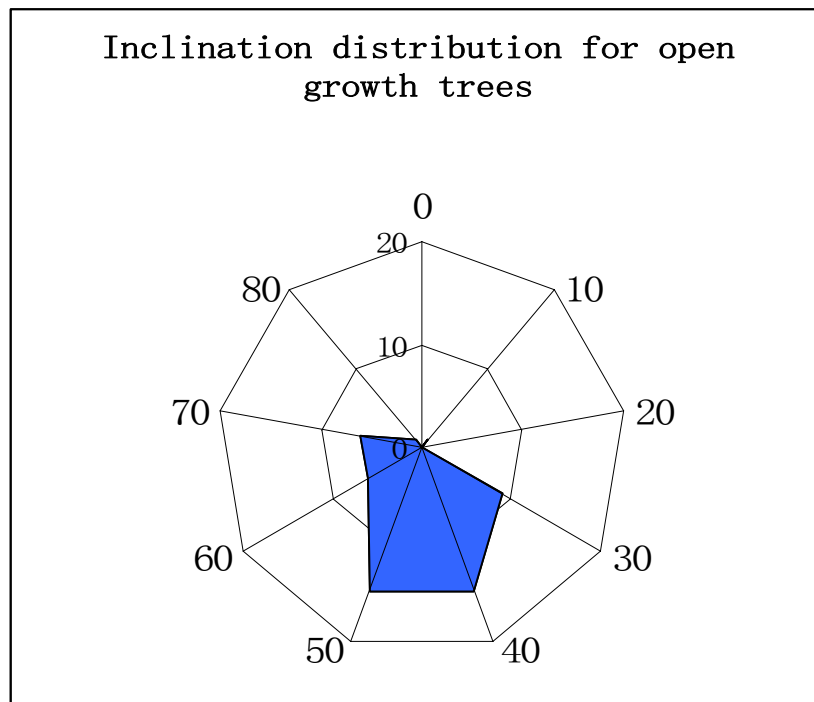


Figure 15. Inclination (vertical bifurcation angle) distribution of branches in cottonwood tree. The inclinations of branches mostly fell into the range from 30° to 70°.

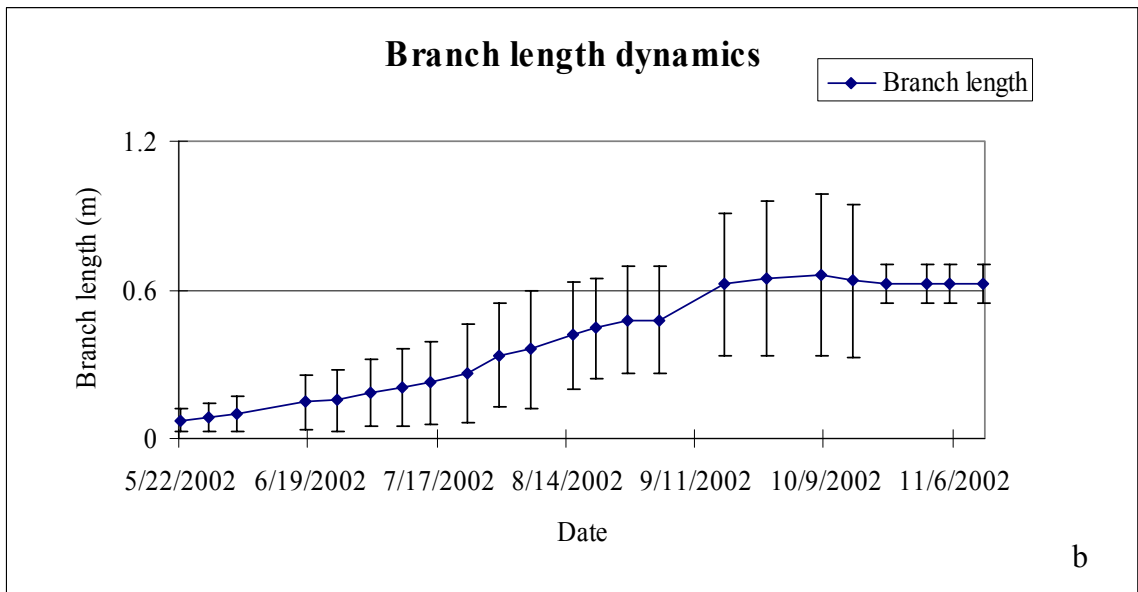
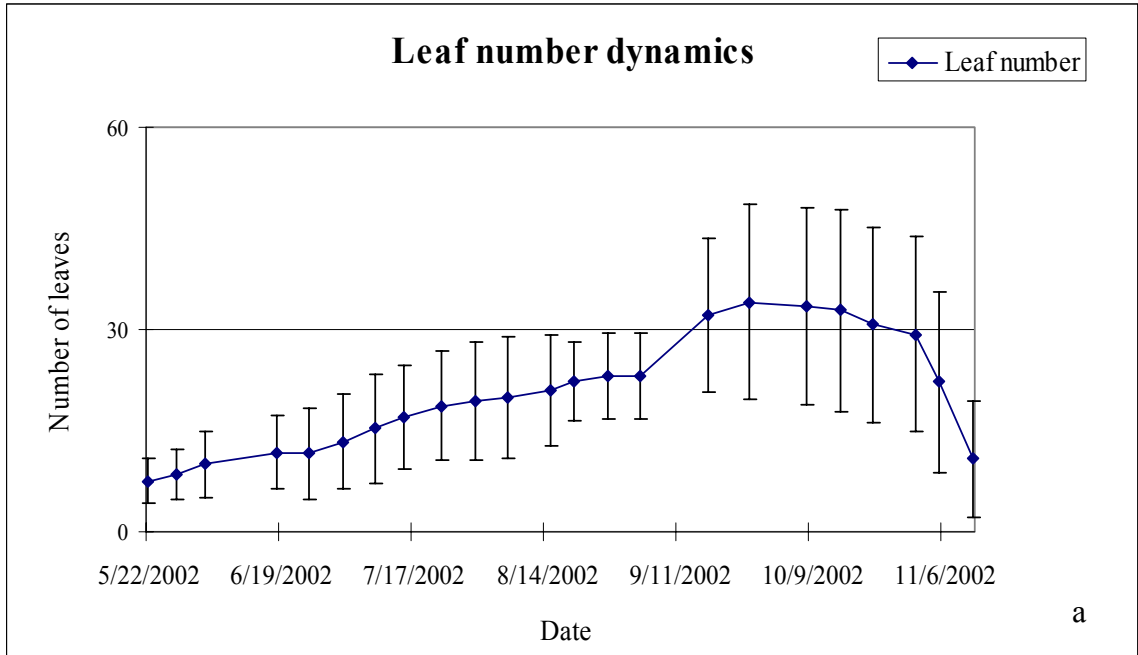


Figure 16. Branch growth dynamics. a) the average leaf number dynamic for branches in one growing season with error bars for standard deviation; b) the average elongation length of new branches in one growing season with error bars for standard deviation.

3.4.2 Model parameterization

Based on the measured result above, the adaptation of LIGNUM to cottonwood simulation utilized the parameters and constants that reflect features specific to cottonwood growth both in terms of structure and physiology. These parameters and constants were used in tree structural pattern construction, modeling of physiological processes, and tree growth allocation (Table 2).

Daily root senescence was estimated as $0.0005 \text{ (kg BM kg}^{-1} \text{ BM)}$ (Dupraz *et al.*, 2004). Root senescence during each structural update is the product of daily root senescence and time period of structural update time step. Sapwood maintenance respiration ratio was set to be $0.015 \text{ kg C kg}^{-1} \text{ C d}^{-1}$ and growth respiration is set to be $0.25 \text{ kg C kg}^{-1} \text{ C}$ of new growth (Rauscher *et al.*, 1990). The average root-shoot ratio for cottonwood sapling in the first two years is about 0.30 (Pallardy *et al.*, 2003). The ratio of root mass growth to new foliage was estimated to be 0.5 based on the root-shoot ratio and leaf-sapwood mass relationship.

Clone-dependent parameters for the CO₂ exchange model are presented in Table 2. Figure 17 shows the differences in net CO₂ assimilation rate with these three sets of photosynthetic parameters. There is no significant difference among these three net CO₂ assimilation curves. The parameters in yellow clone (1112) were selected for photosynthetic production in the cottonwood simulation model. With these parameters, Figure 18 shows the net CO₂ assimilation rate produced with Farquhar's model at temperatures of 15°C, 25°C, and 35°C, which were the typical temperatures for the growing season in Missouri. These curves used parameters from Table 2 for juvenile trees of cottonwood clone 1112. The non-linear photosynthetic function is also affected

by different parameter sets from each clone. Some photosynthetic parameters are critical for photosynthetic production and whole tree growth. The light index curve in Figure 19 was converted from net CO₂ assimilation curve in Figure 18 and will be used in segment growth allocation model.

Table 2. Parameters and constants about structure and physiology.

| Symbol | Meaning | value | Unit | Reference |
|-------------------|---|---------------------|---|---------------------------------|
| Branch Angle | Bifurcation Angle from main branch | 44 ± 14° | degree | measurement |
| Branching Azimuth | Azimuth of branch | random distribution | degree | measurement |
| r | Segment Length Shortening | 1.0 | m m ⁻¹ | measurement |
| sr | Root senescence rate | 0.0005 | Kg BM kg ⁻¹ BM d ⁻¹ | Dupraz <i>et al.</i> , (2004) |
| ar | Root-shoot ratio | 0.3 | kg kg ⁻¹ | Pallardy <i>et al.</i> , (2003) |
| gr | Root growth respiration rate | 0.25 | kg C kg ⁻¹ C | Rauscher <i>et al.</i> , (1990) |
| mr | Root maintenance respiration rate | 0.015 | kg C kg ⁻¹ C | Rauscher <i>et al.</i> , (1990) |
| mf | Foliage maintenance respiration rate | 0.015 | kg C kg ⁻¹ C | Rauscher <i>et al.</i> , (1990) |
| gs | Shoot growth respiration rate | 0.25 | kg C kg ⁻¹ C | Rauscher <i>et al.</i> , (1990) |
| ms | Shoot maintenance respiration rate | 0.015 | kg C kg ⁻¹ C | Rauscher <i>et al.</i> , (1990) |
| C _a | Atmospheric CO ₂ concentration | 350 | μmol mol ⁻¹ | Long, (1991) |
| O _a | Atmospheric O ₂ concentration | 210 | mmol mol ⁻¹ | Long, (1991) |
| K _c | Michaelis constant for CO ₂ | 460 | μmol mol ⁻¹ | Long, (1991) |
| K _o | Michaelis constant for O ₂ | 330 | mmol mol ⁻¹ | Long, (1991) |
| Sg | Wood specific gravity | 350 | kg m ⁻³ | Larson&Isebrands, (1971) |

Table 3. Parameters in cottonwood photosynthesis model with different clones.

| Species | 26C6R51 "red" | | 2059 "white" | | 1112 "yellow" | |
|---|---------------|--------|--------------|-------|---------------|-------|
| Age | old | young | old | young | old | young |
| V _{cmax} (μmol m ⁻² s ⁻¹) | 41.43 | 30.64 | 52.02 | 35.61 | 40.74 | 30.83 |
| CE (μmol m ⁻² s ⁻¹ CO ₂ Pa ⁻¹) | 0.0689 | 0.0546 | 0.0694 | 0.055 | 0.046 | 0.06 |
| QE@amb (mol CO ₂ mol ⁻¹ quanta) | 0.0496 | 0.0472 | 0.0503 | 0.057 | 0.0522 | 0.06 |
| QE@sat (mol CO ₂ mol ⁻¹ quanta) | | 0.0713 | | 0.07 | | 0.07 |
| P _{max@amb} (μmol m ⁻² s ⁻¹) | 11.29 | 10.55 | 11.88 | 10.82 | 9.24 | 13.2 |
| J _{max} (μmol m ⁻² s ⁻¹) | | 102.1 | | 106.6 | | 86.75 |
| R _d (μmol m ⁻² s ⁻¹) | 1.95 | 1.91 | 1.9 | 2.44 | 1.69 | 2.21 |

From unpublished data (Pallardy)

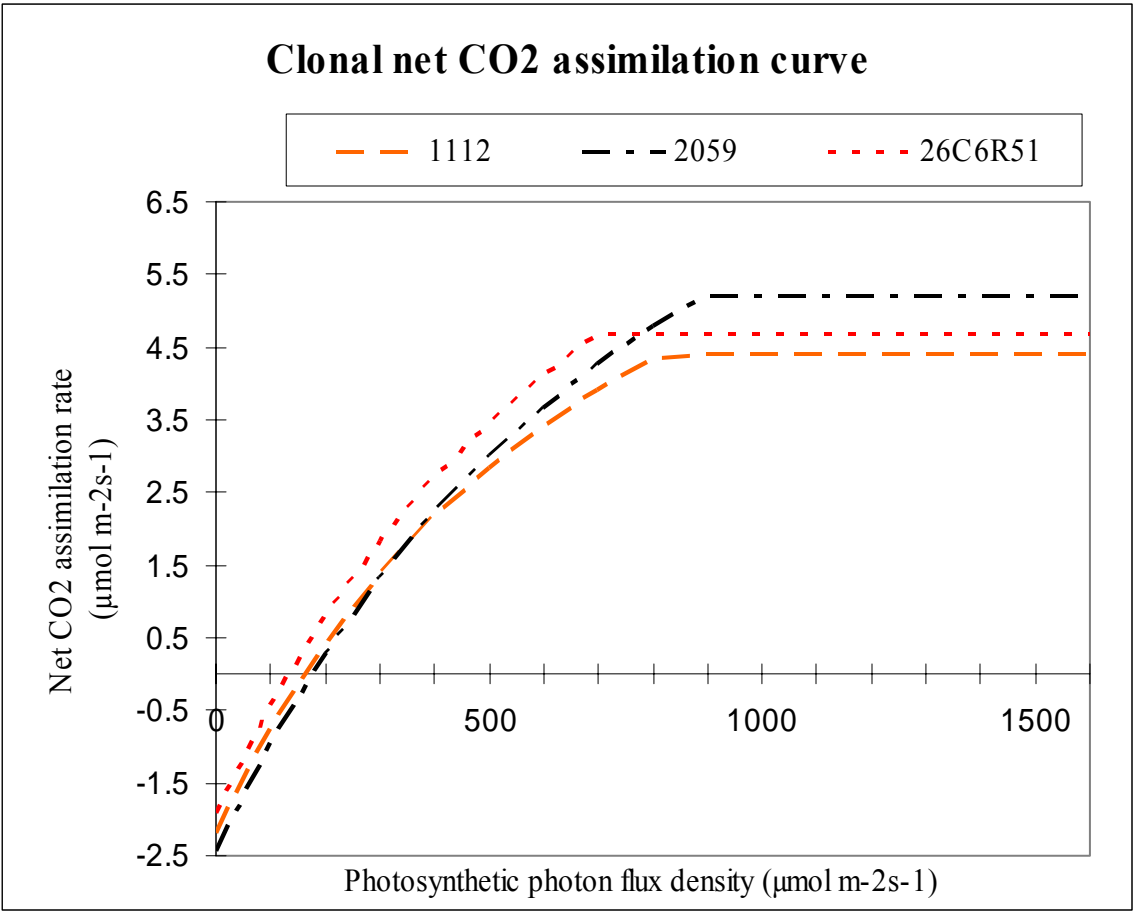


Figure 17. The clonal differences in net CO₂ assimilation rate among three cottonwood clones with parameter sets from Table 2, at 25°C.

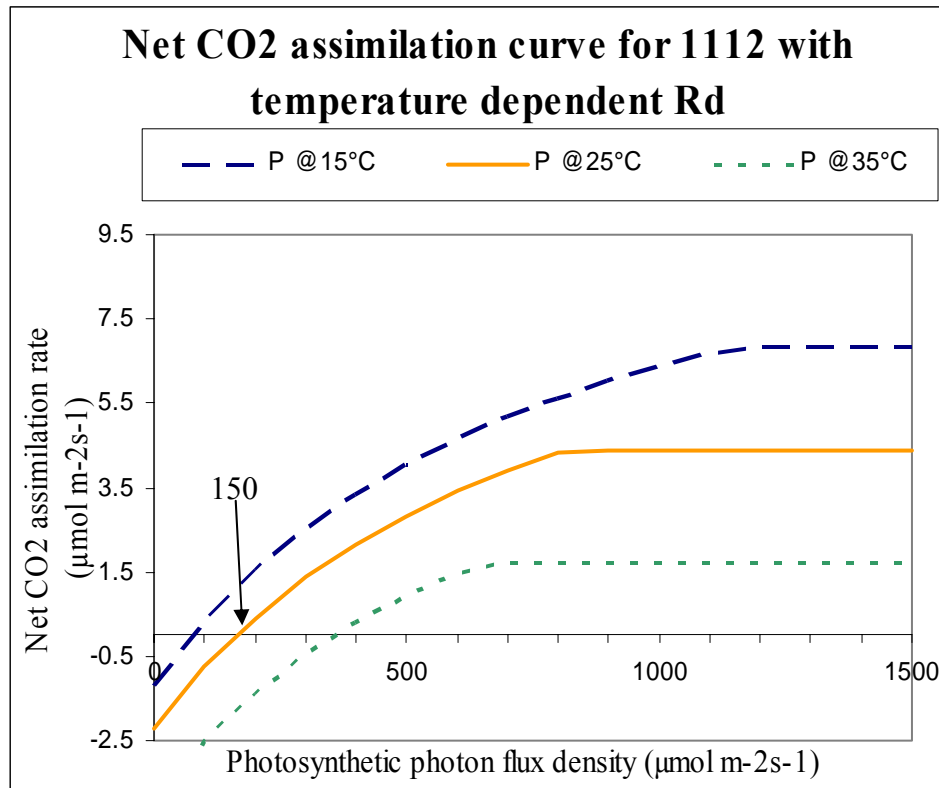


Figure 18. Non-linear relationships between net CO₂ assimilation rate and photosynthetic photon flux density. The net CO₂ assimilation rate decreases with the increase of growing temperature. The light compensation point is *ca.* 180 $\mu\text{mol m}^{-2} \text{s}^{-1}$

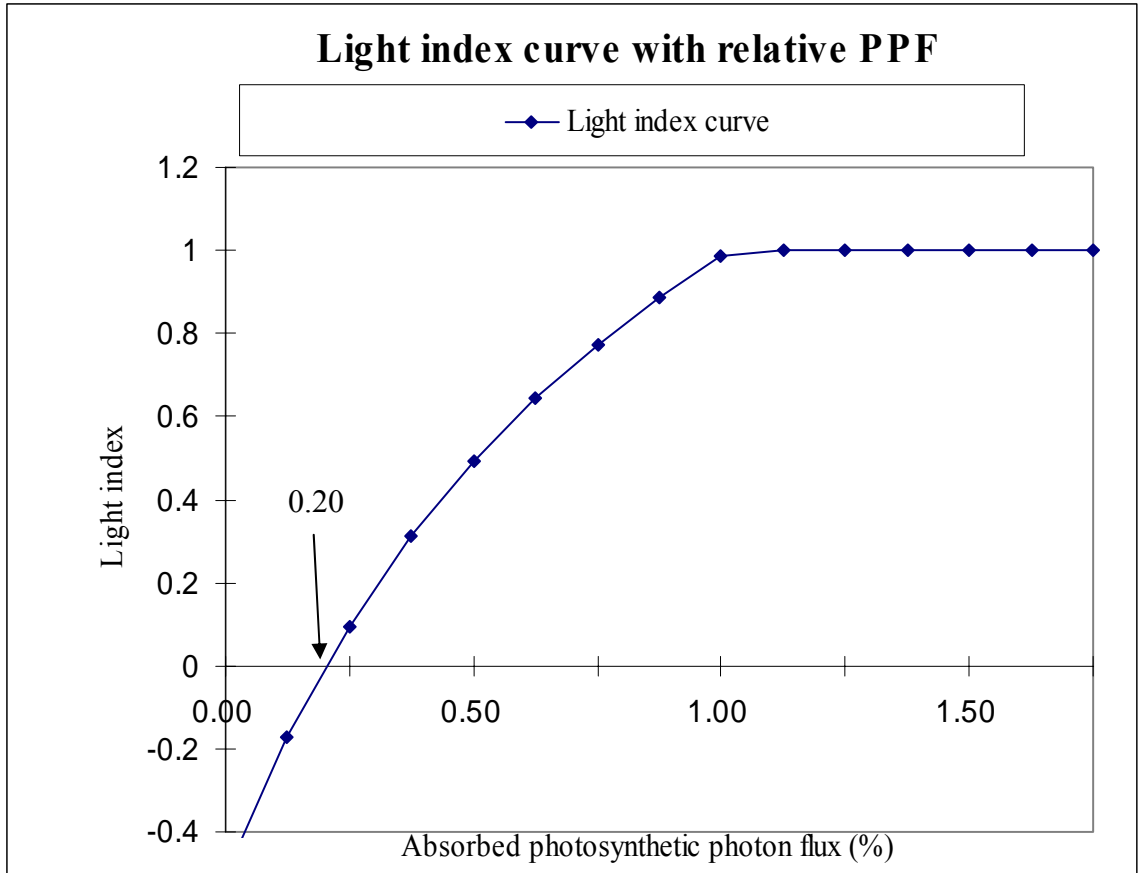


Figure 19. Light index curve with relative photosynthetic photon flux (PPF). The relative PPF value determines the light index in segment elongation in growth allocation. The relative PPF threshold point is 0.20, under which light index equal 0. The curve is borrowed from photosynthetic production curve with 25 degree temperature.

The structural modeling time step and voxel size are determined by branch length development and leaf growth. Figure 16 indicates the branch development in length and leaf emergence during growing season from April to October in field growth. The average length of internode segments is 0.055 meter. The selection of voxel size in LIGNUM model is related to segments' length to some extent. As a simplified representative for calculation unit, voxel size should be bigger than a single segment so as to contain one or more segments completely. At the same time, the resolution of voxel space should be small enough to be able describe the tree structure. The voxel size is set at 0.2 meter in this cottonwood simulation study. The selected voxel size is also reasonable the modeling computational load. For a tree in 4 meters high, there are about 2000 voxels for the whole tree growing space, and it takes about five minutes to simulate a tree growth in this size.

The branch length dynamic (Figure 16) also shows that the branch growth during growing season is stable and almost linear. It took about six weeks for the branch to grow 0.2 meter in average. Thus the structural time step is selected as 6 weeks so that a few new voxels would be created within the growing canopy during that period.

3.4.3 Model output and validation

The simulation result of individual cottonwood tree growth provides the detailed structural and physiological information about cottonwood tree growth under a specific abiotic growth environment. The detailed information includes tree height, total biomass in stem, branches, and roots. Additional information such as branch length and number of leaves and segments are also available on request. In addition to numerical data for model results, simulation results are also presented as a visualized tree. The tree

visualization provides heuristic expression of the simulated results, which can be compared and validated with the visual appearance of real tree growth.

After the modelling parameterization, LIGNUM model simulation for cottonwood growth is implemented and modelling results have to be verified. The model verification involves the comparison of model results with field data to ascertain whether the modelling method could explain the tree growth mechanisms in terms of tree structural development and biomass growth.

There are two general ways in which results of the LIGNUM model may be validated -- qualitative and quantitative approaches. The former involves examining the appearance and the general shape of the tree simulated with computer graphics. The quantitative method entails comparing the numerical data generated by the simulation model with the measurement data from field observations. A satisfactory match between simulation results and field measurements is necessary to validate the model.

Figure 20 shows a simulated 4-year-old cottonwood tree growing in a central Missouri growing environment. The visual image of simulated tree shows apical dominance in the tree crown. Each new branch attaches several new leaves, which split the entire branch into several segments. The bud at the position of each leaf will derive a new branch in next growing season. Branches in lower position bear fewer leaves because of the shading from upper tree crown. Stem diameter tapers significantly from base to tip of the tree. The modelled cottonwood structure appeared to satisfactorily reflect the actual growth of cottonwood trees in the field (Figure 21). The predicted crown shape is close to the actual canopy form.

Quantitative comparison between the tree height for simulation result and field

observations is presented in Table 4. The observation data were from the several trees with difference size growing in the open field shown in Figure 21. There is a good agreement for height growth for each year between the simulated results and field observations. Figure 22 plots the model simulation results and field observations of tree growth in height. The regression line indicates the growth trend of tree height with age in model simulation. The height growth trend matches well with the measurement data from the field. The simulated tree yielded estimates for growth in height, stem biomass, branch biomass, sapwood biomass, and foliage area. Such simulation results could obviously be compared to field measurements (Table 5).

The simulated height growth is closely related to the simulated total leaf area in the tree. As the tree matures, the leaf area gradually becomes stable and begins to drop. The tree height growth also begins to slow down in the sixth growing year (Figure 23). A visual representation of 10-year-old cottonwood individual tree growth in an open growth environment is presented (Figure 24).

The simulated tree growth also responds to the variation of radiation environment as might be expected. The model was implemented with reduced radiation level for a 4-year old tree growth simulation, one with 75% of original photon flux density and the other with 50% of original photon flux density (Figure 25). Under a condition of 75% of normal photon flux density, the simulated tree has much less leaf area compared to such a tree under a normal photon flux environment. Simulated tree height with 75% photon flux density is 6.58 meter in height at four years age, which is a little less than the height (7.34m) at full sun with the same age. In 50% radiation level, the tree growth is dramatically retarded, with the simulated tree attaining a height of only

4.26 meters at age four. The total leaf area is also extremely small (Figure 25). Such a growth response as displayed in the cottonwood tree growth simulation with LIGNUM actually reflects the shade intolerance of the cottonwood species.



Figure 20. The visualization of a simulated 4-year-old cottonwood tree growing in a central Missouri environment without shading by other trees.



Figure 21. Cottonwoods growing in the study field site in central Missouri. The alley cropping experiment (open site) was used for measuring model parameterization and validation data.

Table 4. Comparison between simulation and field data for cottonwood tree growth in open growth environment.

| Age | Measured Height (m) | Simulated Height (m) | Simulation running time |
|------------|----------------------------|-----------------------------|--------------------------------|
| 2 | 3.1±0.46 | 3.77 | 4 minutes |
| 3 | 4.85±0.5 | 5.75 | 13 minutes |
| 4 | 5.25±1.56 | 7.34 | 20 minutes |
| 5 | 7.1±1.5 | 8.23 | 55 minutes |

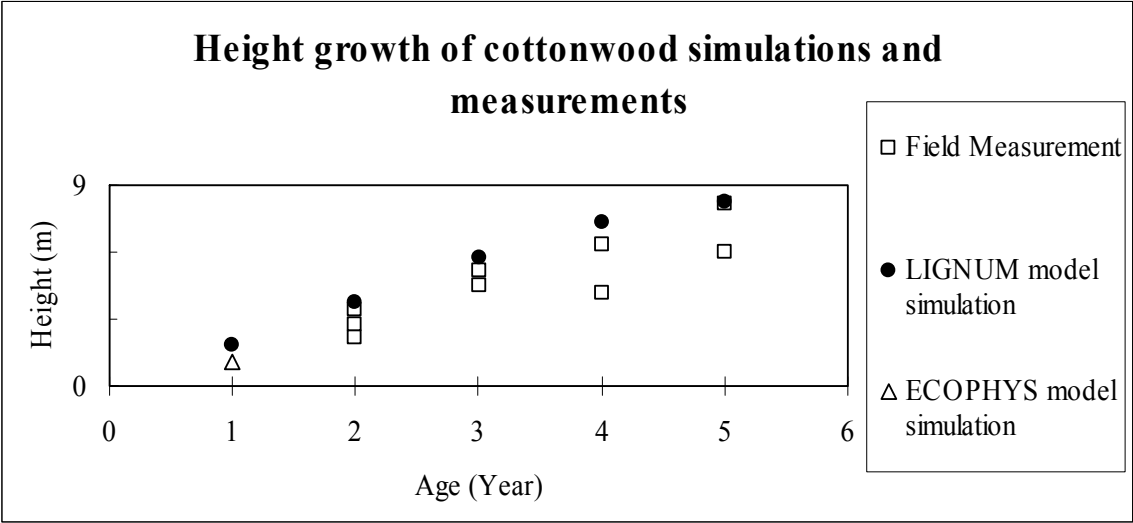


Figure 22. Height growth trend of cottonwood simulation and measurement. The trend line is the regression of LIGNUM modeling simulation results.

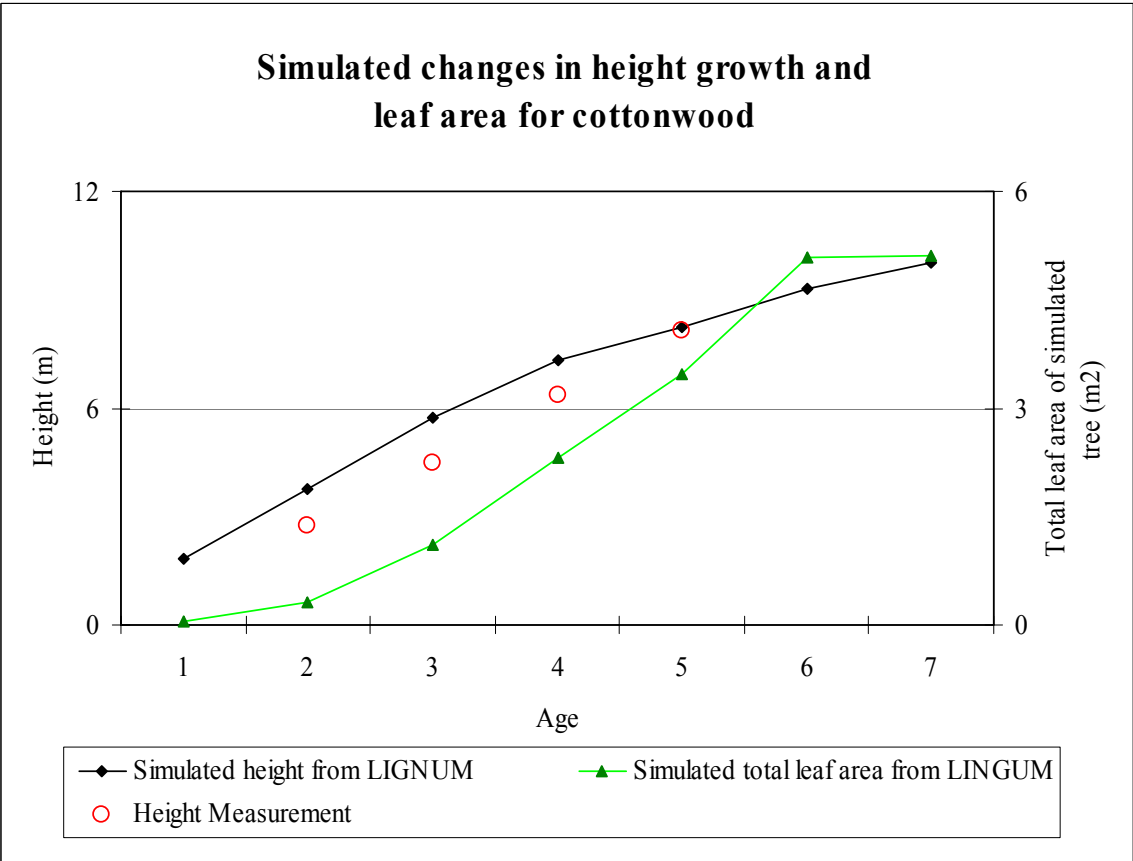


Figure 23. Changes in simulated height and leaf area with age in cottonwood simulation. The height growth is closely related to the leaf area growth in the simulated tree. The tree height and leaf area growth accelerate in the first five years; both acceleration slow down in the sixth growing year. The total leaf area drops from the seventh year.

Table 5. Simulated results of individual tree growth model (4 years) and field observation for 4-year-old tree growth.

| | | Simulation (4 Years) | Measurement (4 Years) |
|---------------------------|--------|---------------------------------|----------------------------------|
| | Stem | 4.91 | |
| Shoot Biomass (kg) | Branch | 0.67 | |
| | total | 5.57 | |
| Root Biomass (kg) | | 0.67 | |
| Height(m) | | 7.34 | 6.35 |
| LeafArea(m ²) | | 2.92 | |



Figure 24. Visualization of results of individual tree growth model for a 10-year-old cottonwood in an open growth environment without shading.

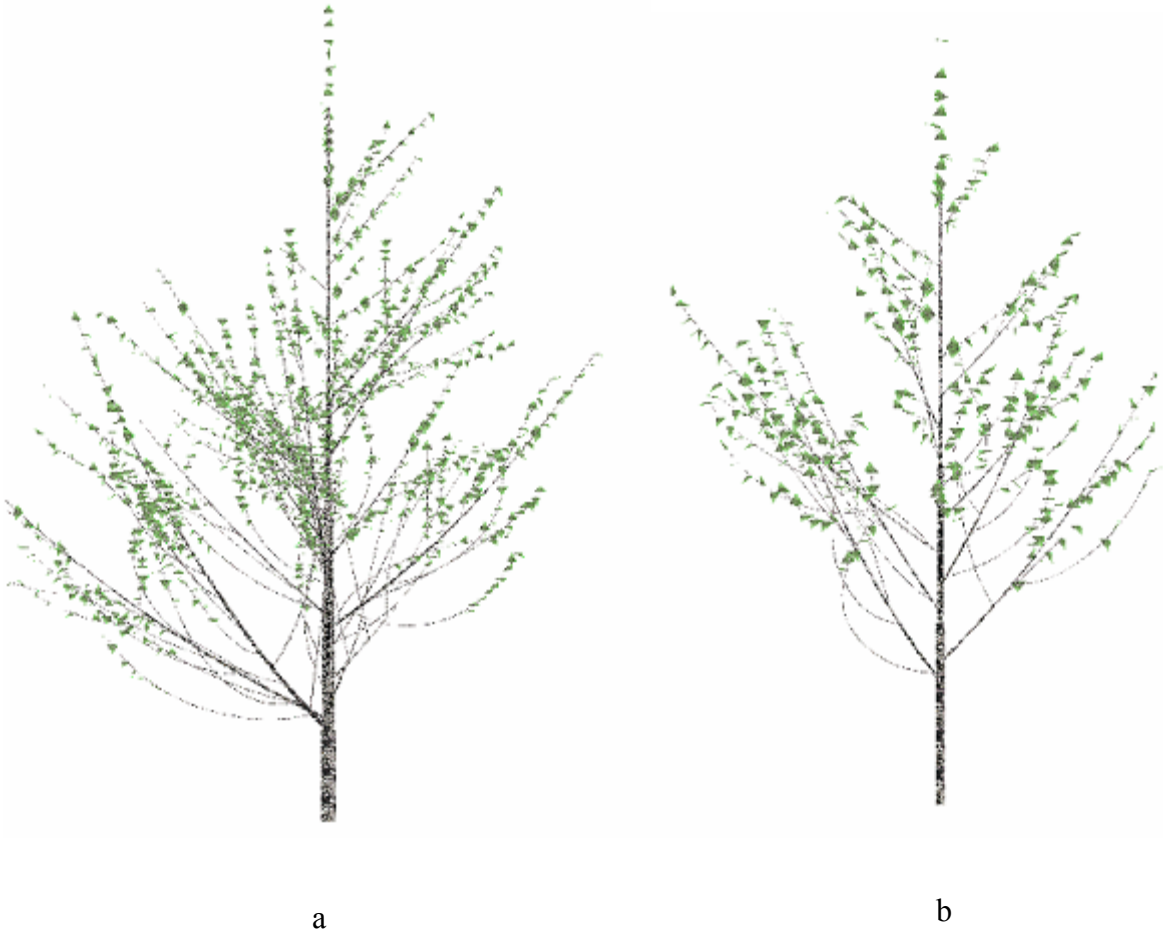


Figure 25. Visualization of tree growth response with decreasing light level. a) the simulated tree with 75% of original photon flux density. b) the simulated tree with 50% of original photon flux density.

3.4.4 Running time consumption in Simulation

The time requirement in LIGNUM calculation is proportional to the second power of the number of units. With pairwise comparisons, the computational time will be fourfold when the number of the tree compartment units is doubled (Sievänen *et al.*, 2000). The application of the short time step simulation significantly increases the calculation tasks for the overall simulation exercise. The voxel model was introduced into the LIGNUM radiation interception model to reduce the calculation task as an alternative to using pairwise comparisons.

The introduction of the voxel space model into cottonwood simulation for photon flux interception calculation resolved the potential danger of computational overload in the model. Instead of using leaves and tree segments as units for calculation, voxels are used to determine photon flux interception. Both the number of tree compartments – leaves and segments – and number of voxels are obtained from tree growth simulation at different ages. The number of voxels is significantly less than the number of total tree compartments (Figure 26). Moreover, the computational time of the voxel space model is proportional to the total number of the valid voxels comprising the tree growing space, as opposed to the computational time in pairwise comparison, which is equal to the second power of the number of tree compartments. As a result, the calculation time with voxel model is much less than that for pairwise comparison.

Computational time between voxel model and pairwise comparison for cottonwood simulation at the same age is compared (Figure 27). The X axis is the increase of computational time with age in voxel model; the Y axis is the possible computational time with pairwise comparison with the same age based on the number of

tree compartments obtained from simulation. The points in figure 27 denoted simulated trees with different ages. The figure indicates that the computational time with pairwise comparison is almost the second power of that in voxel model (the power value for trendline is 1.86 with slope value 10.5).

The use of the extendable voxel space model reduced overall modeling calculation requirements. However, calculation needs do increase dramatically with the increase of growing space. For example, with respect to time required for running the growth simulation model, it takes 1 minute to simulate growth of a 2-year-old tree, 20 minutes for a 4-year-old trees, and more than one hour for an 8-year-old tree.

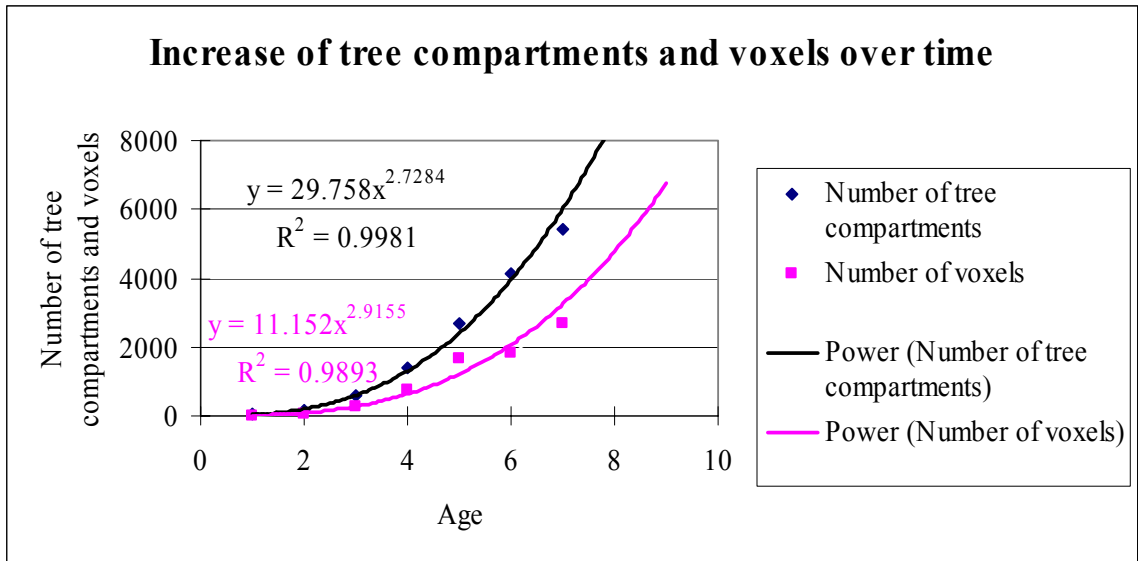


Figure 26. The increase of voxel number and tree compartments with age. The calculation units for radiation interception in voxel model is reduced dramatically.

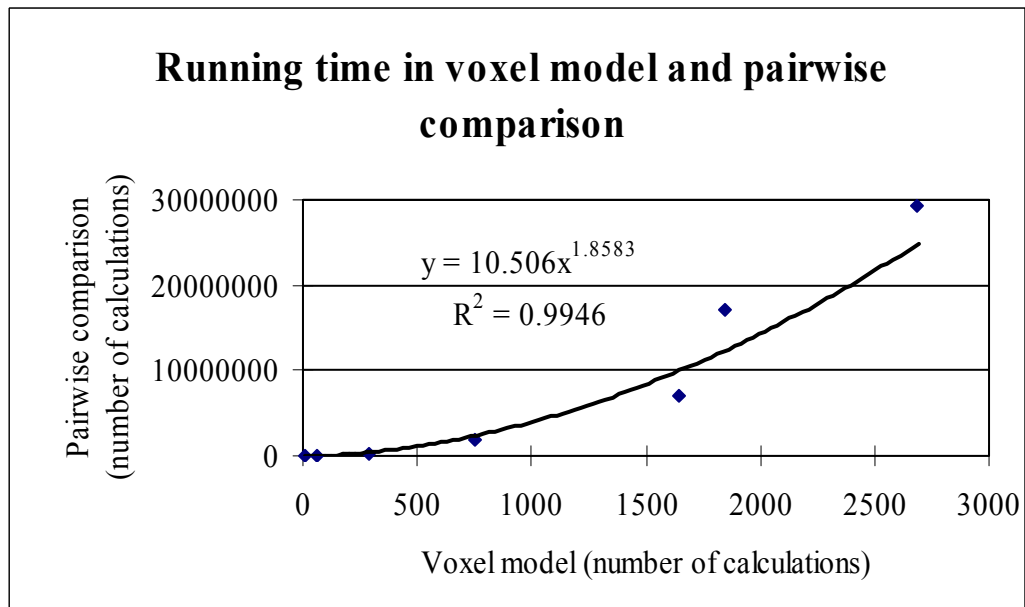


Figure 27. The calculation with pairwise comparison is about the second power of the calculation in voxel model. Running time is the number of calculation times for most time consuming core part in the model.

3.4.5 Sensitivity analyses

A sensitivity analysis was applied to several of the most important tree growth parameters in the cottonwood simulation model to determine the most urgent foci for further model development. The photosynthetic and respiration parameters were the most difficult to measure accurately, due to their dependence on the environment as well as practical issues (Lo, *et al.*, 2001) such as instrument and labour requirements. Tree response to water stress might lead to variation in growth allocation to roots. Morphological parameters and respiration rate might also affect tree growth in terms of resultant biomass and volume.

The seven parameters subjected to sensitivity analysis included: J_{max} (maximum rate of electron transport); V_{cmax} (maximum rate of carboxylation); R_d (day time leaf respiration rate); wood respiration rate; wood specific gravity; specific leaf area (leaf area per unit leaf mass); and root/shoot ratio. In order to test the sensitivity of the model to changes in these parameters, tree growth index data including height, foliage area, stem mass, branch mass, and wood mass were obtained from the simulated tree. Responses of these growth indices to variations in modelling parameters were analyzed, and results are depicted in Table 6.

The parameters were varied by $\pm 25\%$ of their original value. Table 6 displays the variation of these growth indices for both a 25% increase and a 25% reduction in the parameter values tested. In most cases, these growth indices are affected similarly by variation in a given parameter: either all increase or all decrease. The simulation results corresponding to parameter variation are also displayed in Figure 28. Each line is the

difference of simulated tree growth for one parameter's variation in two directions — increase and reduction. In each line, the x axis is the growth indices, and the value in y axis is equal to simulated tree growth with increased parameter minus the simulated tree growth with decreased parameter. The difference of simulated tree growth is used here as the criterion of model sensitivity to parameter variation.

The closer the line to 0, the less sensitive is the parameter. Figure 28 reveals that the model was least sensitive to V_{cmax} value, root/shoot ratio, and specific leaf area. The variation of modelling results is in the same direction as the variation of J_{max} . However, variations in foliage respiration, wood respiration, and specific gravity had opposite effects in resulting modelling growth. The increase of one parameter value (J_{max}) increases the growth indices significantly; the increases of some parameter values (R_d , wood respiration rate, specific gravity) dramatically reduce growth indices; varying other parameters (V_{cmax} , Root/Shoot ratio, specific leaf area) did not make a significant difference in growth index values. For a specific parameter and its relationship to a particular growth index, varying the parameter value in the direction opposite to the initial variation generally resulted in growth index departures of similar amplitude in the opposite directions.

Combined sensitivity analyses were accomplished by applying two sensitive parameters together (Tables 5 and 6). V_{cmax} value, root/shoot ratio, and specific leaf area, the three parameters to which the tree growth indices were not sensitive in the simulation exercise, were not used in the combined sensitivity analysis. The other four parameters included: J_{max} , R_d , wood respiration rate, and wood specific gravity. Each parameter was tested in conjunction with another parameter, yielding four possible scenarios of

combined variation. For example, the combination for parameters a and b can be: a+b+, a-b-, a+b-, and a-b+. The above sensitivity analysis revealed that changes in growth indices such as height, biomass, and leaf area parallel with changes in model parameters. The combined sensitivity test used only one growth index — height — as a representative to test the effects of combined parameter variation.

The combined test for sensitive parameters indicated that changes in two parameters in the same direction can dramatically influence tree growth. On the other hand, changes of two parameters in the opposite direction may cancel each other's effect on tree growth. For example, the variation on parameter J_{max} alone results in height variation with +10.7% and -15.1% (Table 6). While the combination of $-J_{max}$ and $+R_d$ results in 38.4% increase in tree height growth (Table 8). The only exceptions are the combination of specific gravity (+) with wood respiration rate (\pm). The most significant parameter pair was the combination of decreases in both specific gravity and respiration (Table 7). This led to a 62.3% increase in tree height (as the selected index of growth), much bigger than the 25% parameter variation. On the other hand, the combination of J_{max} reduction and R_d increase resulted in the highest reduction with 38.4% in tree growth (Table 8).

Table 6. Sensitivity analysis of parameters for cottonwood growth model. Changes in the value of growth indices with the variation of parameter values:

| Parameters | J_{max} (%) | V_{cmax} (%) | R_d (%) | Respiration Rate (%) | Specific Gravity (%) | Specific Leaf Area (%) | Root/ Shoot Ratio (%) |
|------------------------|------------------|-------------------|--------------|----------------------------|----------------------------|---------------------------------|--------------------------------|
| Height (+) | 10.7 | -0.98 | -14.6 | -8.5 | -14.6 | 0.48 | 2.76 |
| Height (-) | -15.1 | -0.2 | 19.0 | 6.34 | 32 | 0.48 | 2.50 |
| FoliageArea (+) | 30.8 | 0.8 | -58.9 | -29.9 | -50.5 | 1.39 | 4.2 |
| FoliageArea (-) | -51.4 | 0 | 16.8 | 5.6 | 67.3 | -1.39 | 15.7 |
| StemMass (+) | 38.8 | 2. | -55.6 | -26.7 | -42.2 | 2.13 | -2.4 |
| StemMass (-) | -53.3 | 2. | 48.9 | 17.8 | 35.6 | 2.13 | 9.5 |
| BranchMass (+) | 49. | 6.1 | -59.2 | -28.6 | -42.8 | 0 | -10.9 |
| BranchMass (-) | -55.1 | -2.0 | 32.7 | 16.3 | 38.8 | 0 | 13.04 |
| SapwoodMass (+) | 43.6 | 4.3 | -57.4 | -28.7 | -42.6 | 1.28 | -6.7 |
| SapwoodMass (-) | -55.3 | 0 | 41.5 | 17.0 | 37.2 | 0 | 10.1 |

(+): change of sensitivity parameters' value with a 25% increase; (-): change of sensitivity parameters' value with a 25% reduction; the growth indices value in the cell is the increase or reduction rate (%) with parameters variation compared to growth indices value with original parameters.

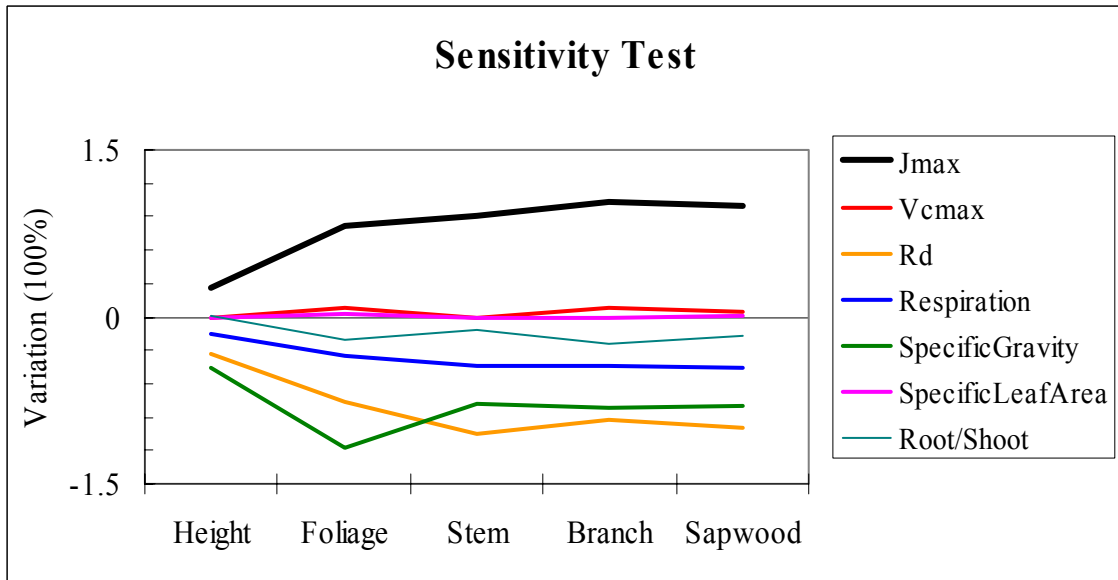


Figure 28. Tree growth variation with 25% variation in modelling parameters. The variation data (Y axis) are the difference of simulated tree growth indices value for one parameter's variation in two directions — increase and reduction. The less the variation is, the less sensitive the parameter. The two parameters V_{cmax} and Specific Leaf Area are close to line $y=0$, which means they are non-sensitive parameters in the model.

Table 7. Sensitivity analysis with variation on parameter combinations. Growth index data – height – is used to test the model sensitivity with parameters.

| 25% ++ / 25% -- | J _{max} | R _d | Respiration | SpecificGravity |
|------------------|------------------|----------------|----------------|-----------------|
| J _{max} | | -0.056* | 0.068* | -0.104* |
| R _d | -0.010* | | -0.251** | -0.321** |
| Respiration | -0.112* | 0.328** | | -0.039*** |
| SpecificGravity | 0.054* | 0.445** | 0.623** | |

Each two parameters are combined as a pair for sensitivity test. The upper triangle of the matrix is the height growth variation with both 25% increases in tested parameters; the lower triangle of the matrix is the height growth variation with both 25% reductions in tested parameters. The height value in the cell is the increase or reduction rate (non-unit) compared to height value with original parameters. The number in bold has greatest increase in tree height growth.

* Changes of two parameters in the opposite direction could cancel each other's effect on tree growth.

** Changes in two parameters in the same direction can dramatically increase their influence on tree growth.

*** Exception

Table 8. Sensitivity test with variation on parameter combinations.

| - / + | J _{max} | R _d | Respiration | SpecificGravity |
|------------------|------------------|----------------|-------------|-----------------|
| J _{max} | | 0.231** | 0.178** | 0.409** |
| R _d | -0.384** | | -0.122* | 0.027* |
| Respiration | -0.248** | 0.088* | | 0.384*** |
| SpecificGravity | -0.328** | -0.010* | 0.051* | |

Each two parameters are combined as a pair for sensitivity test. The upper triangle of the matrix is the height growth variation with 25% increases in column head parameters and 25% reductions in row head parameters; the lower triangle of the matrix is the height growth variation with 25% reductions in column head parameters and 25% increases in row head parameters. The height value in the cell is the increase or reduction rate (non-unit) compared to height value with original parameters. The number in bold has the greatest reduction in tree height growth.

* Changes of two parameters in the opposite direction could cancel each other's effect on tree growth.

** Changes in two parameters in the same direction can dramatically increase their influence on tree growth.

*** Exception

3.5 Discussion

Building on previous applications of the LIGNUM model in simulating conifer and sugar maple growth, this effort relative to cottonwood simulation focused on the adaptation of LIGNUM modeling to another deciduous species. The LIGNUM model itself was modified for improved calculation efficiency and modeling accuracy. These modifications included physiological properties of cottonwood and its specific branching pattern. Developments in LIGNUM model for cottonwood included the system of nested time steps, use of real weather data, application of a new leaf CO₂ exchange model, and use of voxel space for computing the interception of photon flux. At the same time, limitations of this project include the extensive computational time, knowledge required of botanical and physiological dimensions of cottonwood growth and structure, and the continuing need to improve modeling algorithms.

3.5.1 Model evaluation

The cottonwood simulation model using the LIGNUM method includes a complete parameter system with constants and parameters derived from the literature, experimental measurements, and field observations. The model supported with the parameter system produced satisfactory simulation results when compared to current field growth data.

The current cottonwood growth simulation model intends to simulate the cottonwood plantation in flood plain with short rotation. The model assumes that the heartwood in the juvenile cottonwood is negligible (Bruce Cutter, personal communication). However, with the growth of tree height and diameter, the modeled non-senescent sapwood diameter consumes a greater proportion in carbon allocation and

respiration. It would be highly desirable, therefore, to include heartwood in future growth modeling effects for more mature cottonwood trees.

Based on the simulated results, new hypotheses pertaining to tree growth and other additional modeling factors can be embedded into the model to improve model assumptions and parameters and thereby enhance the quality of modeling results.

3.5.2 Precision and efficiency of the model

Modeling accuracy is one of the criteria for defining a good model. Cottonwood simulation with the LIGNUM model provides both accurate and efficient modeling results for individual cottonwood tree growth.

Modeling precision

Modeling results for tree height are close to field measurements. The exponential regression of LIGNUM simulation results on cottonwood growth data produced a good fit with these field data (Figure 22). The one-year result for poplar growth from the ECOPHYS model is 110 cm (Rauscher *et al.*, 1990), which is close to the LIGNUM simulation results in this study for one year old cottonwood growth in an open stand. Compared to the detailed calculations of geometrical shape and size of each leaf required in ECOPHYS, the growth hypothesis in the LIGNUM simulation greatly simplified the tree growth modeling process without sacrificing model accuracy. Furthermore, such simplifications in tree growth modeling enable the LIGNUM model to simulate and predict growth for older trees as well as younger ones.

In previous LIGNUM studies, a linear relationship was used to predict tree photosynthetic production to simplify the modeling process (Perttunen *et al.*, 1996). There are also tree growth simulation models using photosynthesis-PPFD response

curves to calculate the tree photosynthesis precisely (Rauscher *et al.*, 1990). Farquhar's photosynthesis model was applied in this study to reflect the photosynthetic response to the photon flux density and internal crown shading. Farquhar's photosynthesis model yielded a non-linear relationship between photon flux density and photosynthetic production, which represents a reasonable description of actual tree growth. The use of Farquhar's photosynthesis model lends a stronger physiological basis to the overall tree growth simulation effort.

In the cottonwood growth model, photosynthetic production is calculated every 30 minutes with concurrent absorbed photon flux density, temperature, and solar position. Although the use of an annual time step was a reasonable and obvious choice, given that tree growth occurs via a repeated process cycle every year, a short time step simulation was applied in juvenile tree growth (Rauscher *et al.*, 1990) to provide a more detailed tree structural update. Short time step simulation is also a necessary ingredient in simulating the fast-growing cottonwood tree. The application of two nested short time steps enabled the model to update the tree canopy structure more frequently and accordingly adjust photon flux interception in the model. The 30-minute-photosynthesis calculation with real weather data helped to connect the model and local environment so as to reflect the effect of environment on tree growth. The other time step for structure update is intermediate in length to that of the photosynthesis time step and the seasonal time step.

As noted above, the leaf photosynthetic production was calculated every 30 minutes in the model, and tree crown structure was updated four times during one growing season. The model simulated tree growth during growing season from April to November. In each simulated growing season, there are 240 days, 24 hours in a day and

60 minutes in an hour. In contrast a single calculation for structure update and photosynthesis in the previous model, there are $240 \times 24 \times 2$ calculations for direct photon flux interception and leaf photosynthesis calculation. In addition, one diffuse photon flux interception was calculated in each structural time step for all photon fluxes coming from all sectors of sky. Here one calculation is the process of the photosynthesis for the whole tree, including photosynthesis in each leaf.

Selection of voxel size is also a critical element that affects both modeling efficiency and modeling result precision. A small voxel size can catch more detailed tree crown structure pattern, however, it will add heavy load in modeling computation. On the other hand, a big voxel size can simplify the modeling computation, but it may also result into bigger simulation error. The simulation result with one meter voxel size showed that the tree received more photon flux and resulted in overestimate of simulated tree growth in tree height, biomass, and leaf area.

On an overall basis, therefore, the application of real weather data, Farquhar's photosynthesis model, and a short time step simulation combined provide a confidence in modeling accuracy. However, the precision of this model was obtained at the expense of very extensive calculation time, as calculation of photosynthesis at 30-minute intervals put a heavy load on the model. The simulation time for a 2, 3, 4, 5 years old tree growth is 1 minute, 4 minute, 12 minutes, and 20 minutes, respectively. It takes about several hours to simulate growth for a 10-year old tree. In contrast, the simulation process with annual physiological and structural time step needs only several seconds for 10-year-old tree growth simulation.

Stochastic simulation

The Monte-Carlo voxel space model, which is applied in this cottonwood simulation, is stochastic in nature. The chance of radiation interception is related to the leaf density in the voxel. The stochastic Monte-Carlo model accommodates the inherent variety in the growing tree in nature. Every tree is unique, and its growth will be affected by both generic and environmental factors. The results of tree growth simulations will vary from case to case even with the same set of parameters. However, the average result will reflect the actual growth situation.

Calculation simplification

In assessing photon flux interception, the model employed the stochastic Monte-Carlo method to calculate the amount of PPFD received by tree compartments. The photon flux interception was affected by tree structure. In addition, photosynthesis process was implemented every 30 minutes in the model with real radiation input data. However, updates of tree structure did not keep the same pace as those for photosynthesis. Within the tree structure update cycle, diffuse radiation interception was only calculated once with new structure for standard intercepted diffuse radiation. Thereafter diffuse radiation interception was casted from the first one with diffuse radiation input value until next structure update. This method greatly accelerated the speed of conducting model calculations.

3.5.3 Model implications

The application of the LIGNUM method in this simulation of cottonwood growth in flood plain areas of central Missouri is an example of a functional-structural model that combines both the morphological structure of the tree canopy and physiological functions. The simulation examines several botanical hypotheses related to tree growth (tree growth allocation rate in shoot, shoot/root ratio, branch dynamic, and leaf growth development) and applies advanced computational technology in tree growth research. The computational organization for this tree growth simulation provides a complementary method to traditional field experiments in forestry studies, which are more time consuming, labor intensive, and potentially weather-susceptible.

The two properties of cottonwood growth of major importance in this model are its fast growth and shade intolerance. In order to capture the intricacies of rapid cottonwood growth, cottonwood simulation with LIGNUM used a short time step. The length of time steps selected was based on both computational efficiency and simulation accuracy. The time step of a fraction of a growing season for structure update fits well for the simulation of fast-growing cottonwood.

Cottonwood growth is also very sensitive to intercepted photon flux. The use of actual weather data provides the availability of depicting the radiation environment of the growing tree accurately. The link to actual weather data enables better convergence of model results with real world tree growth. It also shows that photosynthetic production is quite sensitive to photosynthetic parameters (Figure 17; Table 3). It can be expected that the model can be used to help to identify cottonwood clones for flood plain forest.

While the use of real weather data and a short time step for estimating NPP increased the actual computational requirements for the model, the use of voxel space considerably speeds up estimation of input radiation compared to earlier LIGNUM versions (Perttunen *et al.*, 1996; 1998; 2001). The voxel model replaces the smaller irregular tree compartments with a larger regular voxel as the basic unit for calculating radiation interception. This significantly simplifies the computer calculations for the model. The stochastic Monte Carlo voxel model provides a method for simulating photon flux interception that effectively mirrors reality.

The simulation results obtained in this study were quite close to field observations for cottonwood growth with the same environmental input in terms of height and biomass. Visual representation of cottonwood simulation enhanced the reliability of the modeling exercise as well as user confidence in such models. The LIGNUM modeling method has proven to be a general one for tree growth simulation for both conifer and deciduous species, whether slow-growing or fast-growing in nature. The modeling results based on field measured branching parameters, photosynthesis parameters, literature-obtained constants; radiation interception assumption, empirical shoot growth rules, and growth allocation distribution were validated by means of field observations. The response of tree growth simulation results to variations in modeling photon flux input was logical. The modeling method can be used as an aid to predicting tree growth, economic analysis, and management decision making.

The computer-based tree growth simulation model may be useful as a complementary tool in predicting the appearance of tree growth in the real world. One of the purposes of tree growth modeling in forest research and management is to predict

future tree growth and to answer questions regarding the potential effects of certain treatments on a forest over time. Tree growth is obviously a long-term process. Its results cannot be observed instantly. Simulation models may be used to predict the effects of forest management on future growth. Moreover, the model in this project also incorporated a weather factor in relation to plant growth. Thus this model could also be helpful in predicting possible effects of environmental changes on plant growth. In these and other ways, modeling cottonwood growth with the LIGNUM method could provide long-term simulation results of tree growth to help predict possible actual tree growth in the future.

3.5.4 Model limitations

A model is a mock-up of reality. A model can never be as good as reality unless that reality is repeated. Each model will have deficiencies in some way. The cottonwood tree growth simulation with LIGNUM also has several restrictions.

Although the simulation is intended to facilitate tree growth research by easing the burden of field experiments, extensive field work will always be necessary to understand tree growth patterns. The morphological analysis requires data on crown branch structure including branch bifurcation, branch direction, branch angle, segment length, and leaf size. Tree growth allocation also requires information about branch diameters and biomass distribution throughout the tree. In this case, sensitivity analysis was applied to determine the most sensitive parameters as the most urgent foci for field measurement.

Even with a large amount of field measurements, the tree structure and

physiological growth rules were simplified for the sake of model simplicity. The branches were assumed to be evenly distributed in all azimuth directions. The four branches in each position were deliberately selected as oriented to south, east, west, and north directions. Root growth was simplified as one part of the sink in biomass as a fraction of total net growth. Growth allocation for the above-ground tree applied empirical rules in segment elongation and thickening such as vigor index and radiation index.

With the application of real weather data and short time step modeling, the simulation was quite time consuming. The number of tree compartments and valid voxels increase at the rate greater than a power of two (Figure 29). Thus, for example, at age 8, the simulated tree will occupy totally about three to four thousand voxels as opposed to 12 voxels at the age of 2.

The model can not be applied to older tree simulation. The conversion from sapwood to heartwood is ignored in current model, nor does it include other tree physiological processes such as seed production and maturation. Further improvements are needed for a wider application of this model.

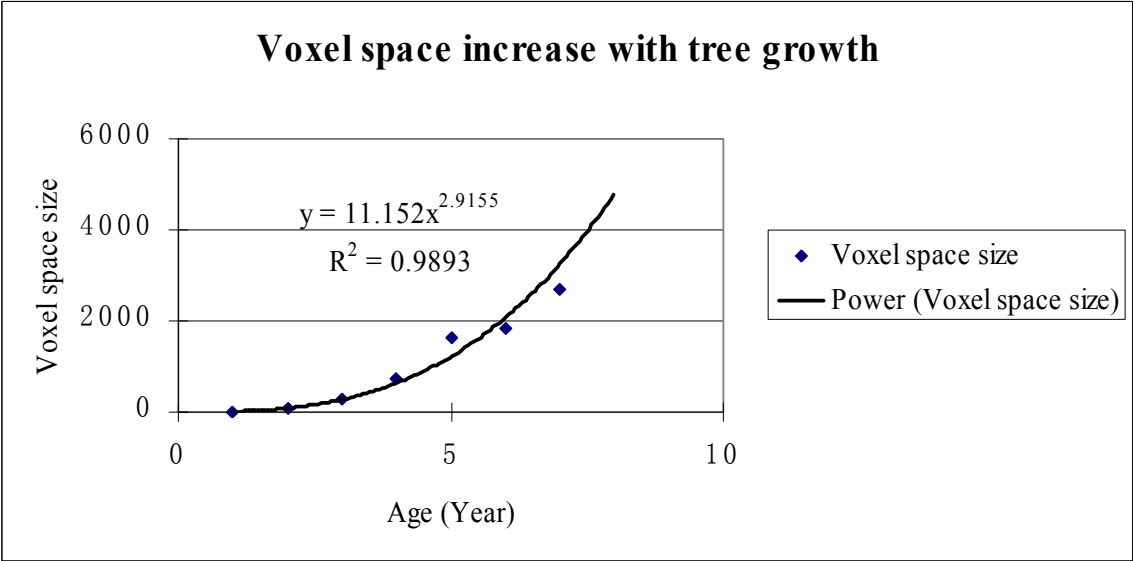


Figure 29. Increase in voxel space number with age and associated tree growth.

3.5.5 Future research needs

This cottonwood growth simulation model focused primarily on the above-ground part of tree growth. Nonetheless, root growth and development is also an important aspect of tree growth. Root structure and dynamic growth will be an important topic for LIGNUM research in the future.

The cottonwood modelling discussed here focuses on tree growth at a young age. Stem and branch heartwood is not considered in the current version. In order to simulate cottonwood at older ages, it will be necessary to include heartwood in the model.

The use of voxels as evenly divided partitions of the growing space greatly simplifies modelling calculations. However, there is great redundancy when tree compartments are clustered in only a part of the voxel space. An octonary voxel space method (a method to divide the growing space according to the tree growth, rather than even-division) can be applied to voxel space division for calculation simplification and detailed structure genesis. When the tree compartment density is high, the voxel can be divided into smaller sizes to obtain more tree detail.

4. TREE STAND GROWTH MODEL

The second objective of this research was to simulate cottonwood growth within a tree stand, with competition among trees for photon flux energy and growing space. Having discussed the modelling framework from individual tree simulation, stand growth simulation represents an extension of the LIGNUM model application in cottonwood growth. The cottonwood stand growth assume that trees in the stand grow in the same way as do open growth trees in terms of physiological processes, structural development, and growth allocation, except that trees in stand are subject to shading from surrounding trees.

4.1 Forest modeling: Purpose and Foci

Knowledge of stand growth and increment is important for effective forest management. One way to learn about stand growth is with the aid of forest modeling methods. Individual tree growth models and forest growth models emerged about the same time in the latter part of the nineteenth century (Botkin, 1972; Greenhill, 1881). During their long history, a wide variety of forest growth models were developed, from simple curve-fitting approaches to complex models dealing with tree physiological processes and crown structure.

As these models have become more complex, the world itself has surely kept pace. Continuing demand for timber products requires more intensive industrial plantation forestry, and the wood products industry needs to be able to predict timber growth and yield accurately in management of forests for desired wood production. World-wide environmental issues, such as species conservation, water quality and

quantity, and carbon sequestration, may be more effectively addressed with the aid of these kinds of models, which have a role to play in the management and preservation of sustainable ecosystems (Vanclay, 2003).

Growth modelling approaches continue to become more efficient at integrating different kinds of growth/yield data and analytical tools with new technologies. Stand growth simulation also continues to be a topic of interest to forest scientists. Scientists are interested in these models not only for their many practical applications in addressing environmental and natural resource issues or meeting economic needs; but also because such models may help them continue to learn about the underlying processes of tree growth.

Forest modelling is concerned with entities on a larger scale than those addressed in individual tree simulation. This larger scale simulation is more complex and at the same time not as detailed as individual tree simulation both in terms of physiology and structure. In general, there have been three main purposes for forest growth simulation: understanding the growth of a *group* of trees; simulation of forest management scenarios, and prediction of timber production. With the emergence of new technologies, more accurate and convenient stand growth models continue to become available.

The growth of individual trees or tree stands may be assessed in terms of three basic components: diameter growth, height elongation, and volume increase. In addressing the above, forest scientists have looked at a variety of processes and entities involved in forest growth. These include: forest growth dynamics (Botkin *et al.*, 1972; *Simile* simulation model [Simulistics Ltd, Scotland, 2005]); carbon sequestration by the

forest canopy (Mäkelä, 1997; Hunt *et al.*, 1991); forest tree height growth strategies (Mäkelä and Sievänen, 1992; Mehtätalo, 2004); crown rise (Valentine *et al.*, 1994); tree competition in forest stands (Mäkelä and Vanninen, 1998; Sorrensen-Cothorn *et al.*, 1993); photosynthesis and radiation use efficiency in forests (Goetz and Prince, 1999; Sands, 1996; Norman and Arkebauer, 1991; Mäkelä and Valentine, 2001); growth response to forest management (Huber, and Stuefer, 1997; Balandier *et al.*, 2000) and fertilization application (van den Driessche, 1999; Brown and van den Driessche, 2002); forest canopy productivity (DeBell and Harrington, 1997; Landsberg and Waring, 1997); and physiological and morphological responses to water stress (Mazzoleni and Dickmann, 1988). All of these research efforts have both contributed to the understanding and refinement of principles related to forest growth as well as been applied in management activities for timber production in the area of industrial forestry.

Forest dynamics and forest production are the most popular topics that have been addressed by those working with conventional empirical and process-based tree growth models. One of the earliest types of empirical forest growth model to be developed was the yield table, which provides expected productivity or volumetric yield for a given stand age, site quality and perhaps other indices such as stand density or certain forest management practices.

Another kind of forest growth model is the process-based model, which is more complex than the yield table in its direct consideration of physiological processes of tree growth. An example of process-based model is FOREST_BGC. This is a forest stand model that calculates the carbon, water and nitrogen cycles within a forest ecosystem. McMurtrie (1991) described another process-based modeling process focusing on the

relationship of forest productivity to nutrient and carbon supply. It is relatively rare for morphological tree growth models to simulate the plant community in a forest. Lane and Prusinkiewicz (2002) used L-system to simulate forest succession and visualize forest growth. There are also some well-developed software packages for forest growth modeling. *Simile* is one such package for forest growth simulation; it uses a diagram-based language to predict the forest growth dynamics under particular growth hypotheses (Simile simulation software [Simulistics Ltd, Scotland, 2005]).

Functional-structural tree growth modeling methods have not usually been applied to forest growth simulation because of their detailed consideration of tree organs such as leaves and segments. However, the more advanced computational capacity of computers and the enhanced efficiency of algorithms developed in recent years provide an opportunity for simulating stand growth with functional-structural growth modeling approaches.

4.2 Simulation of the growth of a cottonwood stand

Cottonwood stand simulation involves simulating and predicting the growth of a group of cottonwood trees on a particular site. Based on the growth simulation of an individual cottonwood tree, a functional-structural growth modeling method — LIGNUM — has been expanded to simulate the growth of a group of trees. The same principles and modeling structure are used for stand or forest simulation as are used for individual tree simulation. The simulated cottonwood tree growth in the stand is also expressed in terms of tree structure derivation and biomass allocation.

4.2.1 General model structure

This project simulates the growth of a tightly-spaced, mono-cohort cottonwood stand. The cottonwood trees are under short-rotation management, in which all trees are harvested by the end of the cycle. In effect, such a time frame does not allow for significant self-thinning of the stand. Thus, the simulation does not take into account events associated with forest development, such as succession and disturbance. Border trees are used around study trees in order to minimize edge effects on focal trees.

As an extension of the LIGNUM modeling method for cottonwood growth simulation, cottonwood stand simulation was based on the techniques of and completed structure derived from individual tree simulation. The stand simulation model focuses on one tree in the center of the stand in terms of detailed physiological process and morphological structure. The growth simulation result for the central tree is assigned or attributed to trees at other locations in the stand to construct overall stand growth. External shading from adjacent trees is taken into consideration in the calculation of photon flux interception (Figure 30).

The tree in the center of the stand is set as the focal tree for tree simulating growth dynamics. The general stand modeling structure begins with photon flux interception and leaf photosynthesis for the focal tree as in individual tree growth. The photon flux interception is affected by shading from adjacent trees. Allocation of growth and updating of tree structure are accomplished in the intermediate time step. Results for the simulated tree are then assigned to trees at different locations in the stand after each structural update. The tree compartments of all trees in the stand are added into voxel space, which subsequently contributes the shading to the focal tree in the next simulation

step.

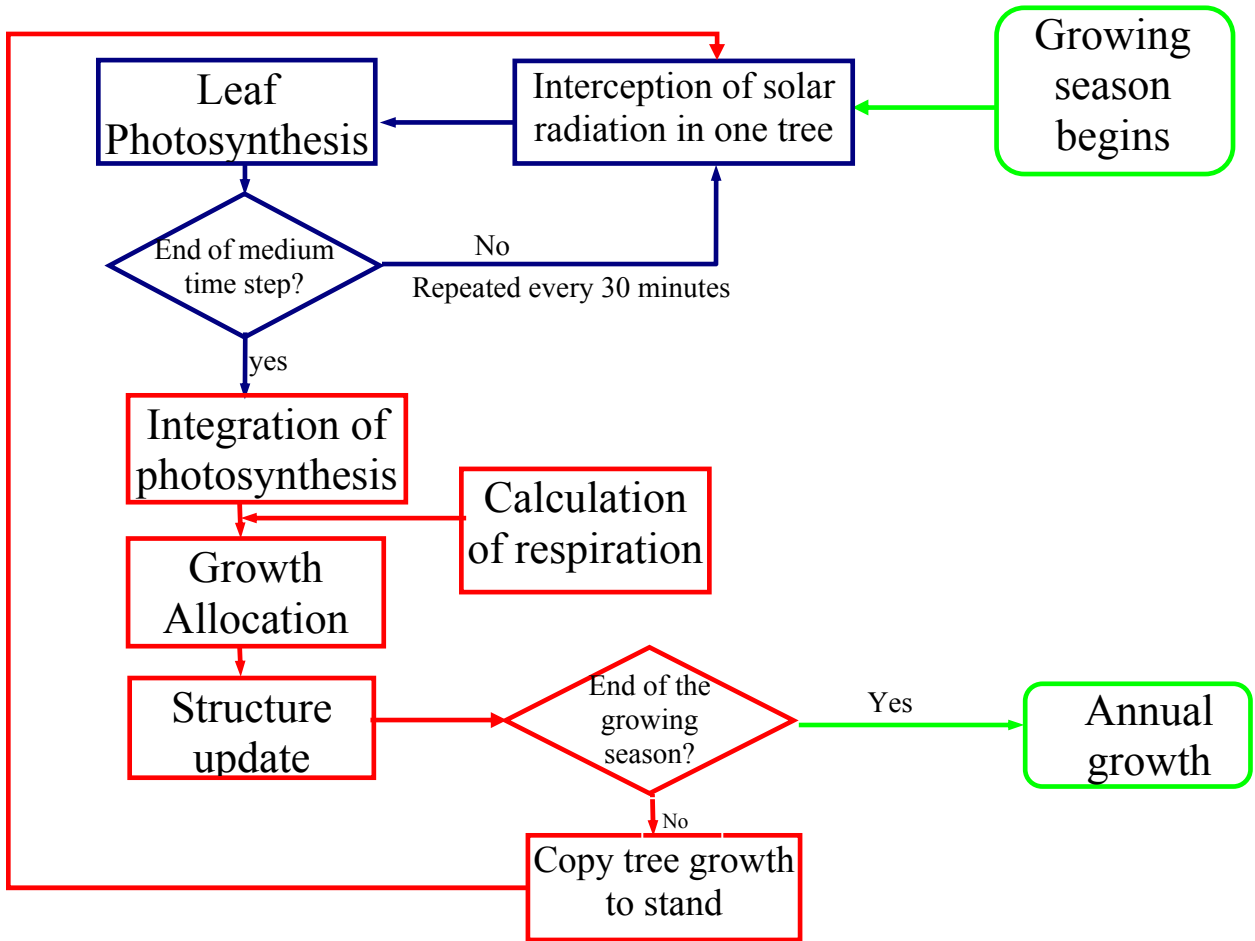


Figure 30. General modeling structure for cottonwood stand growth simulation. Only the focal tree in the center of the stand is simulated in the stand simulation. The structure of the simulated tree is subsequently assigned to other trees in the stand.

4.2.2 Uniformity of tree growth in the stand

The stand simulation is designed to simulate tree growth in a high density plantation. In the field stand, very high uniformity of the cottonwood tree growth was found in the mono-cohort, even-aged, and even spacing stand plantation. Being evenly spaced within a similar growing environment, trees' growths in the field stand are quite similar. The trees in the field have similar height and biomass growth. For example, the measured heights for eight trees from the stand have average 8.6m height with standard deviation 0.67m (unpublished data from Pallardy). There is no dominant tree or suppressed tree observed in the stand. Especially, the leaf area indices for each tree, which is the most critical component in stand shading, show no significant difference between cottonwood clones during most time of the growing season (Pallardy *et al.*, 2003). This uniformity of tree growth in stand allowed a special simulation style in this stand model -- only the growth of the most central tree in the stand was simulated in this exercise.

4.2.3 Voxel model

The voxel model was also applied in estimating interception of photon flux for trees in the stand. Here the voxel space encompasses the entire growing space of the stand rather than exclusively that of a single growing tree. Each tree in the stand is represented in voxel space in the form of compartments. It is possible that tree branches might 'overlap' or 'intersect' in a voxel space so that a voxel may contain compartments from different trees. Moreover, in addition to internal shading within a tree crown,

external shading from adjacent trees may also occur. The voxel space was increased in size to include all trees in the stand, which concurrently and dramatically augmented photon flux interception calculations (Figure 31). In contrast to the extendable voxel space in the individual tree simulation, the overall size of the voxel space for the stand model remained fixed. Increase of individual tree size can be disregarded relative to the overall stand growing space.

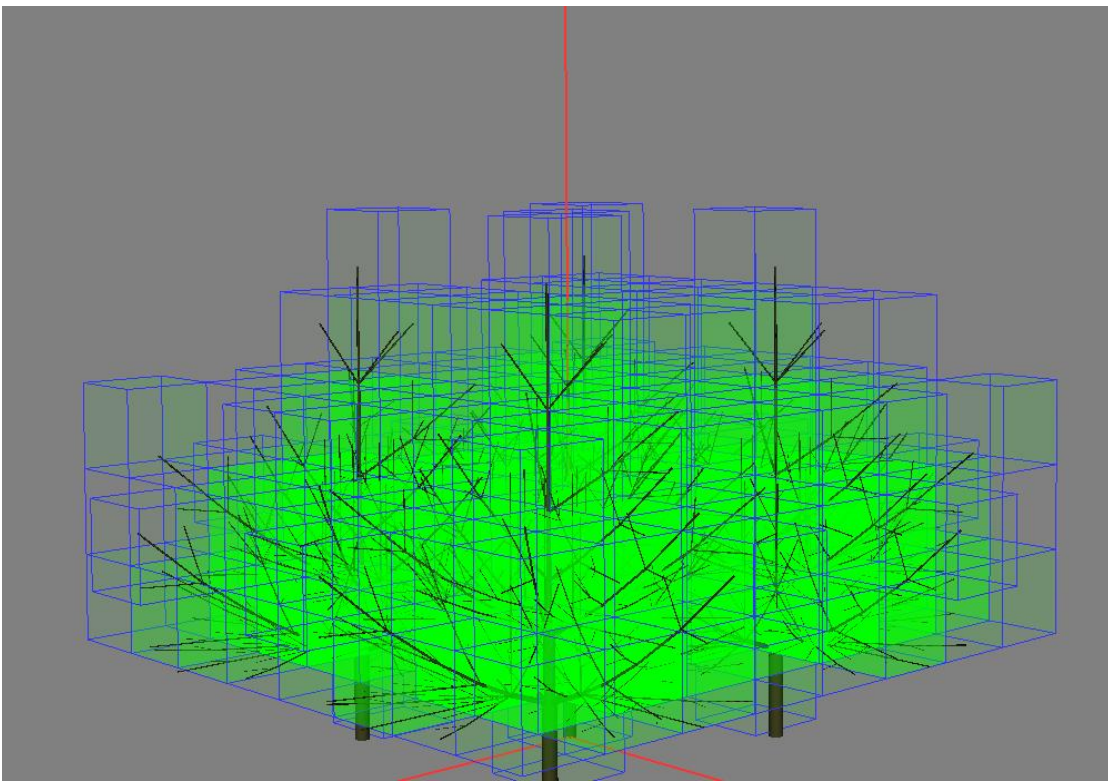


Figure 31. Voxel space for a simulated cottonwood stand. The voxel space includes the growing space of the entire stand. Leaves and segments in all trees are added into corresponding voxels. One voxel may contain tree compartments from different trees. (Figure courtesy of Mika Lehtonen)

4.3 Field data

As was the case with individual tree modeling, field data used in the stand model included real weather data (photosynthetic photon flux density and ambient temperature), tree structure, and photosynthetic parameters. There are both similarities and differences between field data for cottonwood stand growth simulation and open growth simulation. The differences mostly fall into the structural parameters of the tree.

4.3.1 The site

The stand plantation simulation involved a cottonwood stand with the same growth environment as that of the trees in the individual tree growth modeling exercise (chapter 3) -- an area with fertile soil and occasional flooding located in central Missouri (92°46' W; 39°01' N). The climatic conditions for the plantation also were the same as for trees in the individual tree growth modeling exercise.

The cottonwood plantation was established in May 1999 using 20-cm cuttings. The site was treated with a non-selective herbicide to eliminate grass competition. The plantation design is similar to that of Scarascia-Mugnozza *et al.* (1997). Six blocks, each consisting of four single-clone plots (7×10), were used for the plantation research. The plots within a block were distributed randomly. Tree spacing was 1m ×1m (10000 trees per ha). The stand was composed of one hybrid poplar clones (I45/51) and three eastern cottonwood poplar clones (26C6R51; 2059; 1112). The hybrid clones (I45/51) is recommended and widely planted in the upper Midwest; the *P. deltoides* clones were collected by the Missouri Department of Conservation and distributed through the state tree nursery. The three eastern cottonwood clones were measured in this stand growth

simulation study.

The three eastern cottonwood clones in the stand used for the modeling data collection included: *Populus deltoides* 2059 (origin: Osage County, MO); *Populus deltoides* 1112 (origin: New Madrid County, MO); and *Populus deltoides* 26C6R51 (origin: Pope County, IL) (Pallardy *et al.*, 2003).

The soil fertility data for the stand is the average value of the block close to stand plantation. The soil quality shares the similar distribution with that in open growth in nutrition, CEC, and total carbon (Tables 1 and 9). In the uppermost 20cm depth, the amount of CEC, total carbon, calcium, nitrogen, and magnesium content in stand soil are significantly (*ca.* 20%) less than in the soil in open growth site. There is no significant difference of K content between these two locations. The Bray P content in stand soil is significantly (more than 30%) greater than that in open growth soil in the uppermost 20cm depth.

Table 9. Soil fertility data for 1m × 1m spacing stand growth plantation.

| Depth (cm) | Total C (%) | Total N (%) | Bray P (ppm) | CEC(cmol 100g ⁻¹) | Ca(cmol 100g ⁻¹) | Mg(cmol 100g ⁻¹) | K(cmol 100g ⁻¹) |
|------------|-------------|-------------|--------------|-------------------------------|------------------------------|------------------------------|-----------------------------|
| 0 - 10 | 2.0 | 0.219 | 99.2 | 22 | 14.8 | 3.42 | 0.7 |
| 10 - 20 | 1.2 | 0.127 | 68.0 | 19.9 | 13.4 | 3.18 | 0.5 |
| 20 - 30 | 0.8 | 0.076 | 62.2 | 16.6 | 12.1 | 2.62 | 0.4 |
| 30 - 40 | 0.7 | 0.054 | 65.6 | 15.1 | 10.9 | 2.38 | 0.3 |
| 40 - 50 | | | | | | | |
| 50 - 60 | 0.6 | 0.042 | 76.2 | 16.6 | 11.3 | 2.62 | 0.2 |
| 60 - 70 | | | | | | | |
| 70 - 80 | 0.5 | 0.035 | 53.6 | 17.3 | 11.4 | 2.92 | 0.3 |

Additional data were provided from another stand plantation with 3m × 3m tree spacing, which was established in 1997 in central Missouri close to the above 1m × 1m stand. The stand plantation was established to be an even-aged, mono-species, and even

spacing stand plantation. Data on the growth of this stand served only as a reference for the validation of simulation results. Since this stand is two years older than the $1\text{ m} \times 1\text{ m}$ stand, it is useful to validate the predicted modeling results in this project. The climatic condition for this stand is equal to open and the $1\text{ m} \times 1\text{ m}$ stand plantations. Several cottonwood and hybrid clones were planted in this stand; only the three clones – 1112, 2059, and 26C6R51 – were observed with height and DBH value; these three clones are the same as cottonwood clones in the $1\text{ m} \times 1\text{ m}$ plantation.

4.3.2 Tree structure

Same structural parameters were measured in the stand as in the open site. Trees of different sizes in the stand were selected. Twelve branches were measured from each tree -- four from a lower position, four from a middle position, and four from an upper position. The structural data gathered included branch diameter, length of internode segments, horizontal azimuth of branch, vertical inclination of branch, and branch bending angle (Figure 12; Figure 13). The selected branches were tracked until the highest order for branching structural bifurcation. Branch growth dynamics were also followed in stand trees using the same methodology as in open site.

Crown size was measured from eight directions – north, northeast, east, southeast, south, southwest, west, and northwest. The observed objects from $1\text{ m} \times 1\text{ m}$ spacing stand included 81 trees. These 81 trees are from 9 matrices each has 3×3 trees. The center trees of these nine matrices belong to the three clones – three for each. Surrounding trees in the matrices may be any clones of cottonwood trees or hybrid trees in the stand. The trees were measured once a month for 3 consecutive months in summer,

2003. The length of the longest branch was measured in the eight azimuth directions of the tree crown. Of these eight directions, that having the longest branch was recorded for each of the 81 trees.

The same measurements were also conducted in the 3x3-m stand for model validation. There were 108 trees selected in this stand for measurement. These 108 trees were from nine 3×4 matrices. The two center trees in each matrix have the same clone type and belong to one of the three clones – 1112, 2059, and 26C6R51. The surrounding trees of the matrices may belong to any clone type in the stand. The measure was taken at the same time as in above stand.

4.3.3 Weather data and photosynthetic parameters

Both the open plantation and stand plantation are located at the same site, so they share the general climatic conditions. The stand simulation also uses the same set of photosynthetic parameters from cottonwood clone 1112 as used in open growth simulation.

4.4 Results

Attention now turns to the analysis of field measurement data and tree structural patterns were derived. Structural differences between open growth trees and stand trees -- as well as among different clones -- were compared. Model simulation was executed based on these structural patterns and parameters, and simulation results and model evaluation are discussed below.

4.4.1 Results from field measurements

Branch angles

Branch angles include horizontal branch azimuth and vertical inclination angle of the bifurcation branch. Branch angles in the stand plantation display a pattern similar to those in the open plantation (Figure 32). Branch azimuths fall into the range from 0° to 360°, with no significant differences among any directions. Branch inclinations range from 10° to 60°. However, there are still subtle differences between the open and stand plantations, as well as among the different clones within the stand plantation. Table 10 reveals that branch angles differed in terms of vertical inclination and bending for open growth trees as opposed to stand trees. Branches of trees growing in a stand have bigger insertion angles than do those of open growth trees. The average branch insertion angle was 55° in stand trees as opposed to 44° in open growth trees. The average branch bending was 43° in stand trees as opposed to 45° in open growth trees. Compared to the branch origin angle, branches of open growth trees displayed much less bending than did those in the plantation stand. The comparison of the branch insertion angles and bending angles for two plantations (open and stand) and among different cottonwood clones in the stand plantation may be found in Figure 33. Each color denotes either one cottonwood clone in the stand plantation or cottonwood in the open plantation. The insertion angles in stand plantation trees are greater than that for trees in the open plantation. However, the insertion angles of the three cottonwood clones in the stand plantation do not differ significantly among themselves. The bending angles among all four groups are similar.

There are also differences in crown height and crown ratio between stand plantation and open-growth plantation trees (Table 11). In an open growth environment,

the crown ratios increased for juvenile trees in the first three years. The crown ratios for open growth trees in the third year were generally greater than those for trees in the stand plantation in the fourth year.

Data on longest branch directions for all selected trees may be found in Table 12. Information on the longest branch directions indicates a greater tendency of branches to some certain azimuth directions. Table 12 indicates the accumulated frequencies for the directions of the longest branches in both stand plantations. The frequencies of longest branch directions for cottonwood tree crowns are also revealed in figure 34. Among these eight directions, longest branches fell more in the southeast, northeast, and east directions for trees in $1\text{m} \times 1\text{m}$ spacing stand. While more longest-branches fell in the southeast, northeast, and southwest directions for trees in $3\text{m} \times 3\text{m}$ spacing stand.

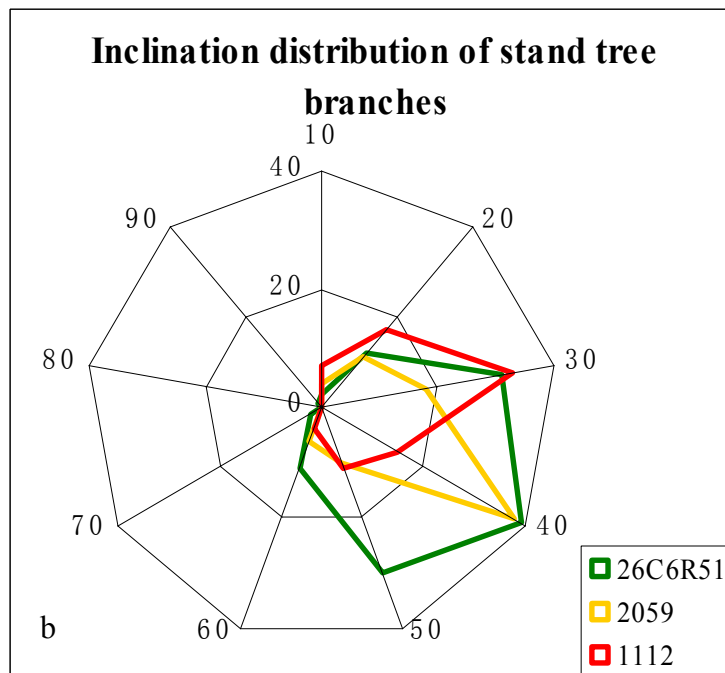
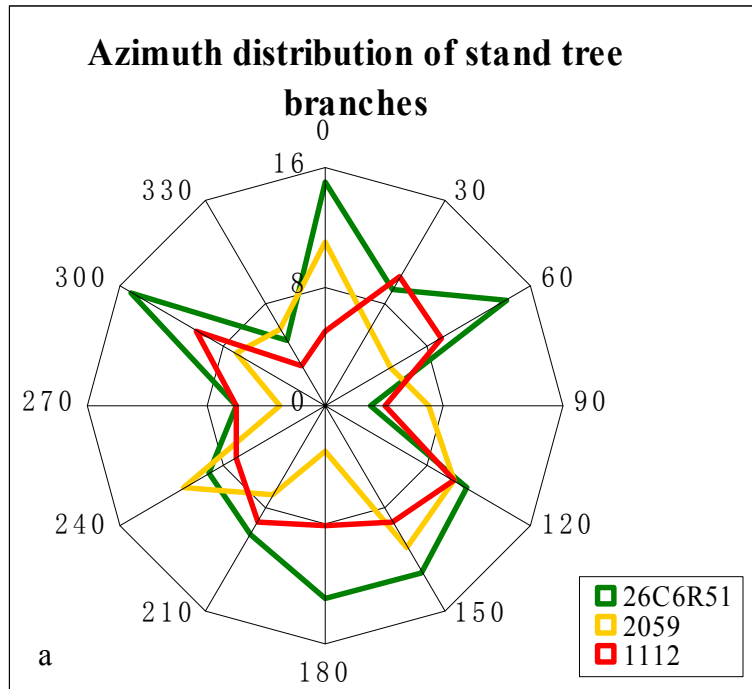


Figure 32. Branch angles distribution for the three clones' cottonwood trees in stand plantation. a) Azimuth (Horizontal bifurcation angle) distribution. The strength in each direction is the frequency of branch azimuths in each direction. Branch azimuths fall into the range from 0° to 360°, with not significant difference among each direction. b) Inclination (Vertical Bifurcation Angle) distribution. The inclinations of branches mostly fell into the range from 10° to 60°.

Table 10. Insertion and bending angles of branches for stand and open growth plantation cottonwood trees.

| Trees | Large Tree (degree) | | Median Tree (degree) | | Small Tree (degree) | | |
|------------------------------------|---------------------|---------|----------------------|---------|---------------------|---------|----|
| | Inclination | Bending | Inclination | Bending | Inclination | Bending | |
| Clone | | | | | | | |
| 2059 | 61 | 47 | 54 | 49 | 51 | | |
| Stand (55 ± 13, 43± 17)* | 1112 | 60 | 47 | 59 | 51 | 58 | 45 |
| | 26C6R51 | 53 | 52 | 48 | | 54 | 45 |
| Open Growth (44± 14, 45± 16) | | 43 | 49 | 43 | 42 | 45 | 45 |

* the average and standard deviation of inclination and bending for stand trees and open growth trees.

Table 11. Crown height and crown ratio for stand and open-growth plantation cottonwood trees.

| Trees | Large Tree | | | Median Tree | | | Small Tree | | | |
|--------------|----------------|-----------------|-------------|----------------|-----------------|-------------|----------------|-----------------|-------------|-------------|
| | Crown Base (m) | Tree Height (m) | Crown Ratio | Crown Base (m) | Tree Height (m) | Crown Ratio | Crown Base (m) | Tree Height (m) | Crown Ratio | |
| Clone | | | | | | | | | | |
| Stand | 2059 | 4.8 | 8.0 | 0.4 | 3.5 | 7.6 | 0.54 | 4.2 | 7.4 | 0.43 |
| (4-year) | 1112 | 5.1 | 8.0 | 0.36 | 5.08 | 8.0 | 0.36 | 3.4 | 6.45 | 0.47 |
| | 26C6R51 | 3.66 | 7.50 | 0.51 | 3.85 | 7.30 | 0.47 | 3.19 | 6.0 | 0.47 |
| Open | | 1.12 | 2.65 | 0.58 | 1.58 | 2.18 | 0.38 | 1.52 | 2.25 | 0.32 |
| 2002(2-year) | | | | | | | | | | |
| Open | | 1.1 | 3.34 | 0.67 | 1.4 | 2.9 | 0.52 | 1.3 | 3.0 | 0.57 |
| 2003(3-year) | | | | | | | | | | |

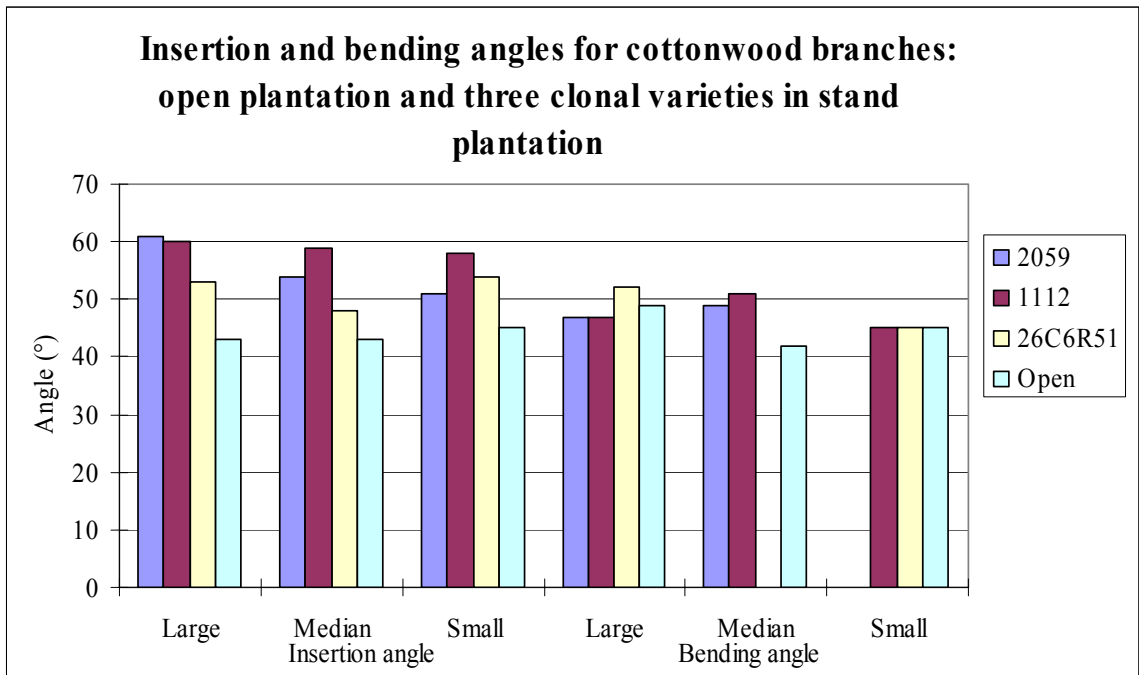


Figure 33. Comparison of the branch insertion angles and bending angles for two plantations and among different cottonwood clones in stand plantation. The left three groups of columns are insertion angles. The right three groups of columns are bending angles. Each color denotes either one cottonwood clone in the stand plantation or cottonwood in the open plantation. The insertion angle in the stand plantation is slightly greater than that in the open plantation. The insertion angles of these three cottonwood clones in the stand plantation are not significantly different from each other. The bending angles among these four series are similar.

Table 12. Frequency of directions for longest branches in cottonwood tree crowns.

| Directions | Frequencies | | Percentages | |
|------------|-------------|-------|-------------|-------|
| | 1mx1m | 3mx3m | 1mx1m | 3mx3m |
| N | 2 | 1 | 0.008 | 0.003 |
| NE | 51 | 76 | 0.21 | 0.235 |
| E | 41 | 17 | 0.17 | 0.052 |
| ES | 52 | 102 | 0.214 | 0.315 |
| S | 32 | 31 | 0.132 | 0.096 |
| SW | 17 | 54 | 0.07 | 0.167 |
| W | 14 | 6 | 0.057 | 0.019 |
| NW | 34 | 37 | 0.14 | 0.114 |
| Total | 243 | 324 | 1 | 1 |

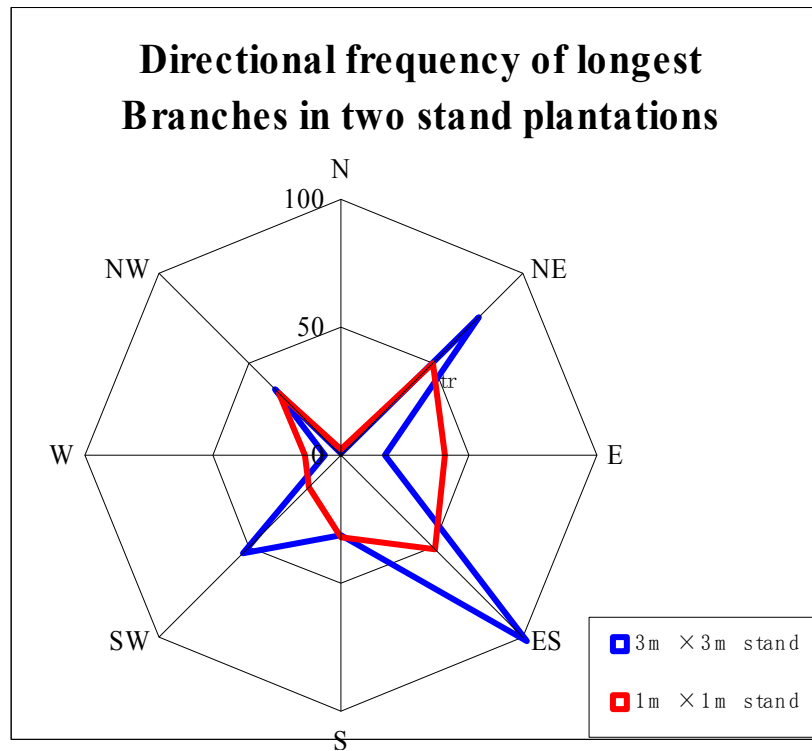


Figure 34. Directional frequencies of the longest branches in cottonwood tree crowns. Greater branch length growth in the crown occurs in the southeast and northeast directions.

Branch growth dynamics

Branch growth dynamics for trees in the stand plantation is shown in figure 35. Branches exhibited active growth from April to September, with final length averaging about 0.18m (Figure 35a). Branch elongations in all clones reveal a similar growth pattern. The elongation process starts from early May and stops at the end of September. The increase in length is slow compared to the branch growth in the open plantation (Figure 35b). The maximum branch length in the stand plantation is less than one third of the total length of 0.7m in the open plantation. Branch elongation in the stand plantation also stops earlier than it does in the open plantation, where it can persist until November.

Leaf growth dynamics

Likewise, leaf emergence in the stand plantation is slow compared to that in the open plantation. The total leaf number in the stand plantation remains steady from May to September. The average leaf numbers reached a maximum number of *ca.* 8 before leaf fall in August (Figure 36a). Some branches may even have 20 leaves. Leaf growth dynamics keeps the same pace as branch length growth dynamics. Again, the leaf emergence growth in the stand plantation stops earlier than it does in the open plantation and the average total leaf number is only one fifth of that in the open plantation (Figure 36b).

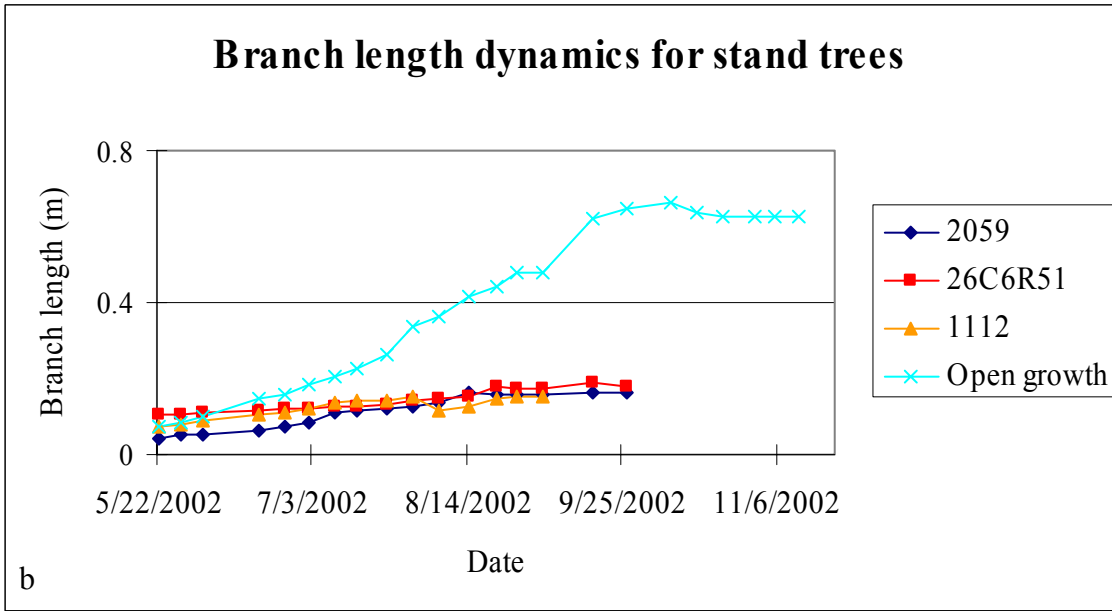
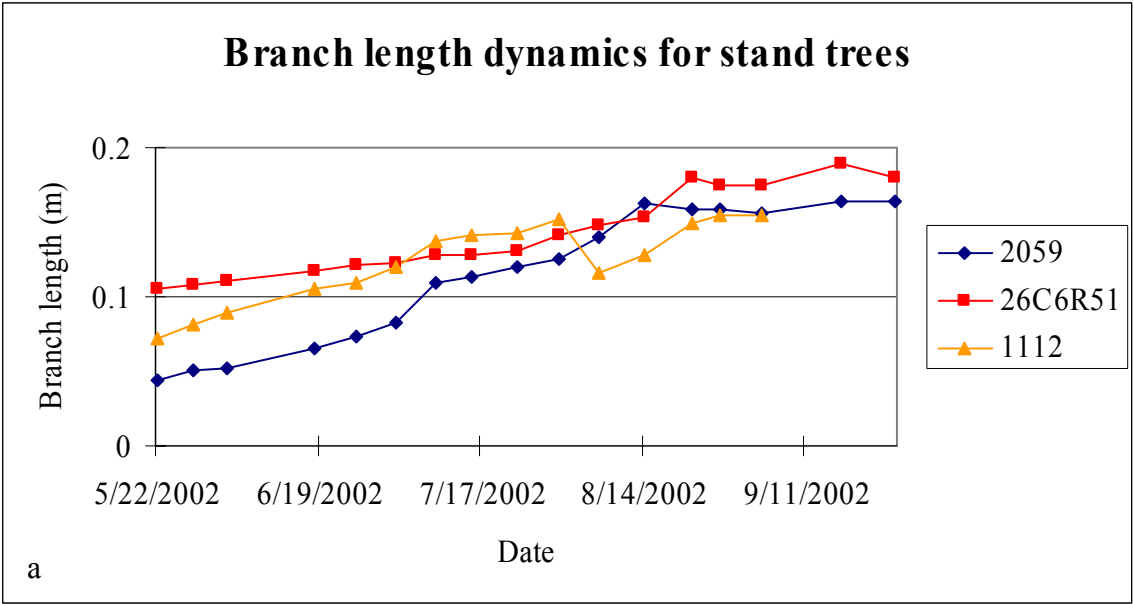


Figure 35. Branch length dynamics for trees growing in stand and open plantations. a) the average length elongation of new branch in one growing season. b) the contrast in branch length development between stand and open plantation trees.

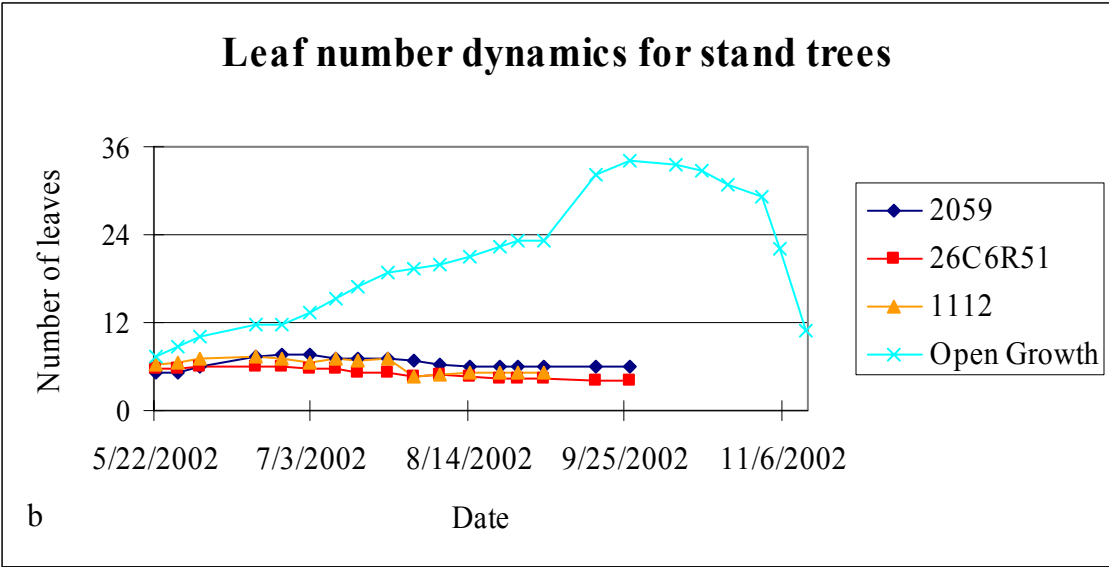
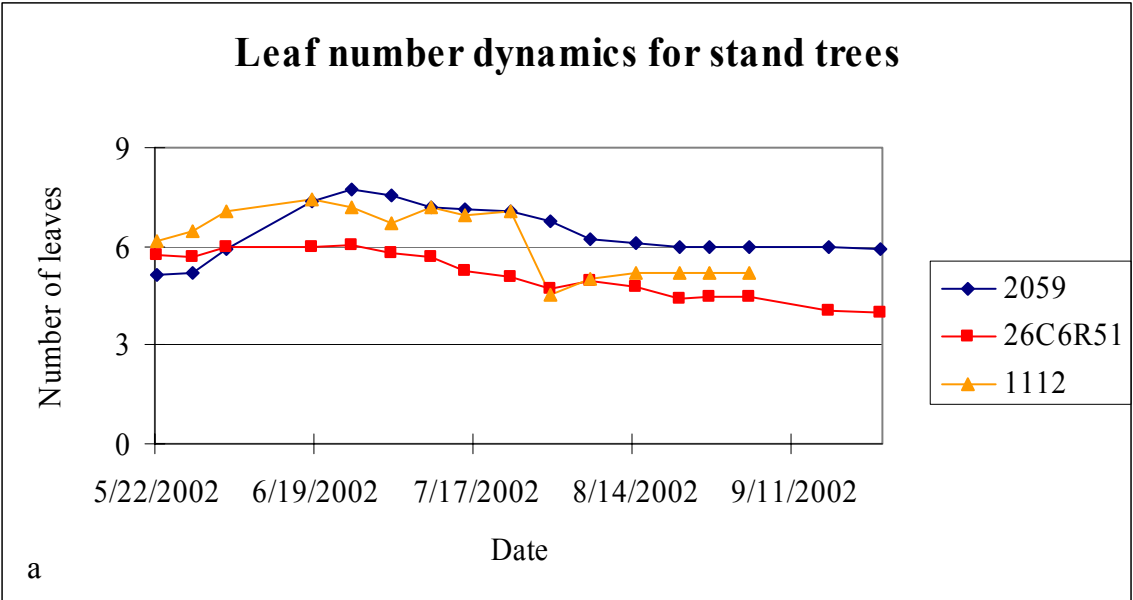


Figure 36. Leaf number dynamics for trees growing in stand plantation and comparison to that of trees in open plantation. a) the average leaves number dynamics for a single new branch in one growing season. b) the contrast of leaves number development between stand plantation and open plantation.

4.4.2 Model parameterization

Most parameters used in the stand simulation were consistent with those of the individual tree growth model (Section 3.4.1). In addition to parameters for stand structure, those for stand spacing were also included in the stand simulation (Table 13).

Table 13. Modelling parameters in cottonwood stand simulation.

| Symbol | Meaning | value | Unit | Reference |
|-------------------|------------------------------------|-------------------|--------|-------------|
| Branch Angle | Bifurcation Angle from main branch | $55 \pm 13^\circ$ | degree | measurement |
| Branching Bending | Bending of branch | $43 \pm 17^\circ$ | degree | measurement |

Branch azimuth distribution was simulated with frequencies shown in Table 12 and Figure 34. Two distinct stand spacing arrangements were simulated, one with 1m×1m spacing, and the other with 3m×3m spacing.

Considering the extension of the entire voxel space into the stand, voxel size was kept the same as that in the individual tree growth simulation even though branch elongation in the stand plantation is slower than that in open plantation. Structural time step length also was kept the same as in the individual tree growth simulation.

4.4.3 Model output and validation

As noted with respect to the individual tree growth model, the results of the LIGNUM model for cottonwood stand simulation may be depicted, assessed, and validated in either quantitative or qualitative terms. Qualitative visualization entails examining the shape and features of the simulated cottonwood stand as it is depicted graphically. On the quantitative side, numerical data describing the simulated stand is

examined, and model validation entails comparing simulated stand data with field measurements of an actual cottonwood stand.

Figure 37 shows the simulated 4-year-old cottonwood stand growing in a central Missouri environment with 1m×1m spacing. All trees in the stand are similar to each other. Crown closure is completed. The stand plantation in the field is shown in Figure 38. The simulated stand growth mirrors closely the real growth of cottonwood stand plantation in the field.

The field data for validation consisted of height and biomass data from a 4-year-old cottonwood stand plantation with 1m×1m spacing measured in fall, 2002 (Figure 38). Additional data included tree height from a 7-year-old cottonwood stand plantation with 3m×3m spacing measured in summer, 2003 (Table 14). Table 14 shows that both height and biomass growth from simulation are a little less than field results at each spacing distance.

Figure 39 shows the height growth trend for both the simulated and field cottonwood stands. The dashed line denotes the linear regression of simulation data for 1m × 1m spacing stand growth. The regression fit well with the simulation data ($R^2 = 0.9773$). Figure 39 shows that the difference between simulation results and field measurements increases with increasing age.

Table 14. Model validation for cottonwood simulation with biomass and height.

| | | 1m×1m Spacing Simu. (4 yr) | 1m×1m Spacing Measu. (2002) | 3m×3m Spacing Simu.(7 yr) | 3m×3m Spacing Measu. (2003) |
|----------------------|--------|---|--|--|--|
| Shoot | Stem | 3.07 | 3.85 | 6.95 | |
| Biomass (kg) | Branch | 0.20 | 0.41 | 0.63 | |
| | Total | 3.28 | 4.27 | 7.58 | |
| Root Biomass (kg) | | 0.47 | 0.966 | 1.25 | |
| Height(m) | | 8.03 | 9.11 | 12.54 | 14.16 |

* Simu. is for simulation, and Measu. is for measurement

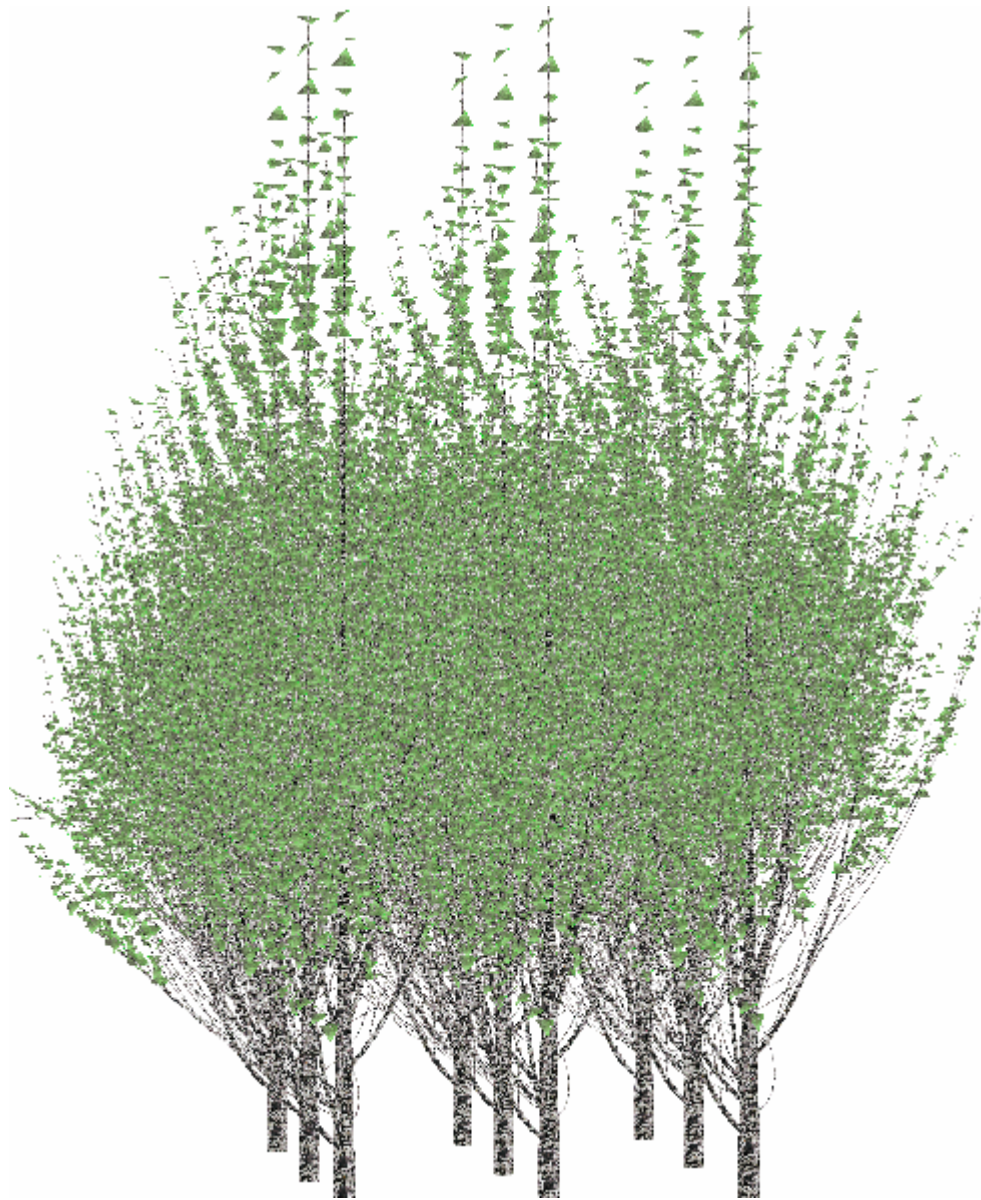


Figure 37. Visualization of a simulated 4-year-old cottonwood stand growing in a central Missouri environment with 1m×1m spacing.



Figure 38. Cottonwood stand plantation growth in the field in central Missouri. The tightly-spaced stand field experiment serves as a source of data for model parameterization and validation.

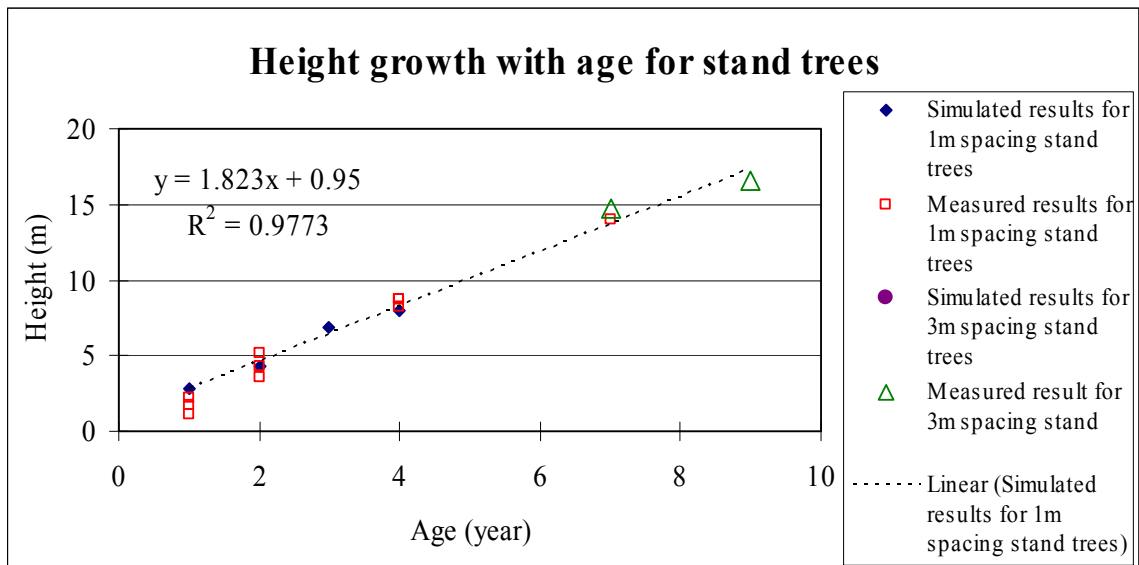


Figure 39. Trend in height for measured and simulated cottonwood growth in stand plantation. The dashed line is the linear regression of the simulation data for a 1×1m stand. The solid red square points are several field measurements from the 1×1m stand with different tree ages. The purple hollow circles are the simulation data for 3m×3m stand. The green hollow triangle point is the field height measurement from the 3m×3m stand.

The purpose of stand simulation is to predict the growth of a forest under certain environmental conditions or forest management regimes. Tree growth simulation can aid in predicting what a forest will look like in the future, including its potential for timber and/or wood products production. Simulation results can thus be used as an input to forest management and economic decision making.

The visual representation of a cottonwood stand after five years growth from establishment is depicted in Figure 40. The simulated stand provides estimates for height growth and increase in tree biomass. The simulation results also provide an estimate of biomass production for a stand or larger scale forest (Table 15).

Table 15. Height and biomass production for 1×1m spacing cottonwood stand growth.

| Age | Simulated Height(m) | Measured Height(m) | Simulated Biomass(Mg/ha) | Measured Biomass(Mg/ha) |
|-----|---------------------|--------------------|--------------------------|-------------------------|
| 1 | 1.84 | 2.22 | 0.5 | 2.49 |
| 2 | 3.77 | 4.33 | 2.7 | 8.4 |
| 4 | 8.03 | 8.42 | 32.8 | 72 |

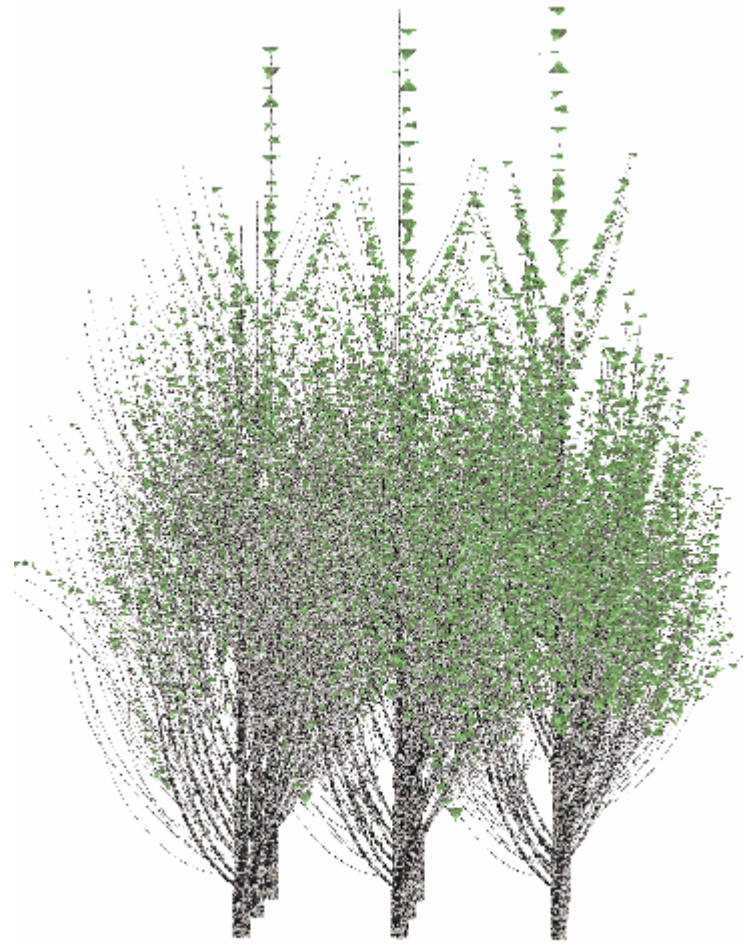


Figure 40. Visualization of 5-year-old tree growth in cottonwood stand.

4.5 Discussion

This project's simulation of a cottonwood stand represents an extension of LIGNUM research and the individual tree-based LIGNUM model to the broader area of forest growth. With the detailed simulation of leaves and branch segments, the stand growth simulation with LIGNUM employed in this study is one of the first applications of functional-structural modeling methods to a broader forest scale. The modeling method can be used in predicting tree growth, as well as in conjunction with economic analysis and management decision making.

4.5.1 Stand shading

Stand growth were retarded both in height and biomass because of the shading from neighboring trees. Compared to the over-estimated height value in individual tree simulation, the height and biomass results in stand simulation were both lower than field measurements (Table 14, 15; Figure 39). One possible reason may be the overestimation of photon flux interception by surrounding trees. The leaf area projection curve for overlapping leaves in one voxel may be overestimated, especially in the higher leaf content level.

4.5.2 Branch azimuth in stand plantation

Pallardy (unpublished) indicated that “there was a sustained, significant trend toward greater branch growth on the south side of trees”. Research conducted by Pallardy (personal communication) shows that the branch azimuths fall mostly in three directions -- southeast, southwest, and northeast – in descending frequency. Although it was

assumed in the individual tree model that all branches were randomly distributed in azimuth, field measurement data in this study revealed that branch lengths were notably longer in certain directions. Assumption is that the branch preference in azimuth direction is mainly determined by environmental factors, such as wind and the moving track of sun. So clones in the same stand are analyzed together. Among these eight directions, longest branches fell more in the southeast, northeast, and east directions for trees in 1m × 1m spacing stand. While more longest-branches fell in the southeast, northeast, and southwest directions for trees in 3m × 3m spacing stand. Combined with finding from Pallardy, results from this study indicate that the branch azimuths are more like to fall in certain directions and branches in these directions likely to have longer length in the whole.

4.5.3 Modeling efficiency

The whole stand is taken as the modeling object in the stand simulation model, which results in dramatically increased simulation time from that required to model an individual tree. The size of the voxel space in whole stand modeling is 10-20 times greater than that for an individual tree growth simulation. While about 1000 voxels are required in the latter for a four-year-old cottonwood tree, approximately 10000 voxels are required for the simulation of a stand of nine trees over that same period. While it requires about 60 minutes for simulating individual tree growth over a ten year period, more than three hours are needed to simulate cottonwood stand growth for a seven-year period.

The stand simulation models provide forest scientists and managers with the

ability to assess tree growth via another method in addition to field experiments.

The simulation of only one central tree to represent all the other similar trees in the stand has both advantages and disadvantages. The former clearly include efficiency improvement and reduction of computational load. Disadvantages include that as a plantation model, it treats all trees in the simulated stand as identical, resulting in the absence of variation. In addition, forest dynamics are not seen to operate in the stand in the form of such process as disturbance and succession.

4.5.4 Short-rotation cottonwood stand growth

The simulation results of the LIGNUM model for cottonwood stand growth were validated by field observations. For two different spacings, the height growth for simulated stands was close to that of stands observed in the field, given the same environmental parameters in terms of height. The linear regression of the LIGNUM simulation on cottonwood growth fit well with the field measurements in both stands with different spacing (Figure 39).

The insertion angle of the branch tends to increase with age (Pallardy, unpublished). Branches in the stand plantation attempt to grow upward to obtain as much radiation as possible because of the shading effect of surrounding trees. In order to avoid shading effects from adjacent trees to the extent possible, these branches also bend during growth. Thus, a branch does not continue growing exclusively in the direction of its initial angle, but increases that angle little by little so as to reach the top of canopy as quickly as possible. As revealed in Table 10, the average branch bending angle in stand trees is 43° , compared to the average insertion angle of 55° at the base of main branches.

The bending angles are significant in modifying the tree structure. The surround shading on the tree also affect the crown height in stand tree.

While in open growth plantation, the average branch bending angle is close to the average insertion angle, with 45° vs. 44°. One reason for these phenomena is that open growth branches can obtain more radiation from the crown edge than the crown top without being subject to shading effects from adjacent trees. In addition, the bending at the beginning of the branch is offset by the effects of gravity on the growing end of long branches.

4.5.5 Future research needs

The application of LIGNUM to stand growth simulation does not extend beyond further than individual-tree-based growth modeling. A variety of concepts relating to forest dynamics are not addressed within the current LIGNUM model for stand growth. Forest stand dynamics such as succession, fire disturbance, and timber harvesting activities must ultimately be incorporated within any realistic stand growth simulation model.

Although a stand of trees with identical characteristics – as assumed in this stand simulation exercise -- is reasonable for a mono-cohort stand, most forests in the world are characterized by diversity in species, tree ages, and spacing densities.

5. CONCLUSIONS

This section offers some final thoughts on the project of cottonwood growth simulation with LIGNUM modeling method. The project focused on the two specific objectives in cottonwood growth study in flood plain area in central Missouri. A single cottonwood tree was first simulated based on the Functional-Structural Modeling frame of LIGNUM. The individual cottonwood tree simulation is a new adaptation of LIGNUM modeling method and several improvements of LIGNUM were accomplished in this new application, which include real weather data input, Monte Carlo photon flux interception, application of Farquhar's model for estimating photosynthetic production, and use of three nested simulation time steps according to natural rates of growth processes. The integration of both features of physiological processes and structural patterns in the tree provided a good interpretation of tree growth.

The application of cottonwood growth simulation was extended into trees in a tightly-spaced plantation. The same assumptions and modeling structure were used in stand simulation as in the individual tree simulation except that stand simulation took into account an additional growth factor – shading from neighboring trees. The parameter system in stand simulation share some consistencies and differences with individual tree simulation. In order to reduce computational load in simulation, the stand simulation simulate only the central tree in the stand. The other trees in the stand were set to be identical to the focal tree.

Both the outputs for individual and stand growth simulation were satisfactorily validated by field measurements and previous simulation results from other models. The computer-based cottonwood growth simulation model provides a promising tool for

research on cottonwood growth in flood plain area. The LIGNUM model can be used in forest dynamics and industrial forest management — short rotation forest and riparian buffer. Simulation result of individual cottonwood provides the detailed structure and physiological information about cottonwood growth in the flood plain area of the Missouri River. This tree growth information, including tree height, biomass, tree structure, and root development, can be used in flood plain forest management, short rotation timber product prediction, and riparian buffer implementation. Moreover, further assumptions on tree growth and structural development can be included in the model so as to better understand tree growth. Based on the simulated results, new hypotheses of tree growth and additional modeling factors can be embedded into the model to make a better tree growth assumption and thus to improve modeling results. Pallardy (2003) indicated that there were obvious clonal differences in root-shoot ratio and growth rate in the first two years for cottonwood clones. A new set of parameters system can be obtained from field measurement for each clone, with which the LIGNUM cottonwood model can be redefined to simulate the possible growth differences. The simulation output can be used as one criterion in identification of potential cottonwood clones for flood plain forest and riparian buffer forest.

The LIGNUM cottonwood simulation model helps forest scientists to further understand tree growth principles and test growth hypotheses obtained from field observations. It provides a fast and flexible method in botanical and forest research. The new developments in LIGNUM model ensure the simulation result with efficiency and accuracy. Real weather data input provides a realistic photon flux environment for the simulated tree. Short time steps used in simulation try to capture the fast structural

change in fast-growing cottonwood growth. Monte Carlo photon flux interception provides a stochastic modeling result for modeling simulation. Farquhar's model on photosynthetic production reflects the current understanding on the functioning of plant photosynthesis. In summary, the cottonwood growth simulation is a new adaptation of LIGNUM modeling method. It includes both inheritance from the general frame of the previous LIGNUM model and new developments for several submodels in the LIGNUM model.

The cottonwood growth simulation with Functional Structural Modeling method – LIGNUM – is a valuable complementary tool for the traditional forest research and practice. Different planting configurations may be tested and the results can be predicted and compared. Hypothetical management questions can be answered before practical management design. In addition to the detail description in digital number, simulation results are also presented as a visualized tree. The tree visualization provides a heuristic expression of the simulated results, which can be compared and validated with the vision of real tree growth. Finally, growth results from modeling simulation can be used as references in the management practices of public forest management and private commercial businesses.

Underlying the structural description and physiological processes, the cottonwood simulation model applied several approximations and assumption with respect to both tree structure and growth allocation, such as the pipe model theory, structural patterns, and root dynamics in both structure and biomass. More detailed information and hypotheses can be embedded into the current model so as to continue to improve cottonwood growth explanation. Other factors affecting tree growth, such as

nutrition and water stress, can also be added into the model by creating more submodels. At the same time, the current stand tree growth simulation model is limited in its application to the forest growth by the fact that it treats all trees in the stand as identical, clearly at odds with most real-world natural stand. However, the model is flexible enough to simulate different scales of objects. Based on the simulations for individual tree, small stand plantation, the model can be extended to simulate more complex forest growth or specific growth purpose – riparian buffer forest. It might be necessary for the model to use some more simplified assumptions – such as forest dynamics principles -- for higher hierarchical simulation.

6. REFERENCES

- Alig, R.J., D.M.Adams, B.A. McCarl and P.J. Ince. 2000.** Economic potential of short-rotation woody crops on agricultural land for pulp fiber production in the United States. *Forest Products Journal* 50: 67-74.
- Aono, M., and Kunii, T.L., 1984.** Botanical tree image generation; *IEEE Computer Graphics Application*. 4: 10-33
- Aratsu, R., 1998.** Leonardo Was Wise: Trees Conserve Cross-Sectional Area Despite Vessel Structure. *Journal of Young Investgators*. 1(1): December.
<http://www.jyi.org/volumes/volume1/issue1/articles/aratsu.html>
- Balandier, P., Lacoite, A., Le Roux, X., Sinoquet, H., Cruiziat, P., Le Dizès, S., 2000.** SIMWAL: A structural-functional model simulating single walnut tree growth in response to climate and pruning. *Annals of Forest Science*. 57(5-6): 571-586.
- Bossel, H., 1996.** TREEDYN3 forest simulation model. *Ecological Modelling*. 90(3): 187-227.
- Botkin, D.B., Janak, J.F., and Wallis, J.R., 1972.** Some ecological consequences of a computer model of forest growth. *Journal of Ecology*. 60: 849-872.
- Botkin, D.B., 1993.** *Forest dynamics: an ecological model*. Oxford, University Press, Oxford, U.K.
- Brown, K.R., and van den Driessche, R., 2002.** Growth and nutrition of hybrid poplars over 3 years after fertilization and planting. *Canadian Journal of Forest Research*. 32: 226-232.
- Bugmann, H. 2001.** A Review of Forest Gap Models. *climatic change*. 51(3-4): 259 - 305
- Bull, H., 1945.** Cottonwood-a promising tree for intensive management. *Chemurgical Digest* 4:53-55.
- Caemmerer, S. von., Farquhar, G.D., 1981.** Some relationships between the biochemistry of photosynthesis and the gas exchange of leaves. *Planta*. 53:376-387.
- Ceulemans, R., Scarascia-Mugnozza, G.E., Wiard, B.M., Braatne, J.H., Hinckley, T.M., Stettler, R.F., Isebrands, J.G., and Heilman, P.E. 1992.** Production physiology and morphology of *Populus* species and their hybrids grown under short rotation. I. Clonal comparison of 4-year growth and phenology. *Canadian Journal of Forestry Research*. 22: 1937-1948.
- Christopherson, Nels, Bnan Barkley, Stig Ledin, and Paul Mitchell. 1989.** "Production Technology for Short Rotation Forestry", *International Energy Agreement (IEA) Report*. 89: 1.
- Cooper, D.T. 2002.** Eastern cottonwood.
<http://na.fs.fed.us/spfo/pubs/silvics%5Fmanual/volume%5F2/volume%5F2/populus/deltoides.htm> accessed in 2006.

- DeBell, D.S., and Harrington, C.A., 1997.** Productivity of Populus in monoclonal and polyclonal blocks at three spacings. *Canadian Journal of Forest Research*. 27: 978–985
- Dickson, R.E. and J.G. Isebrands. 1991.** Role of leaves in regulating structure-functional development of plant shoots. In *Integrated Response of Plants to Stress*. Eds. H.A. Mooney, W.E. Winner and E.J. Pell. Academic press. New York.
- Dupraz, C., Vincent, G., Lecomte, I., Bussi re, F., Sinoquet, H., 2004.** Above-ground modules in Hi-SAFE. The second annual report of SAFE. Montpellier, France
- Dwyer, J., 2004.** A cottonwood clonal trial to identify priority clones for planting in Missouri floodplains. The 6th Annual UMCA Program Review.
- Farquhar, G.D., von Caemmerer, S., Berry, J.A., 1980.** A biochemical model of photosynthetic CO₂ assimilation in leaves of C₃ plants. *Planta*. 149: 78-90.
- Fisher, J.B., 1992.** How predictive are computer simulations of tree architecture? *International Journal of Plant Science*. 153: 137-146.
- Friend, A.D., Schugart, H.H., Running, S.W., 1993.** A physiology-based gap model of forest dynamics. *Ecology*. 74: 792-797.
- Hunt, E. R. Jr., Martin, F. C., and Running, S.W., 1991.** Simulating the effects of climatic variation on stem carbon accumulation of a ponderosa pine stand: comparison with annual growth increment data. *Tree Physiology*. 9: 161-172.
- Gates, D.M., 1980.** Biophysical ecology. Springer-Verlag, New York, USA.
- Godin C., Costes E., Caraglio Y., 1997.** Exploring plant topological structures with the AMAPmod software: an outline. *Sil.a Fennica*. 31: 357-368
- Godin, C., and Caraglio, Y., 1998.** A multiscale model for plant topological structures. *Journal of Theoretical Biology*. 191: 1-46.
- Godin, C., Costes, E., and Sinoquet, H., 1999.** A Method for describing plant architecture which integrates topology and geometry. *Annual of Botany*. 84: 343-357
- Godin, C., 2000.** Representing and encoding plant architecture: A review. *Annals of Forest Science*. 57: 413-438.
- Goetz, S. J., and Prince, S. D., 1999.** Modeling terrestrial carbon exchange and storage: the evidence for and implications of functional convergence in light use efficiency. *Advances in Ecological Research*. 28: 58-92.
- Greenhill, A.G., 1881.** Determination of the greatest height consistent with stability that a vertical pole or mast can be made, and the greatest height to which a tree of given proportions can grow. *Proceedings of the Cambridge Philosophical Society IV, Part II*: 65-73
- Growing short rotation coppice.** Rural Development programme. England. Best practice guidelines for applicants to DEFRA's energy crops scheme. DEFRA, Department for environment, food and rural affairs.

- Guevara, E.A., W.R.N. Edwards, R.H. Morton, P.D. Kemp and A.D. MacKay. 2000.** Tree water use and rainfall partitioning in a mature poplar-pasture system. *Tree physiology*. 20: 97-106.
- Hallé, F., R.A.A. Oldeman and P.B. Tomlinson. 1978.** Tropical trees and forests: an architectural analysis. *Springer-Verlag, Berlin*, 441 p.
- Hamilton, D.A., Jr. 1991.** Implications of random variation in the Stand Prognosis Model. U.S. Forest Service Resource Note INT-394.
- Hanan, J.S., 1988.** PLANTWORKS: a software system for realistic plant modelling. Master's thesis, University of Regina.
- Hearn D., Baker, M.P., 1994.** Computer graphics, 2nd edition. Englewood Cliffs, New Jersey: Prentice Hall.
- Host, G. E., Rauscher, H.M., Isebrands, J. G., and Michael, D. A., 1990.** Validation of photosynthate production in ECOPHYS, an ecophysiological growth process model of *Populus*. *Tree Physiology*. 7(1-4): 283-296.
- Huber, H., Stuefer, J.F., 1997.** Shade-induced changes in the branching patterns of a stoloniferous herb: functional response or allometric effect? *Oecologia*. 110: 478-486
- Hunt, E. R. Jr., F. C. Martin, S.W. Running. 1991.** Simulating the effects of climatic variation on stem carbon accumulation of a ponderosa pine stand: comparison with annual growth increment data. *Tree Physiology*. 9: 161-172.
- Jaeger, M., Reffye (de), Ph., 1992.** Basic concepts of computer simulation of plant growth. *Journal of Bioscience*. 17: 275-291.
- Jaswal, S.C., Mishra, V.K., and Verma, K.S., 1993.** Intercropping ginger and turmeric with poplar (*Populus deltoids* 'G-3' Marsh.). *Agroforestry System*. 22: 111-117.
- Johnson, R. L., and Burkhardt, E. C., 1976.** Natural cotton wood stands-past management and implications for plantations. *In Proceedings, Symposium on Eastern Cottonwood and Related Species*. Sept. 28-Oct. 2, 1976, Greenville, MS. p. 20-29. Bart A. Thielges and Samuel B. Land, Jr., eds. Southern Forest Experiment Station, New Orleans, LA.
- Kawaguchi, Y., 1982.** A morphological study of the form of nature (Proc. SIGGRAPH '82); *Comput.Graphics*.16: 223-232
- Korzukhin, M.D., Ter-Mikaelian, M.T., and Wagner, R.G. 1996.** Process versus empirical models: which approach for forest ecosystem management? *Canadian Journal of Forest Research*. 26: 879-887.
- Kurth, W., 1994.** Morphological models of plant growth: possibilities and ecological relevance. *Ecological Modelling*. 75/76: 299-308.
- Kurth, W., 2000.** Towards universality of growth grammars: Models of Bell, Pagès, and Takenaka revisited. *Annals of Forest Science*. 57(5-6): 543-554
- Landsberg, J.J., 1986.** Physiological ecology of forest production. *London: Academic Press*.

- Landsberg, J.J., and Gower, S.T. 1997.** Applications of physiological ecology to forest management. Academic Press, London.
- Landsberg, J.J., and Waring, R.H., 1997.** A generalised model of forest productivity using simplified concepts of radiation-use efficiency, carbon balance and partitioning. *Forest Ecology and Management*. 95: 209–228.
- Landsberg, J.J., Johnsen, K.H., Albaugh, T.J., Allen, H.L., McKeand, S.E., 2001.** Applying 3-PG, a simple process-based model designed to produce practical results, to data from Loblolly Pine Experiments. *Forest Science*. 47(1): 43-51
- Landsberg, J.J., 2003.** Modelling forest ecosystems: state of the art, challenges, and future directions. *Canadian Journal of Forest Research*. 33: 385-397
- Larson, P.R and Isebrands, J.G, 1971.** The relation between leaf production and wood weight in first year root sprouts of two Populus clones. *Canadian Journal of Forest Research*. 2: 98-104
- Le Roux, X., Grand, S., Dreyer, E., Daudet, F.A., 1999.** Parameterization and testing a biochemically based photosynthesis model for walnut (*Juglans regia*) trees and seedlings. *Tree Physiology*. 19: 481-492.
- LIGNUM.** <http://www.metla.fi/metinfo/kasvu/lignum/index-en.htm>
- Lindenmayer, A., 1968.** Mathematical models for cellular interactions in development i & ii. *Journal of Theoretical Biology*.
- Lindenmayer, A., 1971.** Developmental systems without cellular interactions: Their languages and grammars. *Journal of Theoretical Biology*. 30:455--484.
- Lindenmayer, A., and Rozenberg, G., 1976.** Paracladial systems; in *Automata, languages, development* (eds) Amsterdam, New York, Oxford: North_Holland. pp 57-73
- Lindenmayer, A., 1977.** Theories and observations of developmental biology. In Butts, R. et Hintikka, J., editors, *Foundational Problems in Special Sciences*, pages 103--118.
- Lindenmayer, A., 1982.** Developmental algorithms: Lineage versus interactive control mechanisms. In Subtelny, S. et Green, P., editors, *Developmental Order: Its Origin and Regulation*, pages 219--245. A.R. Liss, New York.
- Lindner, M., Sievänen, R., and Pretzsch, H. 1997.** Improving the simulation of stand structure in a forest gap model. *Forest Ecology and Management*. 95: 183–195.
- Lo, E., Wang, M.Z., Lechowicz, M., Messier, C., Nikinmaa, E., Perttunen, J., Sievanen, R. 2001.** Adaptation of the LIGNUM model for simulation of growth and light response in Jack Pine. *Forest Ecology and Management*. 150:279-291
- Long, S.P., 1991.** Modification of the response of photosynthetic productivity to rising temperature by atmospheric CO₂ concentrations: Has its importance been underestimated? *Plant, Cell & Environment*. 14: 729-739.
- Mäkelä, A., and Hari, P., 1986.** Stand growth model based on carbon uptake and allocation in individual trees. *Ecological Modeling*. 33: 205–229.
- Mäkelä, A., and Sievänen, R. 1992.** Height growth strategies in open-grown trees.

- Journal of Theoretical Biology. 159: 443–467.
- Mäkelä, A., 1997.** A carbon balance model of growth and self-pruning in trees based on structural relationships. *Forest Science*. 43: 7–24.
- Makela, A., and Vanninen, P., 1998.** Impact of size and competition on tree form and distribution of above ground biomass in Scots pine. *Canadian Journal of Forest Research*. 28:216- 227.
- Mäkelä, A., Valentine, H.T., 2001.** The ratio of NPP to GPP: evidence of change over the course of stand development. *Tree Physiology*. 21: 1015–1030.
- Martin, G.L., and Ek, A.R. 1984.** A comparison of competition measures and growth models for predicting plantation red pine timber and height growth. *Forest Science*. 30: 731–743.
- Mazzoleni, S., and Dickmann, D. I. 1988.** Differential physiological and morphological responses of two hybrid *Populus* clones to water stress. *Tree Physiology*. 4(1): 61–70.
- McCullough, E.C. and W.P. Porter. 1971.** Computing clear day solar radiation spectra for the terrestrial ecological environment. *Ecology*. 52: 1008--1015.
- McGraw, 2004. Interactions between trees and crop plants in agroforestry systems: determine if cottonwood tree row orientation affects forage production and growth of reed canarygrass on site subject to periodic flooding.** The 6th Annual UMCA Program Review.
- McKnight, J. S., 1950.** Forest management by Old Man River. *Southern Lumberman*. 181(2273): 233-235.
- McMurtrie, R.E., 1991.** Relationship of forest productivity to nutrient and carbon supply—a modeling analysis. *Tree Physiology*. 9: 87–99.
- McMurtrie, R.E., Landsberg, J.J., 1992.** Using a simulation model to evaluate the effects of water and nutrients on growth and carbon partitioning of *Pinus radiata*. *Forest Ecology and Management*. 52: 243-260.
- Mehtätalo, L., 2004.** A longitudinal height–diameter model for Norway spruce in Finland. *Canadian Journal of forest Research*. 34(1): 131-140
- MHPRC: The Minnesota Hybrid Poplar Research Cooperative: 1999-2003**
<http://www.nrri.umn.edu/default/pt.asp?id=654>
- Mitchell, K.J. 1975.** Dynamics and simulated yield of Douglas-fir. *Forest Science Monograph*. 17: 39.
- Mialet-Serra, I., Dauzat, J., and Auclair, D., 2001.** Using plant architectural models for estimation of radiation transfer in a coconut-based agroforestry system *Agroforestry Systems*. 53: 141-149.
- Monteith, J.L., 1965.** Radiation and crops. *Experimental Agriculture Review*. 1: 241-251.

- Munro, D.D. 1974.** Forest growth models—a prognosis. *In* Growth Models for Tree and Stand Simulation. Proceedings of 1973 IUFRO Meeting, Working Party S4.01-4. Royal College of Forestry, Stockholm. Res. Note 30.
- Nilson, T., 1971.** A theoretical analysis of the frequency of gaps in plant stands. *Agricultural meteorology*. 8: 25-38
- Norman, J.M., and Arkebauer, T.J., 1991.** Predicting canopy photosynthesis and light-use efficiency from leaf characteristics. In 'Modeling Crop Photosynthesis—from Biochemistry to Canopy'. (Eds K. J. Boote and R. S. Loomis.) pp. 75-94. (Crop Science Society of America Inc.: Madison.)
- Nikinmaa, E., Messier, C., Sievänen, R., Perttunen, J. & Lehtonen, M. 2003.** Shoot growth and crown development: effect of crown position in three-dimensional simulations. *Tree Physiology*. 23(2): 129-136.
- Nygren, P., Kiema, P., Rebottaro, S., 1996.** Canopy development, CO₂ exchange and carbon balance of a modelled agroforestry tree. *Tree Physiology*. 16: 733 - 745.
- Oker-Blom, P., Smolander, H., 1988.** The ratio of shoot silhouette area to total needle area in Scots pine. *Forest Science*. 34: 894-906.
- Oppenheimer, P. E., 1986.** Real time design and animation of fractal plants and trees. In *Proceedings of the 13th annual conference on Computer graphics and interactive techniques*, computer graphics. 20: 55-64
- Pallardy, S.G., Gibbins, D.E., Rhoads, J.L., 2003.** Biomass production by two-year-old poplar clones on floodplain sites in the Lower Midwest, USA. *Agroforestry Systems*. 59: 21-26.
- Pallardy, S.G., 2004.** Physiological and morphological determinants of biomass productivity of poplar clones growing in Missouri River floodplains leading to assessment of the carbon budget for cottonwood clonal stands. The 6th Annual UMCA Program Review.
- Perttunen, J., Sievänen, R., Nikinmaa, E., Salminen, H., Saarenmaa, H., Väkevä, J., 1996.** LIGNUM: A tree model based on simple structural units. *Annals of Botany*. 77: 87-98.
- Perttunen, J., Sievänen, R., Nikinmaa, E., 1998.** LIGNUM: A model combining the structure and the functioning of trees. *Ecological Modelling*. 108: 189-198.
- Perttunen, J., Nikinmaa, E., Lechowicz, M.J., Sievänen, R., Messier, C., 2001.** Application of the functional-structural tree model LIGNUM to sugar maple saplings (*Acer saccharum* Marsh) growing in forest gaps. *Annals of Botany*. 88: 471-481.
- Perttunen, J., Sievänen, R., Nikinmaa, E., Lehtonen, M., 2004.** On the structural plasticity of Scots pine during early stand development. 4th International Workshop on Functional-Structural Plant Models, Montpellier, 7-11 June 2004.
- Pienaar, L.V., and Turnbull, K.J. 1973.** The Chapman–Richards generalization of Von Bertalanffy's growth model for basal area growth and yield in even-aged stands. *Forest Science*. 19: 2–22.

- Prusinkiewicz, P., and Hanan, J., 1989.** Lindenmayer systems fractals and plants. No. 79 in Lecture notes in biomathematics. Springer-Verlag, Berlin.
- Pruzinkiewicz, P., Lindenmayer, A., 1990.** The algorithmic beauty of plants. Springer-Verlag, New York, USA.
- Prusinkiewicz, P. and J. Hanan. 1992.** L-systems: From formalism to programming languages. In: G. Tozengerg, A. Salomaa (eds.): Lindenmayer Systems. Springer, Berlin, 193-211.
- Pruzinkiewicz, P., 2001.** The use of positional information in the modeling of plants. In: ACM SIGGRAPH 2001, 12-17 August 2001, Los Angeles, CA, USA, 289-300.
- Prusinkiewicz, P., 2004.** Modeling plant growth and development. Current Opinion in Plant Biology. 7: 79-83.
- Puri, S., V. Singh, B. Bhyshan and S. Singh. 1994.** Biomass production and distribution of roots in three stands of *Populus deltoids*, Forestry ecology and management. 65: 135-147
- Putnam, J. A., Furnival, G. M., and McKnight, J. S., 1960.** Management and inventory of southern hardwoods. U.S. Department of Agriculture, Agriculture Handbook 181. Washington, DC. 102 p.
- Raney, J. W., Wright, L. L., and Layton, P. A. 1987.** Hardwood energy crops: the technology of intensive culture. Journal of Forestry. 85(9): 17–28.
- Rauscher, H. M., Isebrands, J. G., Host, G. E., Dickson, R. E., Dickmann, D. I., Crow, T. R., and Michael, D. A., 1990.** ECOPHYS: an ecophysiological growth process model for juvenile poplar. Tree Physiology. 7: 255-281.
- Reffye (de), Ph., Houllier, F., Blaise, F., Barthélémy, D., Dautzat, J., and Auclair, D., 1995.** A model simulating above- and below-ground tree architecture with agroforestry applications. Agroforestry Systems. 30: 175–197
- Reffye (de), Ph., Fourcaud, T., Blaise, F., 1997.** A functional model of tree growth and tree architecture. Silva Fennica. 31(1): 297-311
- Richards, F.J., 1959.** A flexible growth function for empirical use. Journal of Experimental Botany. 10: 290–300.
- Robinson, A.P., and Ek, A.R. 2000.** The consequences of hierarchy for modeling in forest ecosystems. Canadian Journal of Forest Research. 30: 1837– 1846.
- Robinson, D.F., 2000.** Three gradients in the architecture of trees. Annals of Forest Science. 57(5-6): 439-444
- Ross, J. 1981.** The radiation regime and architecture of plant stands. Dr W. Junk Publishers, The Hague, The Netherlands, 391p.
- Running, S.W., and Coughlan, J.C. 1988.** A general model of forest ecosystem processes for regional applications. I. Hydrologic balance, canopy gas exchange and primary production processes. Ecological Modelling. 42: 125–154.

- Running, S.W. and Gower, S.T., 1991.** FOREST BGC, A general model of forest ecosystem processes for regional applications II. Dynamic carbon allocation and nitrogen budgets. *Tree Physiology*. 9: 147-160.
- Running, S.W., 1994.** Testing FOREST-BGC ecosystem process simulations across a climatic gradient in Oregon. *Ecological Applications*. 4(2): 238-247.
- Sands, P.J., 1996.** Modelling Canopy Production. 111. Canopy Light-utilisation Efficiency and its Sensitivity to Physiological and Environmental Variables. *Austrian Journal of Plant Physiology*. 23: 103-114
- Scarascia-Mugnozza G.E., Ceulemans R., Heilman P.E., Isebrands J.G., Stettler R.F. and Hinckley T.M. 1997.** Production physiology and morphology of *Populus* species and their hybrids grown under short rotation. 2. Biomass components and harvest index of hybrid and parental species clones. *Canadian Journal of Forest Research*. 27: 285–294.
- Shifley, S.R. 1990.** Analysis and modelling of patterns of forest ingrowth in the north central United States. Ph.D. thesis, University of Minnesota, St. Paul.
- Shinozaki, K., Yoda, K., Hozumi, K., Kira, T., 1964.** A quantitative analysis of plant form - the pipe model theory. I. Basic analyses. *Japanese Journal of Ecology*. 14: 97-105.
- Short Rotation Forestry Handbook. 1996.** University of Aberdeen, Wood Supply Research Group, Department of Forestry, 581 King St, Aberdeen. AB24 5UA
wsrcg@abdn.ac.uk <http://www.abdn.ac.uk/wsrcg/index.htm>.
- Short Rotation Woody Crops Program (SRWCP).** <http://www.srs.fs.usda.gov/srwc/>
- Simile.** <http://simulistics.com/index.htm>, accessed in 2006
- Sievänen, R., Nikinmaa, E., Nygren, P., Ozier-Lafontaine, H., Perttunen, J. and Hakula, H., 2000.** Components of functional-structural tree models. *Annals of Forest Sciences*. 57: 399 - 412.
- Sievänen, R., Perttunen, J., Nikinmaa, E., Berninger, F., Nygren, P., 2004.** Modelling tree development with transport/conversion approach in branched architecture. 4th International Workshop on Functional-Structural Plant Models, Montpellier. 7-11 June 2004.
- Singh, B., 1998.** Biomass production and nutrient dynamics in three clones of *populus deltoids* planted on Indogangetic plains. *Plant and Soil*. 203: 15-26.
- Singh, G., Singh, N.T., Dagar, J.C., Singh, H., and Sharma, P.V., 1997.** An evaluation of agriculture, forestry and agroforestry practices in a moderately alkali soil in northwestern India. *Agroforestry System*. 37: 279-295
- Sorrensen-Cothorn, K.A., Ford, E.D., and Sprugel, D.G. 1993.** A model of competition incorporating plasticity through modular foliage and crown development. *Ecological Monographs*. 63(3): 277–304.

- Stage, Albert R. 1973.** Prognosis model for stand development. Res. Pap. INT-137. Ogden, UT: U.S. Department of Agriculture, Forest Service, Intermountain Forest and Range Experiment Station. 32 p.
- Stage, A.R. 1981.** Use of self-calibration procedures to adjust general regional yield models to local conditions. *In* Proceedings, XVII IUFRO World Congress, 6–12 Sept. 1981, Kyoto, Japan. S4.01. Mensuration, growth and yield. pp. 365–375.
- Stage, A.R., and Wykoff, W.R. 1998.** Adapting distance independent forest growth models to represent spatial variability: effects of sampling design on model coefficients. *Forest Science*. 44: 224–238.
- Thornley, J.H.M. 1976.** Mathematical models in plant physiology. Academic Press, London.
- Thornley, J.H.M., and Johnson, I.R. 1990.** Plant and crop modelling: a mathematical approach to plant and crop physiology. Clarendon Press, Oxford, U.K.
- Valentine, H.T., Ludlow, A.R., and Furnival, G.M. 1994.** Modeling crown rise in even-aged stands of Sitka spruce or loblolly pine. *Forest Ecology and Management*. 69: 189–197.
- van den Driessche, R., 1999.** First-year growth response of four *Populus trichocarpa* × *Populus deltoides* clones to fertilizer placement and level. *Canadian Journal of Forest Research*. 29: 554–562
- Vanclay, J.K. 1995.** Growth models for tropical forests: a synthesis of models and methods. *Forest Science*. 41(1): 7–42.
- Vanclay, J. K., 2003.** Realizing opportunities in forest growth modelling. *Canadian Journal of Forest Research*. 33: 536-541
- von Caemmerer, S., Farquhar, G.D., 1981.** Some relationships between the biochemistry of photosynthesis and the gas exchange of leaves. *Planta*. 153: 376-387.
- Wang, Y.P., and Jarvis, P.G., 1990a.** Description and validation of an array model - MAESTRO. *Agricultural and Forest Meteorology*. 51: 257-280.
- Wang, Y.P., and Jarvis, P.G., 1990b.** Influence of crown structural properties on PAR absorption, photosynthesis and transpiration in Sitka spruce: application of a model (MAESTRO). *Tree Physiology*. 7: 297-316.
- Wang, Y.P., Massheder, J.M., Barton, C.V.M., Kruijt, B., Jarvis, P.G., 1995.** Documentation for the model: MAESTRO. Internal document, University of Edinburgh.
- Weinstein, D.A., and Yanai, R.D., 1994.** Integrating the effects of simultaneous multiple stresses on plants using the simulation model TREGRO. *Journal of Environmental Quality*. 23: 418–428.
- Weiss, A., Norman, J.M., 1985.** Partitioning solar radiation into direct and diffuse, visible and near-infrared components. *Agricultural and Forest meteorology*. 34: 205-213.

- Williamson, A. W., 1913.** Cottonwood in the Mississippi Valley. U.S. Department of Agriculture, Bulletin 24. Washington, DQ. 62 p.
- Wu, G. 1999.** ECOPHYS, Master thesis. University of Minnesota.
<http://oden.nrri.umn.edu/ecophys/mathgrad.doc>
- Zeide B. 2004.** Intrinsic units in growth modeling. Ecological Modelling. 175(3): 249-259.

7. APPENDIX

Source code for the photon flux interception in voxel space.

```
// for Poplar: The function calculates the Qin and Qabs-values to every VoxelBox.
LGMdouble VoxelSpace::calculatePoplarLight(LGMdouble diffuse, LGMdouble
structureFlag)
{
    updateStar();
    int vnumber=0, validvn=0;
    for(int i1=0; i1<Xn; i1++)
        for(int i2=0; i2<Yn; i2++)
            for(int i3=0; i3<Zn; i3++)
                {
                    int seed = -rand();
                    Bernoulli ber(seed);
                    vnumber++;
                    int num_dirs = sky->numberOfRegions();

                    if (voxboxes[i1][i2][i3].isEmpty() == false)
                        {
                            validvn++;
                            PositionVector
big_leaf_normal=voxboxes[i1][i2][i3].getBigLeafNormal();
                            if(structureFlag<=0)
                                {
                                    double totaliop=0;
                                    voxboxes[i1][i2][i3].updateValues();

                                    for(int i = 0; i < num_dirs; i++)
                                        {
                                            vector<double> rad_direction(3);
                                            LGMdouble iop =
sky->diffuseRegionRadiationSum(i, rad_direction);
                                            PositionVector radiation_direction(rad_direction[0], rad_direction[1],
rad_direction[2]);
                                            radiation_direction.normalize();
                                            LGMdouble maximum_box_project_area=
abs(Xbox*Ybox*radiation_direction.getZ())
+abs(Xbox*Zbox*radiation_direction.getY())
+abs(Zbox*Ybox*radiation_direction.getX());
                                            vector<VoxelMovement> vec;
                                            getRoute(vec, i1, i2, i3, radiation_direction);
                                            int size = vec.size();
                                            int a=-1;
                                            int flag=0;
```

```

if (size>1)
{
a=size-2;
flag=0;
double result=0;
while (a>=0 && flag<2)
{
result=0;
VoxelMovement v1 = vec[a];
LGMdouble leaf_area=voxboxes[v1.x][v1.y][v1.z].getLeafArea();

if(leaf_area>0)
{
LGMdouble projected_leaf_area=leaf_area*abs(
big_leaf_normal.getX()*radiation_direction.getX()
+ big_leaf_normal.getY()*radiation_direction.getY()
+ big_leaf_normal.getZ()*radiation_direction.getZ());
projected_leaf_area /= maximum_box_project_area;
if(projected_leaf_area>0.2 && projected_leaf_area<=0.8)
projected_leaf_area = 0.51*projected_leaf_area +0.1;
else if(projected_leaf_area>0.8)
projected_leaf_area = 0.7*projected_leaf_area/
(projected_leaf_area+exp(1-2.63*projected_leaf_area));
double p=min(projected_leaf_area, 1.0);
seed=-rand();
result=ber(p, seed);
}
else
result=0;

if (result>0.5)
flag+=1;
a--;
} //while vec
} // if size>1
if (a==-1 && flag<2)
{
double persent;
if (flag==0)
persent=0.8;
else if (flag==1)
persent=0.08;
else
persent=0;
voxboxes[i1][i2][i3].addRadiation(persent*iop*1200/2055.35);
totaliop+= persent*iop*1200/2055.35;
}
}

```

```

    }
    } //num_dirs for diffuse
    voxboxes[i1][i2][i3].setQ_inStdDiff(voxboxes[i1][i2][i3].getQin());
    resetQinQabs();
}

LGMdouble Qin=voxboxes[i1][i2][i3].getQ_inStdDiff()*diffuse/1200;
voxboxes[i1][i2][i3].addRadiation(Qin);

//calculate the light for direct beam
vector<double> direct_direction(3);
LGMdouble iop= sky->directRadiation(direct_direction);

vector<VoxelMovement> vec;
getRoute(vec, i1, i2, i3, direct_direction);
PositionVector radiation_direction(direct_direction[0],
direct_direction[1], direct_direction[2]);
int size = vec.size();

int a=-1;
int flag=0;
if (size>1)
{
    a=size-2;
    flag=0;
    double result;

    LGMdouble maximum_box_project_area=
abs(Xbox*Ybox*radiation_direction.getZ())
+abs(Xbox*Zbox*radiation_direction.getY())
+ abs(Zbox*Ybox*radiation_direction.getX());
    while (a>=0 && flag<2)
    {
        VoxelMovement v1 = vec[a];
        LGMdouble leaf_area=0;
        leaf_area=voxboxes[v1.x][v1.y][v1.z].getLeafArea();

        if(leaf_area>0)
        {
            LGMdouble projected_leaf_area=leaf_area*abs(
                big_leaf_normal.getX()*radiation_direction.getX()
                + big_leaf_normal.getY()*radiation_direction.getY()
                + big_leaf_normal.getZ()*radiation_direction.getZ());
            projected_leaf_area /= maximum_box_project_area;
            if(projected_leaf_area>0.2 && projected_leaf_area<=0.8)
                projected_leaf_area = 0.51*projected_leaf_area +0.1;
            else if(projected_leaf_area>0.8)

```

```

        projected_leaf_area = 0.7*projected_leaf_area/
        (projected_leaf_area+exp(1-2.63*projected_leaf_area));

        double p=min(projected_leaf_area, 1.0);
seed = -rand();
result=ber(p, seed);
    }
else
    result=0;
if (result>0.5)
    flag+=1;
a--;
}
}

if (a==-1 && flag<2)
{
double percent;
if (flag==0)
    percent=0.9;
else if (flag==1)
    percent=0.1;
else
    percent=0;
voxboxes[i1][i2][i3].addRadiation(percent*iop);
}
}
}
return 0;
}

```

VITA

Miaoer Lu, was born on March 7th, 1977, in Yongkang city, Zhejiang province, China. After attending public schools in Yongkang, she received the following degrees: B.S. in Geography from Nanjing University at Nanjing, China (1998); M.S. in Geography from Nanjing University at Nanjing, China (2001); Ph.D. in Forestry from University of Missouri-Columbia at Missouri, USA (2006).